BETA-CARYOPHYLLENE- A NOVEL ADJUNCT TREATMENT FOR BACTERIAL CYSTITIS IN MICE

by

Cassidy Scott

Submitted in partial fulfilment of the requirements
for the degree of Master of Science

at

Dalhousie University
Halifax, Nova Scotia
April 2022

DEDICATION PAGE

I would like to dedicate this thesis to my parents who taught me that through hard work anything is achievable.

TABLE OF CONTENTS

LIST OF TABLES

LIST OF FIGURES

ABSTRACT

Bacterial cystitis (BC) belongs to the family of urinary tract infections (UTIs) and represents one of the most common types of infections. BC occurs when uropathogenic bacteria, mainly *Escherichia coli* (UPEC), enters the bladder. While these infections are typically manageable with antibiotic therapy, painful symptoms may persist. Beta-caryophyllene (BCP), is found in plants such as *Cannabis sativa* and has well described local anesthetic, anti-bacterial and anti-inflammatory activity, the latter mediated through interactions with the cannabinoid type 2 receptor (CB2R).

In a murine model of BC, BCP treatment significantly reduced bacterial growth, demonstrated analgesic effects, and reduced bladder inflammation. *In vitro* experiments in UPEC-infected bone marrow derived macrophages and bladder epithelial cells further demonstrated the antibacterial activity of BCP.

Our results suggest that BCP has potential as a novel adjunct treatment for the management of BC as it is able to reduce bacterial growth, pain and inflammation in experimental BC.

LIST OF ABBREVIATION USED

2-AG	2-Arachidonoylglycerol
ABDH	Alpha/Beta Domain Hydrolases
AEA	*N*-Arachidonoylethanolamide
AMP	Antimicrobial Peptides
BC	Bacterial Cystitis
BCA	Bicinchonic Acid
BCP	Beta-Caryophyllene
BEC	Bladder Epithelial Cell
BMDM	Bone Marrow Derived Macrophages
BSC	Biosafety Cabinet
CACF	Carleton Animal Care Facility
caGa	Cytotoxin-Associated Protein A
cAMP	Cyclic Adenosine Monophosphate
$CB1^{-/-}$	Cannabinoid Type 1 Receptor Knockout
CB1R	Cannabinoid Type 1 Receptor
$CB2^{-/-}$	Cannabinoid Type 2 Receptor Knockout
CB2R	Cannabinoid Receptor Type 2
CBR	Cannabinoid Receptors
CFU	Colony Forming Unit
CNS	Central Nervous System
COX-2	Cyclooxygenase-2
CXCK1	CXC-chemokine ligand 1

DC	Dendritic Cells
DMEM	Dulbecco's Modified Eagle Medium
EA	Encephalomyelitis
EC	Endothelial Cell
ECS	Endocannabinoid System
eNOS	Endothelial Nitric Oxide Synthase
ERK	Extracellular Receptor Kinase
FAAH	Fatty Acid Amide Hydrolase
FCD	Functional Capillary Density
FDA	Food and Drug Administration
FITC-BSA	Fluorescein Isothiocyanate-Bovine Serum Albumin
GM-CSF	Granulocyte-Macrophage Colony Stimulating Factor
GPCR	G Protein-Coupled Receptor
GRAS	Generally Recognized as Safe
H&E	Hematoxylin and Eosin
IBC	Intracellular Bacterial Communities
ICAM-1	Intercellular Adhesion Molecule 1
ICAM-2	Intercellular Adhesion Molecule 2
IFN	Interferon
IL-1	Interleukin-1
IL-6	Interleukin-6
IL-8	Interleukin-8
iNOS	Inducible Nitric Oxide Synthase

IP	Intraperitoneal
IP3	Inositol Triphosphate
IV	Intravenous
IVM	Intravital Microscopy
LPS	Lipopolysaccharide
LUTS	Lower Urinary Tract Symptoms
MAGL	Monoacylglycerol Lipase
MAPK	Mitogen-Activated Protein Kinase
MIF	Migration Inhibitory Factor
MPO	Myeloperoxidase
MS	Multiple Sclerosis
NAAA	N-Acylethanolamine-Hydrolyzing Acid Amidase
NAGL	Neutrophil Gelatinase-Associated Lipocalin
NK	Natural Killer
nNOS	Neuronal Nitric Oxide Synthase
NO	Nitric Oxide
NOS	Nitric Oxide Synthase
Nrf2	Nuclear Factor-Erythroid 2 Related Factor 2
PAC	Prianthocyanin
PAMP	Pathogen-Associated Molecular Patterns
PBS	Phosphate Buffered Saline
PNS	Peripheral Nervous System
PRR	Pattern Recognition Receptors

PTX3	Pentraxin-related protein 3
RBC	Red Blood Cell
TLR	Toll-like Receptor
TMP-SMX	Trimethoprim-sulfamethoxazole
TNF	Tumour Necrosis Factor
TSA	Tryptic Soy Agar
UPEC	Uropathogenic *Escherichia coli*
UTI	Urinary Tract Infection
VacA	Vacuolating Cytotoxin A
Δ^9-THC	Delta-9-Tetrahydrocannabinol

ACKNOWLEDGEMENTS

First, I would like to acknowledge my supervisor, Dr. Christian Lehmann. Thank you for mentoring me over the past five years. From allowing me to volunteer in your lab as a young undergraduate student to now as I work to complete my thesis. Your guidance was essential in my development, and I have learned so much thanks to you. I cannot thank you enough for all you have done for me.

I would also like to thank Dr. Juan Zhou who has always been there to provide support and help with any troubleshooting.

Thank you to my committee members, Dr. Eileen Denovan-Wright and Dr. Jason McDougall for their guidance, feedback, and suggestions over the course of my project.

Tanya Myers and Bithika Ray, thank you for your constant support. This project would not have been possible without your guidance and expertise. You were always there to help and ensure that I had all the necessary tools to succeed.

Kayle Dickson, thank you for being my go-to person over the last few years. From undergrad to now you have taught me so much and have always been there when I needed help.

To my lab mates, past and present, Bashir, Purvi, Geriant, Stefan, Wujood, Maral, Danielle, Ian, Nazli, Daniel, Sophie, Suf, Irene and Hannah thank you not only for your help throughout my project but also for the fun times we had over the course of the last few years.

Thank you to the Jean Marshall lab and Nong Xu for their help with cytokine measurements. Thank you to the CACF staff for their help with my animal studies.

Thank you to Luisa, Sandy and Emma who were always there to provide guidance and answer any questions I had.

Finally, thank you to the animals that were sacrificed for this work.

Chapter 1: Introduction

1.1. Bacterial Cystitis

1.1.1. Definition, Epidemiology and Symptoms

Bacterial cystitis (BC) belongs to the urinary tract infections (UTIs) and is among the most common bacterial infections affecting 150 million people worldwide each year (McLellan & Hunstad, 2016). UTIs consist of infections of the urethra, bladder and kidneys (Grimes & Lukacz, 2011). BC can occur in both men and women, but is traditionally considered a disease of women, among whom 50% will be affected during their lifespan (Foxman, 2014). Women are particularly susceptible as the vaginal cavity and rectal opening are close to the urethral opening. Movement of bacteria from these unsterile environments into the urinary tract is enhanced by manipulation, sexual activity, and urinary catheter insertion. Upon entering the urethra, bacteria are more likely to ascend to the female bladder than the male bladder as a result of shorter urethral length (Foxman, 2014).

BC can be categorized as simple or complicated. Simple BC occurs in young, healthy, non-pregnant women with no anatomical abnormalities. Whereas complicated BC occurs in males, pregnant women, those with anatomic abnormalities, urinary catheters, stents or tubes and those undergoing chemotherapy, presenting with immunosuppression and/or exposed to urological procedures. Complicated BC can be caused by drug-resistant pathogens and is therefore more likely to require longer courses of antibiotic treatment. Furthermore, complicated BC can lead to infection of the upper urinary tract (i.e., kidney infections) (Dubbs & Sommerkamp, 2019).

In non-diseased state, urine is sterile along the urinary tract. The urinary tract system is able to maintain sterility through its constant unobstructed forward flow of urine which flushes

the system. Abnormalities in anatomy or function of the urinary tract which disrupts this flow can allow bacteria colonizing the urethral opening to enter the system and ascend into the bladder, causing infection. Symptoms of BC occur when the host response is engaged. Engagement increases in those who are unable to urinate frequently, empty their bladder completely or are immunocompromised (Foxman, 2014). The most commonly reported symptoms of BC include frequency, urgency, and dysuria. Among postmenopausal women, the elderly and children, suprapubic pressure, malaise, nocturia, incontinence and foul-smelling urine may also present. BC, however, is not always symptomatic. Asymptomatic bacteriuria is a condition where patients have high levels of urinary bacteria without the traditional symptoms of BC such as suprapubic pain, frequency, urgency and dysuria (Hannan et al., 2012). This condition commonly occurs in the elderly, pregnant, young and diabetic women (Nicolle et al., 2005).

Approximately 25% of women who experience BC will suffer a recurrent UTI within 6 months of the initial episode (McLellan & Hunstad, 2016). Women with frequent reoccurrences are more likely to have maternal history of cystitis and a childhood history (Scholes et al., 2000). Frequent or recent sexual intercourse is a common risk factor for BC. The odds of acute cystitis during the 48 hours after sexual intercourse increase by a factor as great as 60. Furthermore, exposure to spermicidal agents increases the risk of infection by *Escherichia coli* or *Staphylococcus saprophyticus* by a factor of two to three. Among elderly women, the risk of urinary tract infection increases with age and debility, especially in those with conditions associated with impaired voiding or poor perineal hygiene (Fihn, 2003). Lastly, genetic factors such as specific blood group antigens and secretor state have been associated with recurrent UTI.

Women of blood groups B and AB are significantly more susceptible to recurrent in comparison to other types (Kinane et al., 1982).

1.1.2. Microbiology – Causative Agent

Bacteria colonizing the urinary tract do not generally cause disease, as the host has effective methods, such as urination, for rapidly removing bacteria from the system (Foxman, 2014). Pathogens that contribute to BC usually originate from the gastrointestinal tract. Uropathogens from the fecal flora commonly colonize the vaginal opening and ascend the urethra to the bladder (Grimes & Lukacz, 2011). Bacteriuria is traditionally defined as the presence of bacteria in the urine, at least 10^5 cfu/mL on culture (Dubbs & Sommerkamp, 2019). Uropathogenic *Escherichia coli* (UPEC) are the most common cause of bacterial cystitis in all settings (Foxman, 2014). In premenopausal women, *Escherichia coli* is responsible for 70 to 90 percent of acute cystitis (Fihn, 2003). *Staphylococcus saprophyticus* accounts for 5 to 15 percent of cases and is mainly found in younger women. *Enterococci* and aerobic gram-negative rods, such as *Proteus mirabilis* and *Klebsiella* species account for the remainder of cases, which are mainly involved in catheter-associated and hospital-acquired BC (Fihn, 2003).

UPEC utilize a variety of virulence factors in order to colonize the bladder. UPEC isolates are able to invade epithelial cells and proliferate intracellularly forming intracellular bacterial communities (IBCs). IBCs are bacterial reservoirs protected from phagocytosis and neutralizing antibodies (Aguiniga, Yaggie, Schaeffer, & Klumpp, 2016). Furthermore, iron acquisition is critical for UPEC survival. The urinary tract is an iron-limited environment; therefore, IBC UPEC have developed mechanisms to acquire iron. UPEC strains produce siderophores, small molecule iron chelators, to scavenge ferric iron. In urine samples from women with cystitis, genes involved in siderophore production and iron acquisition were the

most highly expressed virulence determinants and UPEC isolates produced siderophores that are not synthesized by most non-pathogenic fecal *E. coli* strains, suggesting horizontally acquired genes (Hagan, Lloyd, Rasko, Faerber, & Mobley, 2010). Type 1 and P pili are key components of UPEC's ability to colonize and infect the urinary tract. Pili are protruding fibers on the bacterium which act as an anchoring mechanism allowing UPEC to adhere to their target receptor. Adhesion by type 1 and P pili is strengthened by the quaternary structure of their rod sections which provides mechanical resistance against urine flow. These adhesions appear to be adapted to the bladder environment allowing for maximum colonization of bacteria (Lillington, Geibel, & Waksman, 2014). Lastly, bacterial cell surface virulence factors such as flagella, capsular lipopolysaccharide (LPS) and outer membrane proteins are important virulence factors enabling bacteria to colonize the urinary tract. UPEC isolates from women with acute or recurrent UTIs show the presence of flagellum-mediated motility. Flagella also play a role during biofilm formation, aiding in adherence, maturation and dispersal (Terlizzi, Gribaudo, & Maffei, 2017).

1.1.3. Therapies and Outcomes

Trimethoprim-sulfamethoxazole (TMP-SMX) is the drug treatment of choice for uncomplicated cystitis in women (Fihn, 2003). Three-day therapy with antibiotics provides similar eradication rates and a lower incidence of side effects compared to longer therapy (i.e., seven to ten days). Patients who require longer regiments include pregnant women and those with symptoms lasting over a week. Treatment with either TMP-SMX or fluoroquinolones for three days have shown to result in an eradication rate greater than 90% in those with uncomplicated cystitis (Jancel & Dudas, 2002). However, antimicrobial resistance among uropathogens has been increasing to both TMP-SMX and fluoroquinolones (Critchley, Nicole

Cotroneo, Pucci, & Rodrigo Mendes, 2019). More recently, fosfomycin has been recommended as a first-line antibiotic for treatment of lower urinary tract (LUT) infections. Fosfomycin has a clinical efficacy rate of 91%. However, is likely less effective than TMP-SMX treatment. It has low collateral damage and good resistance profile. Therefore, it is a valuable first line antibiotic, especially in regions where local resistance rates to TMP-SMX are >20% (Chu & Lowder, 2018), Unless pregnant, those presenting with asymptomatic bacteriuria are not typically treated as they can often clear the bacteria without antimicrobials (Hooton et al., 2000). In addition to rise of multidrug-resistant uropathogens, antibiotics fail to eliminate a recurrence. The unmet need of effective therapy calls for novel approaches to this disorder.

Cranberry products in the form of juice or tablets are widely used and self-administered for the prevention of UTIs. No definitive mechanism of action has been established for cranberry products in the prevention of BC. It has been suggested that cranberry prevents UPEC from adhering to uroepithelial cells that line the bladder. Two components of cranberries are responsible for this: fructose inhibits the adhesion of type 1 fimbriated *E. coli* while proanthocyanins (PAC) inhibits the adherence of p-fimbriated *E. coli* (Jepson, Williams, & Craig, 2012). Studies conducted by Singh et al. (2016) found that twelve weeks of receiving cranberry extracts, when compared to placebo, decreased bacterial adhesion. Furthermore, cranberry extracts were able to reduce urine pH and prevent UTI symptoms such as dysuria, bacteriuria and pyuria (Singh, Gautam, & Kaur, 2016). Furthermore, studies by Maki et al. (2016) and Takahasi et al. (2013) concluded that cranberry beverage is superior to placebo in terms of UTI prevention in women with a recent history of UTIs (Maki et al., 2016; Takahashi et al., 2013). These results suggest that cranberry products may function as UTI prevention in otherwise healthy women. However, the literature does report conflicting conclusions as these

studies are mainly directed towards healthy women with recurrent episodes. Further research must be done including participants from a wider population.

Studies have also focused on the potential role of probiotics for UTI prevention and treatment. The vaginal microbiota is dominated by *Lactobacillus* species which are thought to prevent growth of potential pathogens by maintain a low pH (Lewis & Gilbert, 2020). *Lactobacillus* in the vagina may prevent colonization by pathogens such as *E. coli*. Women with lactobacilli-dominated microbiomes commonly carry less vaginal *E. coli* than those with low levels of lactobacilli (Gupta et al., 1998). Changes in the vaginal microbiota can be induced by antimicrobials, hormonal changes, menopause and contraceptive usage (Wawrysiuk, Naber, Rechberger, & Miotla, 2019). Studies by Stapleton et al. (2011) conducted a double-blind placebo-controlled trial of *Lactobacillus crispatus* intravaginal suppository probiotic for prevention of recurrent UTI in premenopausal women. They found probiotic treatment reduced the frequency of recurrent UTIs by 50% (Stapleton et al., 2011). Similarly, studies by Beerepoot et al. (2012) compared the efficacy of treating women with recurrent UTIs with TMP-SMX or *Lactobacillus rhamnosus* and *Lactobacillus reuteri*. Both prophylaxes reduced the mean number of symptomatic UTIs after 12 months. However, in the antibiotic prophylaxis group, resistance to TMP-SMX, trimethoprim and amoxicillin had increased from between 20-40% to between 80-95% in *E. coli* in the feces and urine within one month of therapy (Beerepoot, 2012).

Overall, no conclusive evidence has been found for non-antibiotic approaches to treating and preventing UTIs. Antibiotics therefore remain the gold standard for the treatment of UTIs. However, increasing antimicrobial resistance has raised interest in researching novel treatment options. Non-antibiotics prevention and treatment options could be successful in avoiding antimicrobial resistance and are therefore of great importance.

1.2. Immune Response in Bacterial Cystitis

1.2.1. Innate Immunity

Innate immunity is able to generate an inflammatory response within minutes of pathogen exposure by detecting evolutionary conserved microbial components shared by large groups of pathogens, termed pathogen-associated molecular patterns (PAMPs). This response is primarily mediated through phagocytic immune cells such as macrophages and dendritic cells (DCs), which recognize PAMPs via germ line-encoded pattern recognition receptors (PRRs). Upon PAMP recognition PRRs signal to the host the presence of infection and trigger proinflammatory and antimicrobial responses. Pentraxins, a protein family that can function as soluble PRRs, is an important protein in assessing the severity of infection. The level of pentraxin-related protein 3 (PTX3) in the urine during UTIs is associated with the severity of symptoms. Studies by Jaillon et al. (2014) demonstrated that PTX3 accelerates ingestion of bacteria and phagosome maturation in neutrophils. They found that PTX3 deficient mice had impaired clearance of UTIs and an increased UPEC-induced inflammatory response (Jaillon et al., 2014).

Following PAMP activation, secretion of primary inflammatory cytokines by macrophages and DCs triggers recruitment of other leukocyte subpopulations. The recruitment of leukocytes into tissue occurs through the leukocyte adhesion cascade. This multi-step process begins when inflammatory cytokines and bacteria-derived peptides upregulate adhesion molecules on the endothelial luminal surface which work to capture floating leukocytes onto the surface of endothelial cells (ECs) of postcapillary venules. These interactions are mediated by selectins that promote the “rolling” of leukocytes on ECs. Slow rolling promotes contact between the leukocyte and ECs so that the leukocyte can be further activated by chemokines and other proinflammatory agents on the surface of ECs. Once leukocytes make contact with chemokines,

chemokine receptors on the leukocyte transduces signals that lead to the activation of integrins. Leukocyte integrins enable firm adhesion and arrest of leukocytes on the endothelial surface. Leukocytes bind to members of the immunoglobulin gene superfamily, intercellular adhesion molecules 1 and 2 (ICAM-1 and ICAM-2). Adherent leukocytes crawl to nearby endothelial borders in preparation for extravasation (Muller, 2013).

The bladder epithelial cells (BECs) play an important role in the innate immune response of BC. Upon entering the bladder, UPEC first encounters BECs lining the urinary tract. BECs form a tight barrier and undergo reepithelialisation as a mechanism to reduce bacterial load in the bladder. BECs are replete with PRRs including toll-like receptor 4 (TLR4), a member of the TLR protein family. TLR4 recognizes gram-negative bacteria via the lipid A portion of LPS and induces the LPS-mediated inflammatory response. BECs use TLR4 as an autonomous defence system to sense and eject bacteria. TLR4 mobilizes the cellular trafficking machinery typically used to export hormones to instead export UPEC from infected BECs (Hayes & Abraham, 2016). Bacterial expulsion can be detected within minutes following infection and peaks at 4-hours post infection (Bishop et al., 2007). TLR4 activation can be seen soon after infection through a large secretion of Interleukin-6 (IL-6) which is detectable in the urine (Song et al., 2007). Secretion of IL-6 along with other inflammatory mediators result in a robust influx of immune cells to the epithelium. In addition to IL-6, BECs respond to UPEC by secreting IL-1 and IL-8 which leads to the recruitment of neutrophils into the infected bladder.

The submucosa of the urinary tract contains a substantial population of macrophages, and more are recruited to the site, following infection. Macrophages produce cytokines and chemokines that modulate the activity of other immune cells in the bladder. CXC-chemokine ligand 1 (CXCL1) and macrophage migration inhibitory factor (MIF) are important chemokines

which recruit neutrophils to the epithelial region. Following recruitment, tumor necrosis factor (TNF) released from macrophages permits transepithelial migration of neutrophils. Crosstalk between bladder macrophages allows for efficient bacterial clearance while minimizing damaging inflammation (Schiwon et al., 2014). Large numbers of neutrophils are found in the urine of patients with UTIs, indicating that neutrophils are capable of breaking through the tight junctions between epithelial cells (Hayes & Abraham, 2016). Neutrophils are among the first immune cells to be recruited to the bladder following infection. They respond to CXCL1 and other chemoattractant produced by BECs, mast cells and macrophages. The number of neutrophils closely correlates to the bacterial burden in the urinary tract, as bacterial numbers decrease so do neutrophils. Activated neutrophils release reactive oxygen species and other cytotoxic products in order to kill invading microbes (Abraham & Miao, 2015). However, excessive neutrophil responses can cause inflammatory damage to the bladder tissue. In the bladder, mast cells are found in the detrusor muscle region in close proximity to blood and lymphatic vessels. They are capable of releasing pre-stored pro-inflammatory mediators such as TNF, histamines and chemokines. Mast cell-deficient mice show impaired neutrophil responses and decreased bacterial clearance, indicating an important role of mast-cell activation during infections (Abraham & Miao, 2015).

BECs also release antibacterial agents which inhibit bacterial growth by eliminating bacterial growth factors in the urine. The neutrophil gelatinase-associated lipocalin (NGAL) protein, produced by α-intercalated cells, restricts bacterial growth by binding bacterial siderophores. Studies by Paragas et al. (2014) demonstrated that mice deficient in NGAL or α-intercalated cells showed increased susceptibility to UPEC infection (Paragas et al., 2014). Furthermore, antimicrobial peptides (AMPs) play an important role in the innate immune

defence. BECs function as the initial source of AMPs but at a later stage, secretion of AMPs occurs mainly by recruited neutrophils. The uroepithelium expresses two main families of AMPs, the defensins (e.g. β-defensin 1) and cathelicidins (e.g., LL-37). LL-37 is constitutively expressed at low levels in urothelial cells. Rapid production and secretion of LL-37 by neutrophils and epithelial cells occurs upon bacterial presence to increase epithelial production (Nielsen et al., 2014). Chromek et al. (2006) found that clinical *E. coli* strains that were more resistant to LL-37 caused more severe UTIs, demonstrating the protective nature of cathelicidin (Chromek et al., 2006). Furthermore, LL-37 has been shown to have direct killing mechanisms towards *E. coli* (Johansson, Gudmundsson, Rottenberg, Berndt, & Agerberth, 1998). β-defensin 1 is another AMP which mainly originates from kidney epithelial cells. However, both AMPs contribute to cytokine production and neutrophil recruitment in the bladder.

Upon activation of the immune system, immune cells evoke a robust immune response to recognize and destroy invading pathogens. Overexaggerated or prematurely terminated responses can both have detrimental effects on the host. Therefore, tightly controlled response consisting of innate immune cell crosstalk is necessary for a coordinated and effective response.

1.2.2. Adaptive Immunity

Unlike the wide-ranging innate immune response to BC, the adaptive immune response in the bladder tends to be limited. The majority of studies focus on the innate immune response in UTIs and therefore many adaptive immunity mechanisms remain unclear. UTIs that progress to kidney infections often lead to the production of specific antibodies however, not as much is known about infections confined to the bladder (Abraham & Miao, 2015). Studies by Thumbikat et al. (2006) used a murine model of UPEC-induced BC to demonstrate that transfer of serum or T cells from UPEC-infected animals is capable of initiating an adaptive immune response

through the activation and recruitment of B and T lymphocytes to the bladder in naïve mice. They found that cellular and humoral immune response peaked two weeks post infection. The cellular response was driven by Ag-specific activated T cells while the humoral was by Ag-specific IgG and IgM antibodies in both the serum and urine (Thumbikat, Waltenbaugh, Schaeffer, & Klumpp, 2006). Furthermore, studies by Asadi Karam et al. 2013 have been able to show humoral and cell-mediated immunity through vaccine studies. A vaccine was created from flagellin FliC protein of *Salmonella Typhimurium,* which binds TLR5, and recombinant antigen of UPEC to enhance the protective immune response against the antigen. Immunized mice showed significantly higher humoral (IgG1 and IgG2a) and cellular (IFN-γ and IL-4 immune response (Asadi Karam, Oloomi, Mahdavi, Habibi, & Bouzari, 2013). Lastly, a phase 2 clinical trial using a vaginal vaccine containing 10 heat-killed uropathogenic bacteria was done at the University of Wisconsin. Uehling et al. (2003) found that women who received primary immunization plus 5 booster doses remained free of infection for significantly longer than those who received placebo or only primary immunizations. Fifty-five percent of women who received 6 immunizations did not experience an infection, compared to 89% of placebo treated women who had UTIs. However, the basis for this protection remains unclear as no specific increase in IgG or IgA levels in immunized subject was found (Uehling, Hopkins, Elkahwaji, Schmidt, & Leverson, 2003). These studies suggest that the urinary tract system is able to mount a protective adaptive immune response. An important question remains regarding the duration of protection in the urinary tract. Approximately 25% of women who experience BC will suffer a recurrent UTI within 6 months of the initial episode, despite having no underlying immune deficiency (McLellan & Hunstad, 2016). It is possible that the adaptive immunity generated in the urinary

tract is short lived. Further studies must be done in order to better comprehend the underlying mechanisms of the immune response in the urinary tract.

1.3. The Endocannabinoid System

1.3.1. Cannabinoid Receptors (CB1R & CB2R)

The endocannabinoid system (ECS) is composed of cannabinoid receptors (CBRs), bioactive lipids (i.e. endocannabinoids) and enzymes responsible for synthesis and degradation of endocannabinoids. Cannabinoid type 1 receptors (CB1R) are the most abundant cannabinoid receptors, found primarily in the CNS. After the discovery of CB1R, cannabinoid type 2 receptors (CB2R) were described in splenic macrophages. CB2R has been found to be predominantly expressed in immune cells and other peripheral tissues, including the liver, bone, reproductive system, adipose tissue, GI tract and cardiovascular system (Zou & Kumar, 2018). Both CB1R and CB2R are members of the G protein-coupled receptors (GPCRs) family. Their activation inhibits adenylyl cyclases and certain voltage-dependent calcium channels and activates mitogen-activated protein kinases (MAPK), inwardly rectifying potassium channels (Ibsen, Connor, & Glass, 2017). Activation of either cannabinoid receptor exerts a broad spectrum of physiological changes. CB1R is largely involved in aspects of central nervous activities and disorders such as appetite, depression, stroke, neurodegeneration, multiple sclerosis, epilepsy and addiction. CB1R also plays a role in conditions of the peripheral nervous system (PNS) including pain, inflammation, cancer, reproductive and cardiovascular functions and musculoskeletal disorders (Rhodes et al., 2017). CB1R have attracted wide interest as a mediator of psychoactive properties.

1.3.2. Cannabinoid Ligands and Enzymes

There are five structurally distinct chemical classes of cannabinoid compounds: the classical cannabinoids (e.g., Δ^9-THC, Δ^8-THC- dimethylheptyl (HU210)); bicyclic cannabinoids (e.g., CP-55,940); indole-derived cannabinoids (e.g., WIN 55212-2); eicosanoids (e.g., anandamide, 2-AG) and antagonist/inverse agonists (e.g., SR141716A for CB1R, SR145528 and AM630 for CB2R) (Howlett & Abood, Mary, 2017). Some agonists show little selectivity between CB1R and CB2R receptors. However, antagonist compounds are usually highly selective, allowing for discrimination of CB1R vs. CB2R-mediated effects. The classical cannabinoids are dibenzopyran derivates. Δ^9-THC is the main psychoactive constituent of cannabis. HU-210 is a synthetic analog of Δ^8-THC, with a higher affinity for CB1R and CB2R and a higher potency and relative intrinsic activity as a cannabinoid receptor agonist than Δ^9-THC. The bicyclic analogs of Δ^9-THC lack a pyran ring. CP55,940 is a well-known member of this group and has been found to have slightly lower CB1R and CB2R affinities, compared to HU-210. Indole-derived cannabinoids have structures that differ markedly from the previously mentioned groups. WIN 55212-2 is the most studied indole-derived cannabinoid. WIN 55212-2 is similar to HU-210 and CP55,940 as it has intrinsic activity at both CB1R and CB2R. However, unlike these cannabinoids it has been found to have slightly higher CB2R than CB1R affinity. The two main endocannabinoids in the eicosanoid group are *N*-arachidonoylethanolamide (anandamide/AEA) and 2-arachidonoylglyverol (2-AG). These are the primary endogenous ligands that bind and activate CB1R and CB2R. Anandamide and 2-AG are both synthesized on demand, in response to elevations of intracellular calcium (Pertwee et al., 2010).

Anandamide is rapidly hydrolyzed in the CNS by fatty acid amide hydrolase (FAAH) (Cabral, Rogers, & Lichtman, 2015). Additionally, anandamide can be degraded via oxidation by cyclooxygenase-2 (COX-2). COX-2 is reasonably selective for anandamide over other acyl ethanol amides, so its inhibition allows for a more selective way to increase anandamide concentrations. Lastly, anandamide degradation can occur via N-acylethanolamine-hydrolyzing acid amidase (NAAA) (Hermanson, Gamble-George, Marnett, & Patel, 2014).

2-AG degradation is primarily due to monoacylglycerol lipase (MAGL) and alpha/beta domain hydrolases 6 and 12 (ABHD6 and 12). Enzymes that degrade 2-AG have different subcellular localization which allows for degradation of 2-AG in different cellular compartments. MAGL is widespread within the CNS and accounts for the majority of 2-AG degradation in the brain. ABDH6 is primarily localized to dendrites and dendritic spines of excitatory neurons in the cortex. Lastly, ABDH12 is involved in the hydrolysis of 2-AG in the brain.

The last chemical class of cannabinoid compounds is the antagonist/inverse agonists group. The development of CB1R and CB2R antagonists is of particular importance as they have been used as a tool for exploring the physiological functions of endocannabinoids. However, antagonists developed to date including the CB1R antagonist SR141716 and the CB2R antagonists SR145528 and AM630 have inverse agonist properties. Therefore, their effects cannot entirely be concluded as reversal of the tonic action of an endocannabinoid (Pacher, Bátkai, & Kunos, 2006).

1.3.3. CB2R Involvement in Immune Response

As previously mentioned, CB2R is highly expressed by immune cells such as macrophages, lymphocytes, and mast cells. In humans, the highest to lowest immune cell populations expressing CB2R are B cells > natural killer (NK) cells > macrophages >

polymorphonuclear cells > CD4 T cells > CD8 T cells (Galiègue et al., 1995). CB2R is involved in the immune response, regulating the inflammatory processes by enhancing apoptosis, suppressing immune cell activation, pro-inflammatory mediator release (e.g., cytokines, ROS, nitric oxide) and immune cell proliferation. CB2R expression changes are dependent on the activation status of different immune cell populations, highlighting the immunomodulatory role of the cannabinoid system. In vitro, the endocannabinoid, 2-AG, has be shown to induce the migration of human monocytes, neutrophils, and NK cells. In all studies, the effects of 2-AG were reverse by the CB2R-selective antagonist SR144528 demonstrating that immune cells migrate in response to 2-AG in a CB2R-dependent manner (Kishimoto et al., 2003, 2005; Kurihara et al., 2006). Additionally, studies by Sardinha et al. (2014) explored the effects of modulating the CB2R pathway using HU308, a CB2R agonist. HU308 reduced the number of adherent leukocytes in a murine model of sepsis, while AM630, a CB2R antagonist maintained the levels of adherent leukocytes (Sardinha, Kelly, Zhou, & Lehmann, 2014).

The endocannabinoid, 2-AG, has been shown to decrease inflammatory cell recruitment and enhance anti-inflammatory cytokine production in numerous experimental models. Studies using experimental autoimmune encephalomyelitis (EA) to model multiple sclerosis (MS) examined the effects of 2-AG treatment on the inflammatory response. It was shown that expression of both CB1R and CB2R were increased in the 2-AG-treated acute EAE mice compared to EAE control mice. Furthermore, 2-AG treatment potentiated a qualitative change of the inflammatory process, increasing microglial population and M2-shifting of inflammatory macrophages/microglia activating them towards a neuroprotective phenotype within the inflammatory environment (Lourbopoulos et al., 2011). Additionally, studies examining the role of MAGL, the main enzyme responsible for the inactivation of 2-AG, have been done to further

characterize the anti-inflammatory role of 2-AG. Studies by Comelli et al. (2007) used URB602, a MAGL inhibitor in a murine model of inflammation. URB602 administration elicited a dose-dependent anti-edemogen effect that was reversed by the CB2R antagonist SR144528 (Comelli, Giagnoni, Bettoni, Colleoni, & Costa, 2007). Similarly, studies using the MAGL inhibitor JZL184 have shown ability to decrease leukocyte migration as well as cytokine/chemokine levels and adhesion molecule expression in bronchoalveolar lavage fluid in a mouse model of acute lung injury. Furthermore, all anti-inflammatory effects were blocked by the CB2R selective antagonist, AM630 (Costola-de-Souza et al., 2013). The ability of MAGL inhibitors to prevent the inflammatory process alone but not in the presence of CB2R antagonists highlights the role of CB2R activation by 2-AG in modulating inflammation.

The endocannabinoid, AEA, is present at very low levels and has a short half-life due to the action of FAAH. Anti-inflammatory effects of AEA have been shown including its ability to inhibit the release of NO and TNF-α and decrease IL-6 production in LPS-stimulated astrocytes (Molina-Holgado, Molina-Holgado, & Guaza, 1998; Molina-Holgado, Molina-Holgado, Guaza, & Rothwell, 2002). Similarly, studies by Ortega-Gutiérrez et al. (2005) examined the effects of anandamide uptake inhibition on the production of nitric oxide (NO) and the release of cytokines. It was found that the selective anandamide uptake inhibitor, UCM707, is able to reduce the production of TNF-α, IL-6, IL-1β and NO release in LPS-stimulated astrocytes. Additionally, these results were shown to be reproduced with administration of the synthetic agonist, HU210 (Ortega-Gutiérrez, Molina-Holgado, & Guaza, 2005). Furthermore, studies using the FAAH inhibitor, URB497, in a rat model of LPS-induced inflammation found that increased AEA levels attenuated the LPS-induced increase in IL-1β and IL-10 (Kerr et al., 2012).

1.3.4. CB2R Involvement in Pain

The role of the CB2 receptor in pain is of particular interest as CB2R agonists show potential to treat acute pain without CNS side effects. The antinociceptive effects of CB2R agonists have been proposed to exert their effects via inhibition of inflammatory cells in the periphery, suppressing the production of proinflammatory cytokines and reducing painful behaviours in wide range of animal pain models (Shang & Tang, 2017). CB2R agonists have been considerably studied in inflammatory hyperalgesia. Intrapaw administration of AM1241 has been shown to reverse the increase in paw volume associated with carrageenan-induced paw edema. This inhibitory effect was completely blocked with AM630 administration. Additionally, local administration of AM1241 produced antinociception to thermal stimuli (Quartilho et al., 2003). Studies have also been done testing CB2R involvement in antinociception using mice lacking CB2R receptors, $CB2^{-/-}$. AM1241 inhibited nociception in $CB2^{+/+}$ mice but had no effect in $CB2^{-/-}$ mice. These results complete previous studies and reinforce the idea that activation of the CB2R via AM1241 has antinociceptive activity (Ibrahim et al., 2006). Similarly, studies by Hanus et al. (1999) found that HU-308, a CB2R specific agonist, reduced both inflammation and pain behavior in a murine model of arachidonic acid-induced ear swelling. These analgesic effects were partially blocked by the CB2R antagonist, SR-144528, but not by the CB1R antagonist, SR-141716A (Hanuš et al., 1999).

The role of the CB2R in pain modulation has also been studied using SR144528, a highly selective CB2R inverse agonist. SR144528 injection into the hind paws of mice was shown to prolong and enhance the pain behaviour associated with formalin tissue damage (Calignano, Rana, Giuffrida, & Piomelli, 1998).

Studies using CB1R knockout mice have further suggested the antinociceptive activity of CB2R activation. Δ^9-THC interacts with both CB1R and CB2R, having a higher affinity for CB1R. Studies by Zimmer et al. (1999) measured nociceptive responses to acute pain using the tail-flick test in $CB1^{-/-}$ mice. Δ^9-THC induced analgesic effects in the tail-flick test in both knockout and wild-type mice, demonstrating that Δ^9-THC has analgesic action mediated by the CB2R. Furthermore, Δ^9-THC produced catalepsy, hypothermia or hypomobility in wild-type mice but not in knockout mice, suggesting that these negative actions are mediated by CB1R alone (Zimmer, Zimmer, Hohmann, Herkenham, & Bonner, 1999).

Additionally, it has been shown that cannabinoids can interact synergistically with opioid receptors to produce analgesic effects. It has been shown that the CB2R agonist, AM1241, stimulates β-endorphin release from rat skin tissue and cultured human keratinocytes. Additionally, stimulation of endogenous opioid release was reversed by AM630 suggesting that CB2R activation acts on local μ-opioid receptors to inhibit nociception (Ibrahim et al., 2005).

1.4. Terpenes - Beta-Caryophyllene

1.4.1 Overview

Terpenes are the primary constituents of essentials oils and are responsible for the aroma of many plants, fruits and herbs. Terpenes are hydrocarbons with small isoprene units linked to one another forming chains. These lipophilic volatiles are able to freely cross cellular membranes (Sommano, Chittasupho, Ruksiriwanich, & Jantrawut, 2020). *Cannabis* is interesting for terpene research as diverse terpenes have been identified in the plant (Booth & Bohlmann, 2019). The terpene, beta-caryophyllene (BCP) has been of particular interest recently due to its dietary availability and safety, holding Food and Drug Administration (FDA) approval for food use and granted GRAS (Generally Recognized as Safe) status. BCP is a sesquiterpene prominent in many

cannabis strains as well as in other plants such as oregano, cinnamon, and black pepper. BCP selectively binds to the CB2R with an inhibitory constant K_i of 155 ± 4 nM and lacks binding activity to the human CB1R (Scandiffio et al., 2020).

Activation of CB2R by BCP leads to cellular activation and anti-inflammatory effects, activating the $G_{i/o}$ α -subunit inhibits adenylate cyclase thereby inhibiting cyclic adenosine monophosphate (cAMP) stimulation and activating phospholipase C, determining calcium release from inositol triphosphate (IP3), increasing intracellular levels of the of Ca^{2+}(Francomano et al., 2019). Furthermore, BCP has shown to increase phosphorylation of MAP kinase p38 and extracellular receptor kinases 1/2 (Erk1/2) (Gertsch et al., 2008).

1.4.2. Anti-Inflammatory Action of Beta-Caryophyllene

Beta-caryophyllene has been shown to have anti-inflammatory properties both *in vivo* and *in vitro.* Studies by Zhang et al. (2021) found phosphorylated levels of p38 MAPK, ERK and JNK were reduced by 85%, 90% and 75%, respectively in LPS challenged BMDMs pre-treated with BCP. Additionally, using an *in vivo* model of LPS-induced acute lung injury they found that BCP reduced mRNA levels of IL-6, IL-1β and TNF-α by approximately 50% (Zhang, Zhang, Li, Wang, & Qian, 2021). Similarly, BCP has been shown to decrease levels of pro-inflammatory cytokines, IL-6 and IL-1β, and inflammatory mediators, iNOS and COX-2, in doxorubicin-injected rats compared to control rats (Al-Taee et al., 2019). These results were further supported in studies using a murine model of rotenone-induced Parkinson disease. Both studies found that BCP attenuates levels of pro-inflammatory cytokines, IL-6, IL-1β and TNF-α, and inflammatory mediators, COX-2 and iNOS (Javed, Azimullah, Haque, & Ojha, 2016; Ojha, Javed, Azimullah, & Haque, 2016). Studies by Javed et al. (2016) went further providing evidence that neuroprotective effects are CB2R mediated, finding that pre-treatment with

AM630 significantly diminished the beneficial effects of BCP on pro-inflammatory cytokines and inflammatory mediators (Javed et al., 2016).

BCP has also shown cytoprotection towards the central nervous system, modulating the redox state and inflammation. Upon binding to CB2R, BCP stimulates nuclear factor-erythroid 2 related factor 2 (Nrf2), a transcriptional factor stimulated by oxidative stress. Nrf2 increases genes involved in cell survival and the reduction of the inflammatory process (Francomano et al., 2019). In a murine neurodegenerative model of MS, BCP was shown to significantly reduce the infiltration of inflammatory cells in the CNS and reduce levels of IFN-γ, TNF-α and IL-17 (Fontes et al., 2017). IFN-γ and TNF-α are cytotoxic and may provoke tissue injury therefore reducing secreted levels of these mediators plays an essential role in mitigating the effects of inflammation.

1.4.3. Anti-Bacterial Action of Beta-Caryophyllene

In addition to the anti-inflammatory effects of Beta-caryophyllene, recently BCP has been shown to have antibacterial activity against both Gram-negative and Gram-positive bacteria such as *Escherichia coli* and *Bacillus cereus* (Dahham et al., 2015). Studies by Yoo et al. (2018) found that BCP significantly inhibited the growth of *Streptococcus mutans* and reduced the formation of *S. mutans* biofilm (Yoo & Jwa, 2018) . Research has also shown BCP to inhibit the growth of *Helicobacter pylori* both *in vivo* and *in vitro* (Jung et al., 2020; Woo et al., 2020). In a mouse model of *H. pylori* infection, BCP dose-dependently decreased bacterial levels in the gastric mucosa of experimental animals. Additionally, bactericidal activity was accompanied by a significant reduction in *H. pylori*-induced inflammation compared to untreated mice (Jung et al., 2020). The mechanisms behind BCPs antibacterial activity remain largely unknown. However, *in vitro* studies on *H. pylori* reveal potential methods of action. *H. pylori* has many

known virulence factors associated with its pathogenesis. Cytotoxin-associated protein A (CagA) is an immunogenic protein injected into host cells which once translocated to the nucleus, dysregulates the homeostatic signal transduction of gastric epithelial cells. Additionally, vacuolating cytotoxin A (VacA) protein is known as a pore-forming secreted toxin that once translocated to the host cells, leads to cellular alterations including cell death. Studies by Woo et al. (2020) found that BCP inhibited CagA and VacA protein translocation into infected cells. To further investigate this finding, they then studied the effect of BCP on *H. pylori* mRNA and protein expression finding that that BCP downregulated mRNA and protein levels of both CagA and VacA (Woo et al., 2020). Studies have also investigated BCP's mechanisms of anti-bacterial action on *Bacillus cereus*, finding that BCP increases membrane permeability leading to intracellular content leakage and cell death (Moo et al., 2020).

1.5. Hypothesis

BCP treatment is beneficial in an acute model of experimental BC by providing anti-inflammatory and analgesic effects, based on its activity on CB2R and local anesthetic properties. Furthermore, administration of BCP in experimental BC will reduce bacterial growth - both *in vitro* and *in vivo*.

1.6. Study Objectives

The objective of the study was to examine the therapeutic potential of the CB2R agonist, BCP, in cellular and murine models of acute bacterial cystitis.

First, a pilot study was performed in order to characterize the development of infection after intravesical administration of UPEC in mice. The focus here was to ensure that intravesical administration of UPEC was an effective method of modeling bacterial cystitis and did not lead to the development of an upper urinary tract infection nor a systemic infection. Therefore, it was

first aimed to confirm bacterial burdens within the bladder unaccompanied by infection within the kidney and spleen tissues.

Once the model of bacterial cystitis was established it was used to assess the potential analgesic and anti-inflammatory properties of BCP comparing its efficacy to that of the FDA approved standard-of-care antibiotic, Fosfomycin, both alone and in combination. We aimed to study changes in pain and behaviour by von Frey aesthesiometry and behavioural assessment and evaluated anti-inflammatory effects through intravital microscopy (IVM) of the bladder microcirculation. To further explore the anti-inflammatory properties of BCP treatment we analyzed histological changes and cytokine levels in the bladder tissue of UPEC-infected mice.

In order to evaluate CB2R-dependent mechanisms of BCP treatment we then aimed to examine the analgesic and anti-inflammatory properties of BCP in the presence of the specific CB2R antagonist, AM630.

Lastly, we aimed to study the interactions between UPEC and bone marrow derived macrophages from mice as well as human bladder epithelial cells with and without BCP treatment. The goal of this objective was to study the potential effects of BCP on the clearance of UPEC *in vitro*.

Chapter 2: Material and Methods

2.1. Animal Models and Ethics Statement

Female BALB/c mice (8-12 weeks old; 20-30g) were purchased from Charles River Laboratories International Inc. (Wilmington, MS) and housed in ventilated plastic cage racks in a pathogen free room at the Carleton Animal Care Facility (CACF), Faculty of Medicine, Dalhousie University, Halifax, NS, Canada. Animals were provided with a standard diet of rodent chow and water *as libitum*. Animals were kept on a 12-hour light/dark cycle at 21℃. Prior to experimentation, animals were acclimatized in the CACF for one week. All animal experiments were performed following guidelines and standards set forth by the Canadian Council on Animal Care and were approved by the Dalhousie University Committee on Laboratory Animals under protocols #19-024 and #21-032.

2.2. Drugs and Reagents

The drugs and reagents used in experiments were purchased from commercial suppliers. CFT073 *Escherichia coli* (Maryland, USA) was purchased from American Type Culture Collection. BCP and highly refined olive oil (low acidity) were purchased from Sigma-Aldrich (Oakville, ON, Canada). 1X sterile phosphate buffered saline (PBS) used as our BC control and AM630, the CB2R antagonist used in our studies were purchased from Thermo Fisher Scientific (Massachusetts, USA). Saline (0.9% Sodium Chloride Injection USP, B. Braun Medical Inc., Bethlehem, PA, USA) was purchased from an in-house supplier at the Sir Charles Tupper Medical Building.

2.3. Inducing Spontaneous Rifampicin Mutations in *Escherichia coli*

Rifampicin resistance was induced in CFT073 *E. coli* by subculturing *E. coli* in fresh nutrient broth with varying concentrations of rifampicin (Sigma Aldrich, Oakville, ON, Canada).

The highest concentration of rifampicin-stressed bacteria still showing growth was then selected and serially diluted in 1X D-PBS (Thermo Fisher Scientific, Massachusetts, USA). Serial dilutions were then plated on Tryptic Soy Agar plates (TSA; Millipore Sigma, Etobicoke, Ontario, Canada) containing 200 μg/ml of rifampicin and left to incubate overnight at 37℃. Any colonies present following incubation are mutants. Mutant colonies were then isolated and serially passaged in between broth and plates containing rifampicin for 7 days to ensure mutant stability. Mutants were then preserved in a glycerol stock.

2.4. Experimental Groups

Two experimental timelines were established for these experiments. UPEC instillation of 50 µl (1-2x10^8 CFU/ml) occurred at T_0 following the induction of anesthesia in all groups. Animals in the pilot studies received treatment (BCP or saline) at T_0 immediately following UPEC instillation, given by intraperitoneal (IP) injection. Animals in the main and antagonist studies received treatment at T_6, given by IP injection. Description of treatments are shown in Table 1.

Table 1: Description of experimental groups

Group Name	Instillation and Treatment
Group 1: SHAM (control) Pilot Studies	50 µL PBS at T_0 (instilled via catheterization) Saline at T_0 (I.P.)
Group 2: BC (control) Pilot Studies	50 µL UPEC (1-2 X 10^8) at T_0 (instilled via catheterization) Saline at T_0 (I.P.)
Group 3: BC + BCP (100 mg/kg) Pilot Studies	50 µL UPEC (1-2 X 10^8) at T_0 (instilled via catheterization) BCP (20mg/mL) at T_0 (I.P.)
Group 4: SHAM (control) Main Studies	50 µL PBS at T_0 (instilled via catheterization) Saline at T_6 (I.P.) Olive oil at T_6 (I.P.)
Group 5: BC (control) Main Studies	50 µL UPEC (1-2 X 10^8) at T_0 (instilled via catheterization) Saline at T_6 (I.P.) Olive oil at T_6 (I.P.)
Group 6: BC + BCP (100 mg/kg) Main Studies	50 µL UPEC (1-2 X 10^8) at T_0 (instilled via catheterization) BCP (20 mg/mL) at T_6 (I.P.) Saline at T_6 (I.P.)
Group 7: BC + Fosfomycin (10 mg/kg) Main Studies	50 µL UPEC (1-2 X 10^8) at T_0 (instilled via catheterization) Fosfomycin (33.33 mg/mL) at T_6 (I.P.) Olive oil at T_6 (I.P.)
Group 8: BC + Fosfomycin (10 mg/kg) + BCP (100 mg/kg) Main Studies	50 µL UPEC (1-2 X 10^8) at T_0 (instilled via catheterization) BCP (20 mg/mL) at T_6 (I.P.) Fosfomycin (33.33 mg/mL) at T_6 (I.P.)
Group 9: BC + BCP (100 mg/kg) + AM630 (2.5 mg/kg) Antagonist Studies	50 µL UPEC (1-2 X 10^8) at T_0 (instilled via catheterization) AM630 (2.5 mg/kg) at $T_{5.5}$ (I.P.) BCP (20 mg/mL) at T_6 (I.P.) Saline at T_6 (I.P.)

2.5. Bacterial Cystitis Induction

BC induction was conducted in a Biosafety cabinet (BSC) using appropriate aseptic technique. General anesthesia was induced using 5% isoflurane by inhalation. After the induction, anesthesia was reduced to 2% isoflurane and 1L/min oxygen by inhalation. The bladder was then manually emptied by applying pressure to the suprapubic region. Animals' vaginal area was cleaned with an alcohol wipe and lubricated with warm saline. Sterile Vaseline (sterilized by UV light function of BSC for 30 minutes) was put on the catheter to provide lubrication and catheterization was performed at a 45-degree angle then changed to parallel when entry is secured. A transurethral catheter was made by inserting a 30G needle (0.3 mm x 13 mm, BD PrecisionGlide, Franklin Lakes, NJ, USA) into 4 cm of polyethylene tubing (PE10, inner diameter: 0.28mm, BD Intramedic, Sparks, MD, USA). All catheters were steam sterilized by the CACF prior to use. BC was induced by instilling 50 µL of the appropriately dilute ($1\text{-}2x10^8$) CFT073 *Escherichia coli* (American Type Culture Collection, Maryland, USA) or sterile 1X D-PBS (Thermo Fisher Scientific, Massachusetts, USA) slowly over 10 seconds into the bladder. Treatments were given either immediately following BC induction (T_0, pilot studies) or 6 hours later (T_6, main and antagonist studies) via IP injection. Urine samples were collected at the 6-hour timepoint to confirm infection. Food and water were given *ad libitum.*

2.6. Von Frey Aesthesiometry and Behavioural Assessment

Electric von Frey aesthesiometry (IITC Inc. Life Science 2390 series, Woodland Hills, California, USA) was performed to assess pain tolerance by measuring the amount of force applied (in grams) before the animal reacted (e.g., withdraw) to a noxious stimulus directed at the suprapubic region of the lower abdomen. Animals were scored prior to the experiments in order to set a baseline. The lower abdomen of the animal was shaved, and the suprapubic region

marked with a marker. Animals were then allowed to acclimatize within the procedure room for 1h prior to scoring. The animal was then placed in a plexiglass enclosure with a mesh floor (IITC Life Sciences, Woodland Hills, CA, USA) and allowed to acclimatize for 15 min (Figure 1). Following the acclimatization period baseline behaviour and von Frey measurements were taken. Animals were scored to set an individual baseline (i.e., breathing rate, posture, motor activity, eye opening). Each behavioural parameter can receive a maximum score of 10 (worst case), summing to a maximum cumulative score of 40. A minimum score of 0 implies no signs of pain. Animals in pain typically exhibit the following: increased breathing rate, fully or partially closed eyes, hunched posture and overall, less motor activity. The behavioral scoring system was adapted from Boucher et al. [(Boucher et al., 2000), Table 2]. For von Frey measurements, a rigid tip probe attached to the aesthesiometer was applied to the marked region of the abdomen, until withdrawal was noted. Five values were recorded, with 30s intervals between measurements. Following baseline measurements, bacterial cystitis induction took place, as described in section 2.4. The animals were then left to recover for twenty-four hours before the von Frey measurements and behavioural scoring were repeated using the same parameters. A timeline of von Frey measurements and behaviour assessment is shown in Figure 2.

A) **B)**

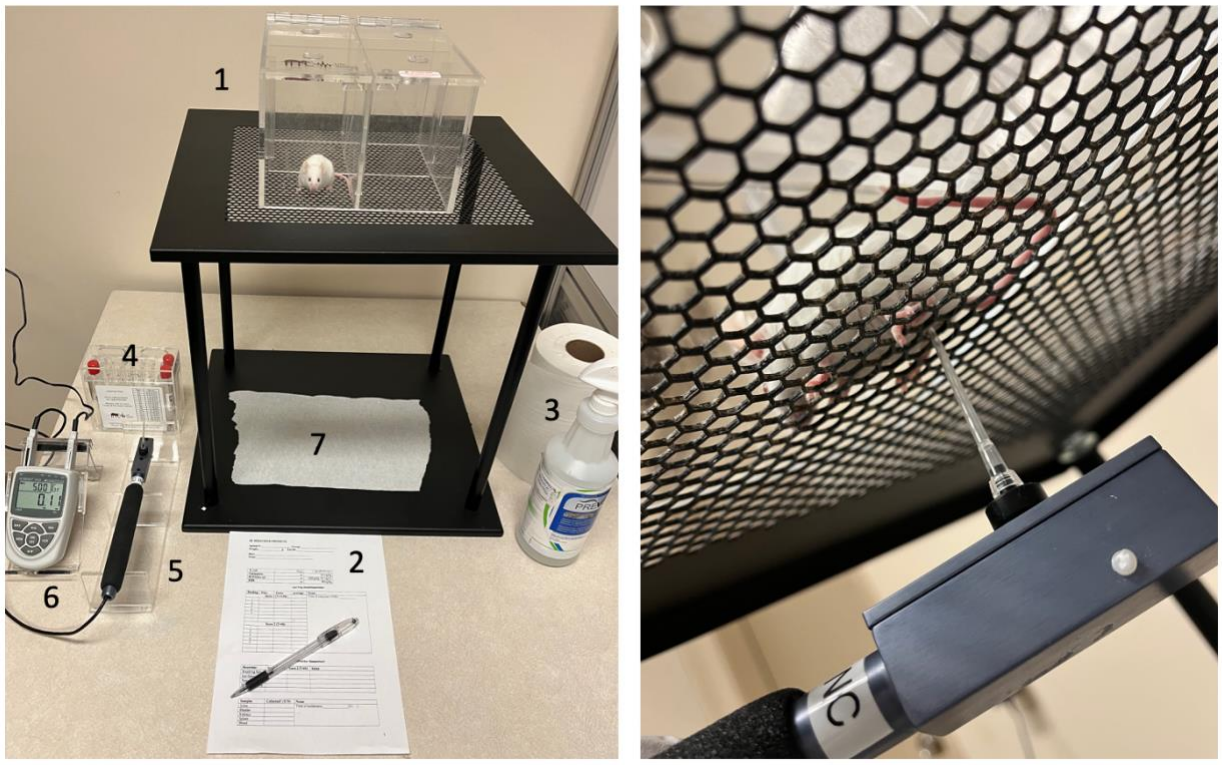

Figure 1. von Frey Aesthesiometry set up. A. 1) Plexi glass enclosure housing experimental animal 2) von Frey and behaviour scoring sheet 3) Plexi glass and stand cleaner 4) von Frey probe tips 5) Electronic von Frey force transducer 6) Electronic force readout device 7) Mesh stand with paper towel. B. von Frey measurement location on the suprapubic region of the animal.

Table 2. Parameters used in behavioural assessment system

Behavioral Parameter	Description
Eye opening/closing	Completely open eye lids receive a score of 0. Half opened eye lids receive a score of 5. Fully closed eye lids receive a score of 10. Intermediate positioning of eyelids receives a score of 2 or 7 based on the observer's assessment.
Posture	Normal posture (i.e., no back curvature, full extension of the body) receives a score of 0. Moderately hunched receives a score of 5. Fully rounded receives a score of 10. Intermediate posture receives a score of 2 or 7 based on the observer's assessment.
Motor Activity	Animals were observed for activity (e.g., exploring, grooming) over a 20 second time window. Exploring and grooming within the 20 second time window receives a score of 0. No movement for 10 seconds (50% of time window) receives a score of 5. No movement over the entire time window receives a score of 5.

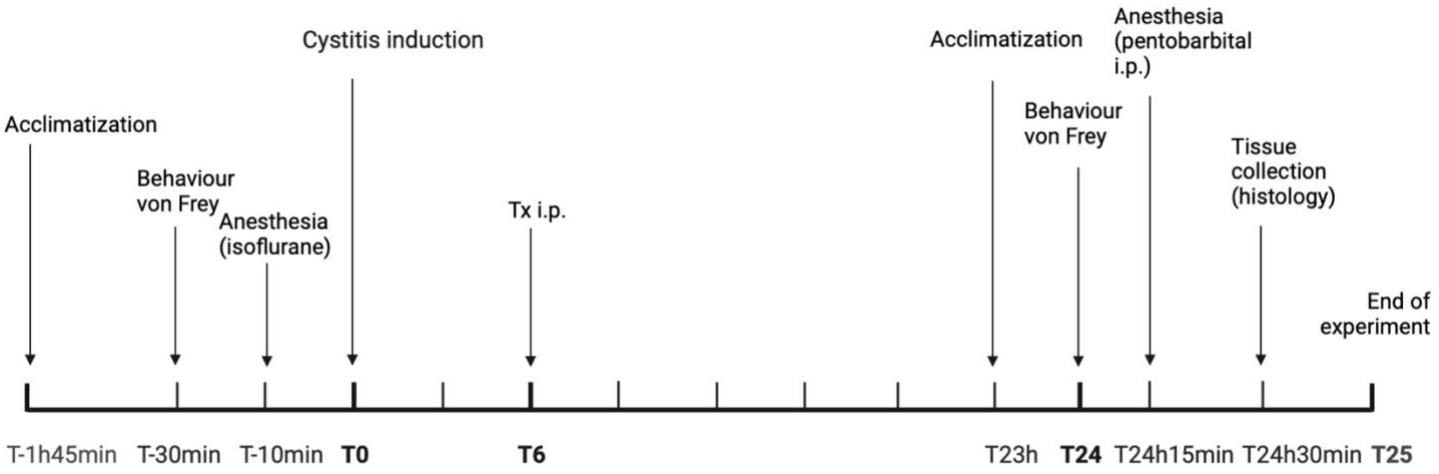

Figure 2. von Frey aesthesiometry and behavioural assessment timeline.

2.6.2. Plasma and Tissue Collection – Post von Frey Aesthesiometry and Behavioural Assessment

Under general anesthesia, the chest cavity was opened, and blood samples were collected aseptically by cardiac puncture using a 1mL syringe containing anticoagulant (0.1mL heparin). The bladder was voided by pressing gently with cotton swabs and urine was collected for assessment of bacterial burdens. Blood was put in a 1mL Eppendorf tube (Axygen Maxyclear Microtube, Acygen Inc, NY, USA) and centrifuged at 4°C for 10 minutes at 2500 rpm. The plasma was transferred to a new 1mL Eppendorf, frozen in liquid nitrogen and stored at -80°C. Cervical dislocation was performed to ensure euthanization of the animal. The bladder was surgically removed using fine tip scissors and cut on the transverse plane using a scalpel. The top section was frozen in liquid nitrogen and placed in the -80°C. The bottom half was placed in a histology cassette and submerged in 10% neutral buffered formalin (NBF) for twenty-four hours before being placed in ethanol.

2.7. Intravital Microscopy

2.7.1. Anesthesia and Surgical Preparation

Twenty-four hours after BC induction, IVM of the bladder wall was performed using an epifluorescence microscope (Leica, DM LM, Wetzlar, Germany).

Animals were anaesthetized for IVM via IP injection of sodium pentobarbital (65mg/kg; Ceva Sante Animale, Montreal, QC, Canada). Following induction of anesthesia, mice were placed on a heating pad to maintain a body temperature of 37°C. Anesthesia was maintained with repeated i.p. administration of 5 mg/kg sodium pentobarbital, while the depth of anesthesia was monitored by clinical examination (return of pedal withdrawal reflex).

Animals received fluorochrome dyes via tail vein (IV) injection fifteen minutes prior to IVM. The fluorochrome dye mixture consisted of Rhodamine 6G (1.5 mL/kg, 0.75 mg/kg body

weight, excitation wavelength 515-560nm, Sigma-Aldrich, ON, Canada) and fluorescein isothiocyanate-bovine serum albumin (FITC-BSA, 1 mL/kg, 50 mg/kg, excitation wavelength 450-490nm, Sigma-Aldrich, ON, Canada). The injection was done using a needle bevel of 39G x ½ inch 1mL syringe facing upwards parallel to the vein. Rhodamine 6G allows for visualization of leukocytes while FITC-albumin is used to study functional capillary density by illuminating capillary beds of the bladder. Fluorochrome solutions were stored in tin foil-covered receptacles to minimize photobleaching.

2.7.2. Microscopy

Once animals achieved a surgical depth of anesthesia, an abdominal midline incision using surgical scissors was made. The abdominal muscle layer was lifted using forceps, and an incision made along the linea alba to expose the bladder. The bladder was gently exteriorised, and a glass cover slip (18mm diameter) was placed on top of the bladder and the animal was placed under the microscope in a supine position on a heating pad (Figure 3). If the bladder was inflated with urine, catheterization was performed at a 45-degree angle then changed to parallel when entry is secured and a hundred microliters of sterile 1X D-PBS (Thermo Fisher Scientific, Massachusetts, USA) was slowly instilled into the bladder. During the IVM procedure, the bladder was kept moist with warm normal saline. The bladder was positioned under a 20X objective (Leica, Germany) and visualized using a 10X eyepiece (HC Plan, Leica, Germany). Leukocyte activation within the microcirculation of the bladder was visualized under a 530-550nm bandpass excitation filter allowing green light to pass and excite the Rhodamine-6G (emission wavelength 515nm). Six to eight randomly selected visual fields containing submucosal bladder venules were recorded for 30s. Capillary blood flow was then examined using FITC-albumin (emission wavelength 520nm) using a 460-490nm bandpass filter, allowing

blue light to pass. Again, six to eight randomly selected visual fields with capillaries in focus were recorded for 30s.

2.7.3. Plasma and Tissue Collection – Post IVM

Following IVM, the bladder was voided by pressing gently with cotton swabs and urine was collected for assessment of bacterial burdens. Cervical dislocation was performed to ensure euthanasia of the animal and the bladder, kidneys and spleen were surgically removed using fine tip scissors and placed in a 1mL Eppendorf tube on ice for bacterial counts. The full IVM timeline is shown in Figure 4.

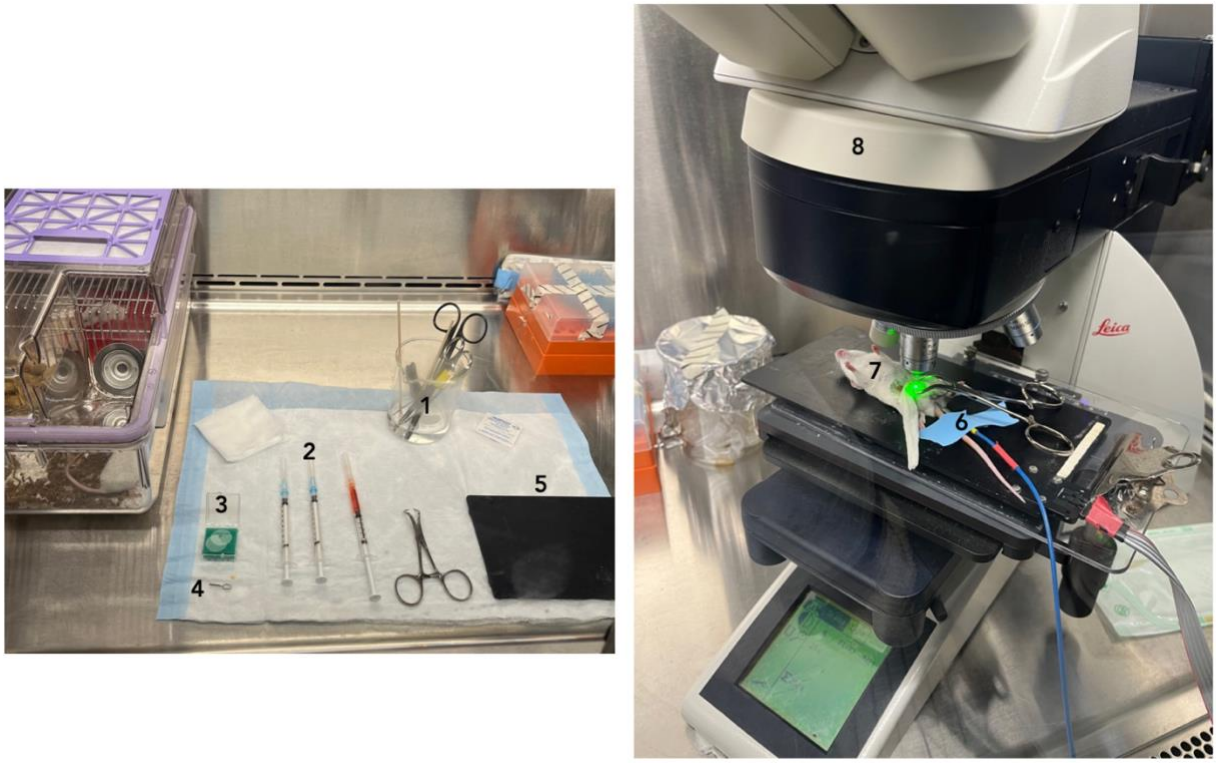

Figure 3. Intravital microscopy set up inside a biosafety cabinet. 1) Surgical tools in 70% ethanol (scissors, forceps, tweezers, cotton tipped applicators), 2) reagents (pentobarbital, fluorescents, heparin), 3) 18mm coverslips, 4) aneurysm clip, 5) Physitemp heating pad, 6) Physitemp heating pad with attached rectal temperature probe and 7) animal placed in supine position, 8) Epifluorescent Leica Microscope with Hamamatsu camera connected to Mac computer monitor.

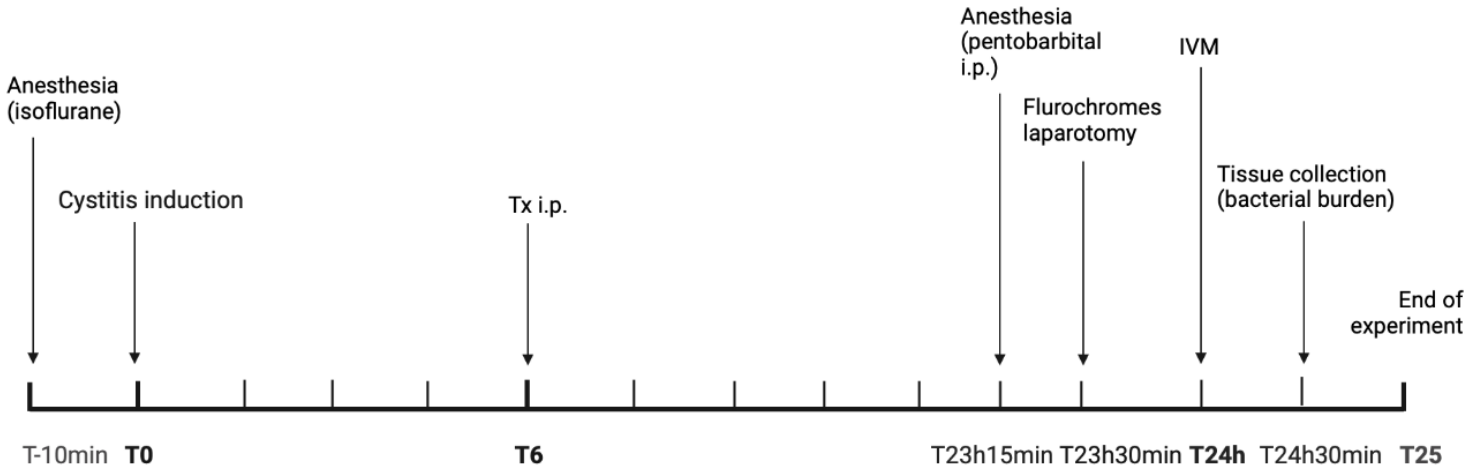

Figure 4. Intravital microscopy experimental timeline

2.7.3. Offline Video Analysis

Using Volocity software (Perkin Elmer, Waltham, MA, USA), videos were captured using a digital EM-CCD camera C9100-02 with AC-adapter A3472-07 (Hamamatsu, Herrsching, Germany). Offline IVM video analysis was performed in a blinded fashion using Image J software (Bourne & Bourne, 2010) (NIH, USA). Immobile leukocytes adhering onto the same position of the venule under the study for 30s were counted as adherent leukocytes. To quantify adhesion, an area of the venule was outlined and adherent leukocytes within that area were counted. The area and number of leukocytes counted were used to calculate the number of adherent cells in cells/mm^2. Still-frame images from leukocyte adhesion videos obtained by IVM are shown in Figure 5.

Rolling leukocytes were measured by counting the number of rolling leukocytes per minute to cross an arbitrary line perpendicular to the vessel being measured. Rolling leukocytes were defined as leukocytes travelling slower than the surrounding flow.

Capillary perfusion was quantified as the lengths of perfused capillaries with observable erythrocyte movement measured in a defined area. Functional capillary density (FCD) was calculated by summing the total length of capillaries and dividing by the selected area (cm/cm^2). Still-frame images from leukocyte adhesion videos obtained by IVM are shown in Figure 6.

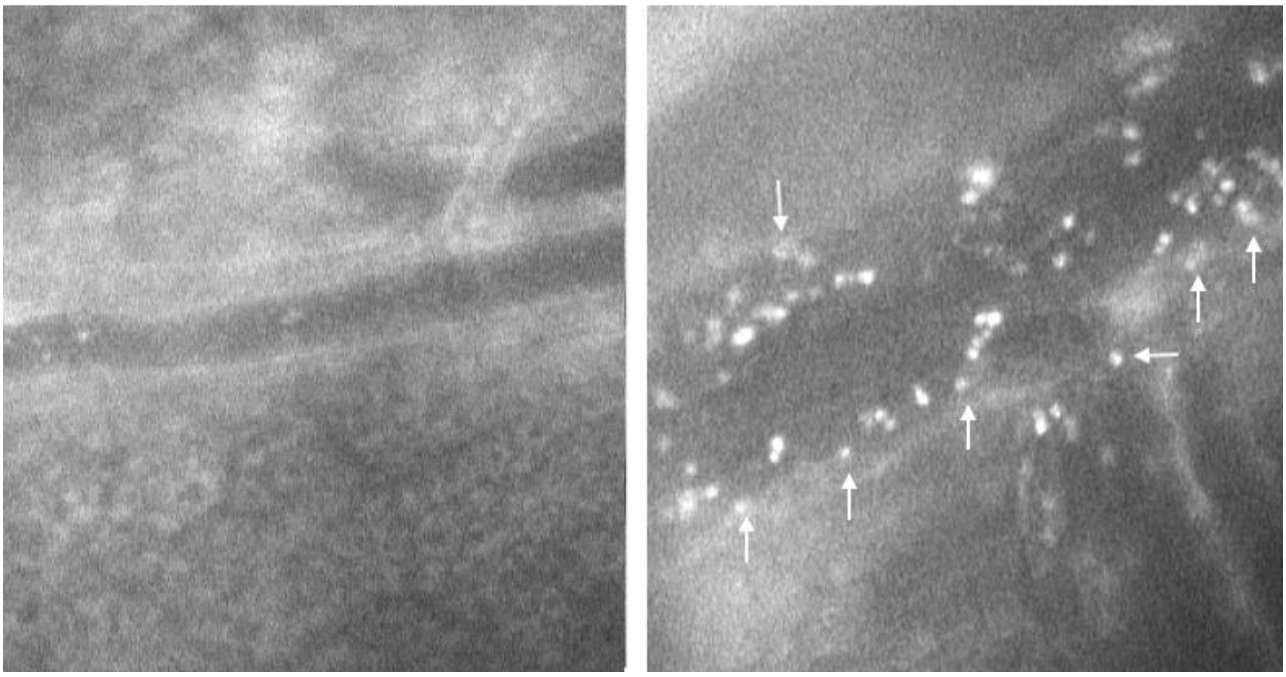

Figure 5. Still-frame image of leukocyte adhesion within the microcirculation of female BALB/c mice. Images obtained by intravital microscopy (magnification= 200x). Images taken from (A) control animal and (B) untreated BC animal are shown. Arrows indicate adherent leukocytes.

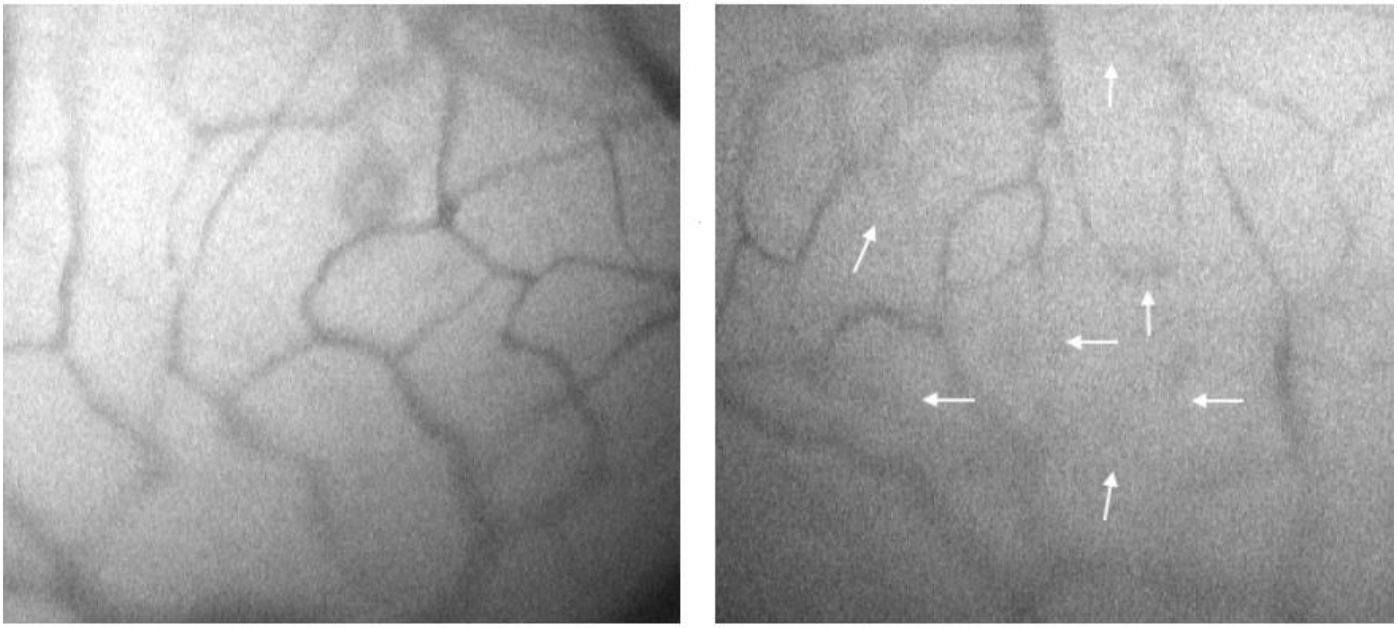

Figure 6. Still-frame image of capillary perfusion within the microcirculation of female BALB/c mice. Images obtained by intravital microscopy (magnification= 200x). Images taken from (A) control animal and (B) untreated BC animal are shown. Arrows indicate areas of irregular capillary perfusion.

2.8. Bladder Histopathology

2.8.1. Tissue Processing and Staining

Following von Frey Aesthesiometry and behaviour assessment studies, the bladder was surgically removed using fine tip scissors and cut on the transverse plane using a scalpel. The bottom half was placed in a labelled histology cassette and submerged in 10% neutral buffered formalin (NBF) for 24 hours. After 24 hours the cassettes were transferred and stored in 70% ethanol. The tissue samples were processed and embedded in paraffin by the IWK Department of Pathology and Laboratory. Paraffin-embedded tissue blocks were placed on ice for 10 minutes and then three 5µm sections were cut using a HistoCoer Multicut Semi-automated Rotary Microtome (Leica Biosystems). Sections were then placed onto a 42℃ float water bath (Lipshaw MFG Co. Detroit, MI, USA) and transferred onto glass slides (Fisherbrand Microscope Slides, Thermo Fisher Scientific, Ottawa, Ontario, Canada). Slides were then left in an 80℃ oven for 8 hours to melt excess paraffin.

Bladder samples were then stained using hematoxylin and eosin (H&E). Slides were deparaffinized in two changes of xylene followed by three changes of varying concentrations of ethanol (100%, 95% and 70%), then rehydrated using water. Nuclei were then stained using Harris hematoxylin, rinsed in tap water, differentiated using 1% Acid (HCl) alcohol, blued in Scott's tap water and counterstained with eosin. Stain quality was checked using an Optika B-290TB brightfield microscope (Optika Microscopes, Ponterica, Italy). Slides that were stained properly were then washed in 70%, 95% and 100% ethanol and dehydrated in three changes of xylene. Cover slips were then placed over the stained slides using Cytoseal-60 mounting media (Electron Microscopy Science, Fort Washington, PA, USA). Slides were left to dry in the fume

hood overnight and then scored as described in 2.7.2. A detailed hematoxylin and eosin staining procedure can be found in table 3.

Table 3. Detailed protocol for hematoxylin and eosin staining of bladder tissue. Steps involving multiple immersions used new reagents for each subsequent immersion.

Reagent	**Method**
Xylene	5-minute immersion (x2)
100% Ethanol	5-minute immersion (x2)
95% Ethanol	2-minute immersion (x2)
70% Ethanol	2-minute immersion (x2)
Running tap water	2-minute immersion
Harris Hematoxylin	3-minute immersion
Running tap water	5-minute immersion
1% Acid (HCl) Alcohol	30-second immersion
Running tap water	1-minute immersion (until clear)
Scott's tap water	1-minute immersion
Running tap water	5-minute immersion
Eosin	10 dips
70% Ethanol	10 dips (x3)
95% Ethanol	10 dips (x2)
100% Ethanol	10 dips (x3)
Xylene	5-minute immersion (x3)

2.8.2. Bladder Histopathology Scoring

Bladder samples were scored using a bladder inflammation grading scale based off of Hopkins et al., 1998 (Hopkins, Gendron-Fitzpatrick, Balish, & Uehling, 1998). The score was modified based on the suggestions made by Dr. Cheng Wang (Department of Pathology, Department of Urology, Dalhousie University, Halifax, Nova Scotia, Canada). The full scoring system used can be seen in Table 4. Bladder sections were divided into four quadrants and each quadrant received an individual score. An average of the four quadrants was then taken. Sections were analyzed using an Optika B-290TB brightfield microscope (Optika Microscopes, Ponterica, Italy) on the 40x objective lens. Histology images were captured using the Optika Vision Lite 2.1. software microscope (Optika Microscopes, Ponterica, Italy).

Table 4. Histopathological grading scale assessing bladder inflammation. Adapted from Hopkins et al. 1998.

Score	**Criteria**
0	Normal; inflammatory cells largely confined to vessels
1	Subepithelial inflammatory cell infiltration (focal)
2	Subepithelial inflammatory cell infiltration (multifocal); ± mild edema
3	Diffuse subepithelial inflammatory cell infiltration; edema; ± neutrophil necrosis
4	Score 3 criteria; Inflammatory cells extend to mucosal epithelium
5	Score 4 criteria; inflammatory cells in muscle layer
6	Score 5 criteria; loss of surface epithelium

2.9. Bacterial Burdens

Following IVM, bladder, kidney and spleen samples were collected for bacterial counts. Urine was collected from all animals. During the following steps, aseptic technique was used to maintain the integrity of all bacterial data. Bladder and kidney samples were individually placed in separate Eppendorf's containing 200µL of sterile 1X D-PBS. Bladder and kidney samples were homogenized using the Micro Tube Homogenizer System (Thomas Scientific, SP Bel-Art, Ottawa, Canada). Spleen samples were placed in a small petri dish containing 1 mL of sterile 1X D-PBS. The back end of a 3 mL syringe was used to mash the spleen and remove the capsule. Tissue samples were then centrifuged at 1000rpm for 2 minutes to pellet out the tissue. Using a 96 well plate, 20 µL of homogenized bladder sample was transferred into 180 µL of sterile 1X D-PBS to make a 1:10 dilution. The transfer was repeated from well 1 to well 2, and then each subsequent well until a 1:10000 dilution was achieved (well 4). A new tip was used between each transfer. Each dilution of bladder sample was then plated out using a triplicate spot method on Tryptic Soy Agar (TSA) plates (TSA; Millipore Sigma, Etobicoke, Ontario, Canada) supplemented with 100 µL/mL of rifampicin (Sigma Aldrich, Oakville, ON, Canada). This process was then repeated for spleen, kidney, and urine samples as well as the UPEC inoculum. Plates were then incubated at 37℃ for 16-24 hours. Following incubation, plates were enumerated to determine the number of colony-forming units (CFU) per millilitre. Calculations were based on the mean value obtained from the triplicate spots and the dilution factor using the following formula. CFU/ml = (no. of colonies x dilution factor)/ volume of culture plate.

.

2.10. *In vitro* Studies

2.10.1. Murine Bone Marrow Derived Macrophages Isolation

Animals were anaesthetized via IP injection of sodium pentobarbital (65mg/kg; Ceva Sante Animale, Montreal, QC, Canada). Once a surgical depth of anesthesia was reached animals were sacrificed by cervical dislocation. Femur and tibia bones were isolated, skinned and washed with ethanol. The top and bottom of the bones were cut using scissors and then placed in punctured 0.5mL microfuge tubes supported by 1.5 mL microfuge tubes. The bones were then centrifuged at 2000rpm for five minutes, until the inner cavity of the bones is clear, to flush the bone marrow. Bone marrow was then resuspended in Dulbecco's Modified Eagle Medium (DMEM), high glucose, pyruvate media (ThermoFisher, Grand Island, New York, USA) supplemented with 10% heat inactivated fetal bovine serum (Sigma Aldrich, Oakville, ON, Canada), 100µg/ml Penicillin-streptomycin solution (Sigma Aldrich, Oakville, ON, Canada) and 2mM HEPES (Gibco, Paisley, Scotland, UK), filtered through a 70µm Nylon cell strainer (Corning, NY, USA), and centrifuged at 1000rpm for 5 minutes at 4℃. The pellet was then resuspended in 2 ml of 1X red blood cell (RBC) lysis buffer (Invitrogen™, Burlington, Ontario, Canada) to remove contaminating red blood cells and neutralized after 1 minute using complete DMEM media. Dissociated cells, seeded at $2x10^6$ cells per well, were then transferred into a 6-well plate containing 30ng/ml murine granulocyte-macrophage colony stimulating factor (GM-CSF) (Peprotech, Rocky Hill, NJ, USA) and complete DMEM media and incubated for 7 days at 37℃, 5% CO2. On days three and six GM-CSF was added (30 ng/ml and 15 ng/ml, respectively) to induce hematopoietic cell differentiation into macrophages. Cells were checked every day and fresh media was added if the media became yellow in colour.

2.10.2. Intracellular Macrophage Infections with UPEC

Following the seven-day incubation period, matured bone marrow derived macrophages (BMDM) were harvested and seeded into 24-well plates at a density of 1 x 10^5/well. Cells were infected with UPEC by adding 10 µl of an of an OD_{600}= 0.8 bacterial suspension (~1x10^7 colony forming units (CFU)) or multiplicity of infection (MOI) of 10) in PBS. Treatment groups were as follows (1) BMDM control, (2) BMDM+UPEC, (3) BMDM+UPEC+BCP (500 µg/ml), (4) BMDM+UPEC+BCP (250 µg/ml), (5) BMDM+UPEC+BCP (100 µg/ml), (6) BMDM+UPEC+BCP (50 µg/ml), (7) BMDM+BCP (500 µg/ml) and (8) BMDM+BCP (100 µg/ml). Groups 1 and 2 received polysorbate 80 (Sigma Aldrich, Oakville, ON, Canada) in place of BCP as a vehicle control. 24-well plate was then centrifuged in a swinging bucket clinical centrifuge with microtray adaptors at 1000rpm for 5 minutes to bring bacteria in contact with the cell monolayer and then incubated for 1h at 37℃, 5% CO2.

2.10.3. Primary Bladder Epithelial Cells

Human bladder epithelial cell (BEC) line PCS-420-032 was obtained from ATCC (Cedarlane Corporation, Burlington, Ontario, Canada). Cells were grown in bladder epithelial cell basal medium supplemented with the bladder epithelial cell growth kit (ATCC, Cedarlane Corporation, Burlington, Ontario, Canada). One ml of cell suspension was added to each pre-equilibrated culture flask (Corning Incorporated, New York, USA) and seeded culture flasks were placed in the incubator 37℃, 5% CO2 for 24 hours. Once the culture had reached 80% confluence cells were passaged. Cells were detached using trypsin-EDTA solution (ATCC, Cedarlane Corporation, Burlington, Ontario, Canada). And once the majority of cells had detached an equal volume of trypsin neutralizing solution (ATCC, Cedarlane Corporation, Burlington, Ontario, Canada) was added. Dissociated cells were then transferred to a sterile

falcon and the culture flask was washed with DPBS (Thermo Fisher Scientific, Massachusetts, USA) to collect any additional cells. Cells were centrifuged at 150 x g for 5 minutes, the cell pellet re-suspended in 5 ml of fresh media, cells were seeded in a new flask at a density of 3,000 cells per cm^2 and placed in the incubator at 37℃, 5% CO2 until they were ready to passage after 6 to 7 days. Cells were used between passage 5 and 7.

2.10.4. Intracellular Bladder Epithelial Cell Infection with UPEC

BECs were seeded into 24-well plates at a density of 0.5 x 10^5/well and incubated for 24 hours at 37℃, 5% CO2 until reaching 99% confluency. Cells were infected with UPEC by adding 10µl of an of an OD_{600}= 0.8 bacterial suspension (~1x10^7 colony forming units (CFU)) or multiplicity of infection (MOI) of 10) in PBS. BCP at four doses was added 500 µg/ml, 250 µg/ml, 100 µg/ml, 50 µg/ml to BECs ± UPEC. Additionally, a vehicle control group received polysorbate 80 (Sigma Aldrich, Oakville, ON, Canada) in place of BCP ± UPEC. 24-well plate was then centrifuged in a swinging bucket clinical centrifuge with microtray adaptors at 1000rpm for 5 minutes to bring bacteria in contact with the cell monolayer and then incubated for 1h at 37℃, 5% CO2.

2.10.4. Nitric Oxide Assay

After one hour of infection, supernatant was collected from each well (either BMDMs or BECs). A nitric oxide assay kit (Lot# GR3418350-8, Abcam, Cambridge, MA, USA) was used for the measurement of extracellular nitric oxide levels. Samples were deproteinated before use by mixing 150 µl of sample with 8 µl of $ZnSO_4$ followed by 8 µl of NaOH, the mixture was then vortexed, and centrifuging for 10 minutes at 14,000 rpm. Samples were then ready to be used as the kit protocol described. In short, 100 µl of each sample was added to individual 1.5 ml Eppendorf tubes, 200 µl of Working Reagent was added and then tubes were incubated for 1

hour at 37℃. Tubes were then centrifuged at 2000rpm for 5 minutes and 250 µl of each sample was transferred to a 96 well plate. The plate was then read at an optical density of 540nm ± 20nm.

2.10.5. Phagocytosis Killing Assay

After one hour of infection, supernatant was collected from each well for the nitric oxide assay. The infected monolayer was then washed three times with 0.5 ml PBS followed by a fourth wash with PBS containing 100 µg/ml gentamicin (Sandoz, Boucherville, Quebec, Canada) to remove extracellular bacteria. Cells were then lysed using 1 ml PBS + 0.1% Triton-X (Corning, Manassas, VA, USA) Intracellular bacterial burden was then determined by plating serial dilutions on agar plates an incubating at 37℃ overnight. Following incubation, plates were enumerated to determine the number of colony-forming units (CFU) per millilitre. Calculations were based on the mean value obtained from the triplicate spots and the dilution factor using the following formula CFU/ml = (no. of colonies x dilution factor)/ volume of culture plate.

2.11. Plasma and Tissue Sample Analysis

2.11.1 Tissue Preparation and Bicinchonic Acid Protein Assay

Prior to the Luminex assay, a Bicinchonic acid (BCA) protein assay was conducted to determine the protein concentration in the bladder samples. Bladder samples were taken from the -80℃ freezer and placed on ice. Samples were placed in 2 ml polypropylene screw cap tubes pre-filled with 2.4 mm metal beads (Fisher Scientific, Pittsburgh, PA, USA) and 100 µL of Tissue Protein Extraction Regent (T-PER, Thermo Fisher Scientific) containing protease inhibitor (PI, 10ml T-Per:1 PI tablet, Thermo Fisher Scientific) was added to each sample. Samples were then homogenized for 90 seconds using the PowerLyzer 24 bead mill Homogenizer (Qiagen Sciences, MA, USA). Following homogenization, samples were spun in a refrigerated centrifuge set to

4℃ at 5000g for 15 minutes. The supernatant was transferred to a 1.5 ml Eppendorf tube and diluted 50-fold in double deionized water (10 µl sample, 490 µL double deionized water). The BCA was performed according to the manufacturer's protocol for a 96 well plate (Rapid Gold BCA, Protein Assay, Thermo Fisher Scientific). The protein concentration in the samples was then calculated using the equation provided from the standard curve on Microsoft Excel. Samples were aliquoted, placed in a -20℃ freezer for 4 hours and then transferred and stored in a -80℃ freezer.

2.11.2. Bladder tissue cytokine and adhesion molecules measurements

A custom designed mouse cytokine 10-plex kit (Lot # l144219, R&D Systems, Minneapolis, MN, USA) was used to determine the concentration of the following cytokines, chemokines, and adhesion molecules. In the bladder tissue homogenates: intercellular adhesion molecule 1 (ICAM-1), interleukin 1 (IL-1), interleukin 10 (IL-10), interleukin 6 (IL-6), chemokine CXC ligand 1 (CXCL1), chemokine CXC ligand 2 (CXCL2) P-selectin, interferon-gamma (IFN-γ), LIX recombinant mouse CXC motif chemokine 5 (LIX), and tumour necrosis factor alpha (TNF-α). Briefly, all samples aliquoted following BCA protein assay were thawed and prepared according to the manufacturer's instructions. Samples were run in duplicates and diluted three-folds using the Bio-Plex® sample diluent (50 µl sample mixed with 100 µl if diluent. Fifty microliters of diluted sample or standard was added to each well of a flat-bottom 96 well plate. Then 50 µl of diluted microparticle cocktail was added to each well and the incubated for 2 hours at room temperature, in the dark on a horizontal orbital microplate shaker (0.12" orbit, 800rpm. The plate was then washed 3 times to remove unbound beads using a Bio-Plex Pro magnetic wash station (Bio-Rad) Next, 50 µl of diluted Biotin-Antibody Cocktail was added to each well and the plate was incubated for 1 hour at room temperature, in the dark on a

horizontal orbital microplate shaker on the same settings. The plate was then washed again for three cycles using the magnetic wash station. Lastly, 50 µl of diluted Streptavidin-PE was added to each well and the plate was incubated for 30 minutes at room temperature, in the dark on a horizontal orbital microplate shaker on the same settings. A final cycle of 3 washes was performed and the beads were then resuspended in 100 µl of supplied R&D wash buffer in each well. The plate was incubated for 2 minutes before being read using a Bio-Plex 200 Analyzer and Bio-Plex Manager software (Bio-Rad Mississauga, ON, Canada) calibrated according to the manufacture's protocol. Analysis was performed in Dr. Jean Marshall's lab (Department of Microbiology and Immunology, Dalhousie University).

2.12. Statistical Analysis

Data are expressed as mean ± standard deviation (SD). Statistical analyses were conducted using GraphPad Prism 6.0 (GraphPad Software Inc., La Jolla, CA, USA). Data was evaluated for normality using the Kolmogorov-Smirnoff test. Outliers were removed using the ROUT method or Tukey's method for parametric and non-parametric data, respectively. Parametric data was then assessed by one-way ANOVA with Tukey's multiple comparison test. Non-parametric data was assessed using the Kruskal-Wallis test with Dunn's multiple comparison test. Differences of $p<0.05$ were considered statistically significant.

Chapter 3: Results

3.1. Pilot Bacterial Studies

3.1.1. Urine

Urine was collected from animals twenty-four hours after intravesical administration of UPEC. No bacteria were found in the urine of sham animals. Intravesical administration of UPEC significantly ($p<0.05$) increased bacterial burden in the urine of BC animals when compared to sham control. Treatment with BCP (100 mg/kg) was able to significantly ($p<0.05$) reduce bacterial growth compared to the untreated BC group (Figure 7).

3.1.2. Bladder

Bladder samples were collected from animals twenty-four hours after intravesical administration of UPEC. No bacteria were found in the bladder samples of sham animals. Intravesical administration of UPEC significantly ($p<0.05$) increased bacterial burden within the bladder of BC animals when compared to the sham control group. Treatment with BCP (100 mg/kg) was able to significantly ($p<0.05$) reduce bacterial growth compared to the untreated BC group (Figure 8).

3.1.3. Left and Right Kidneys

Left and right kidneys were collected from animals twenty-four hours after intravesical administration of UPEC to evaluate the development of pyelonephritis. After twenty-four hours, no animals developed pyelonephritis within the left or right kidney (Figure 9). No significant difference ($p>0.05$) was detected between any groups.

3.1.4. Spleen

In order to detect the systemic spread of infection, spleen tissue was evaluated for bacterial burden twenty-four hours after intravesical administration of UPEC. After twenty-four

hours, no bacteria were detected in spleen tissue from any animals (Figure 10). No significant difference ($p>0.05$) was detected between any groups.

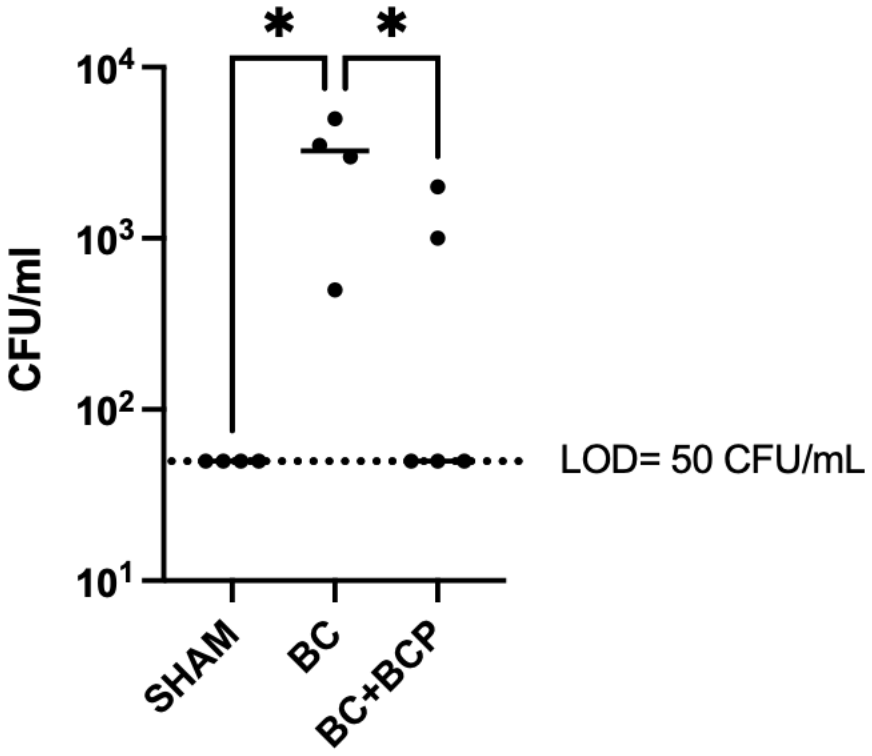

Figure 7. The effects of BCP treatment on bacterial growth in the urine of BALB/c mice 24 hours after instillation of UPEC or PBS (SHAM). The following groups are included: sham animals (sham; n=4), untreated BC (BC; n=4), BCP treated BC (BCP, 100 mg/kg, n=5). Bacterial burdens are expressed as CFU/ml (LOD: limit of detection). Individual data points and group means are shown. * $p < 0.05$.

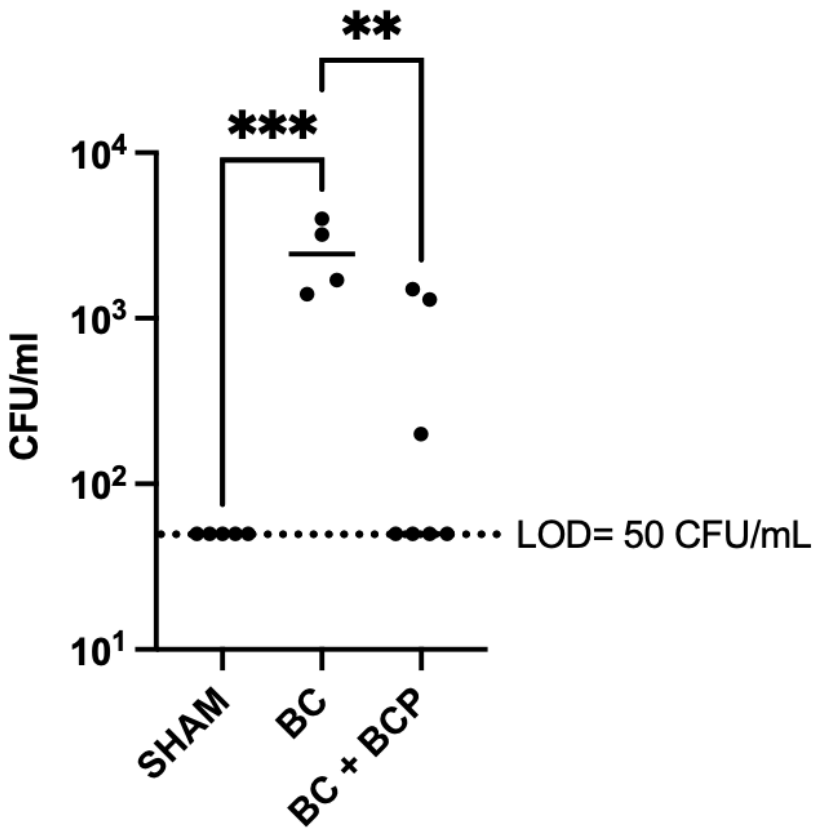

Figure 8. The effects of BCP treatment on bacterial growth in homogenized bladder tissue of BALB/c mice 24 hours after instillation of UPEC or PBS (SHAM). The following groups are included: sham animals (sham; n=5), untreated BC (BC; n=4), BCP treated BC (BCP, 100 mg/kg, n=7). Bacterial burdens are expressed as CFU/ml (LOD: limit of detection. Individual data points and group means are shown. * $p < 0.05$.

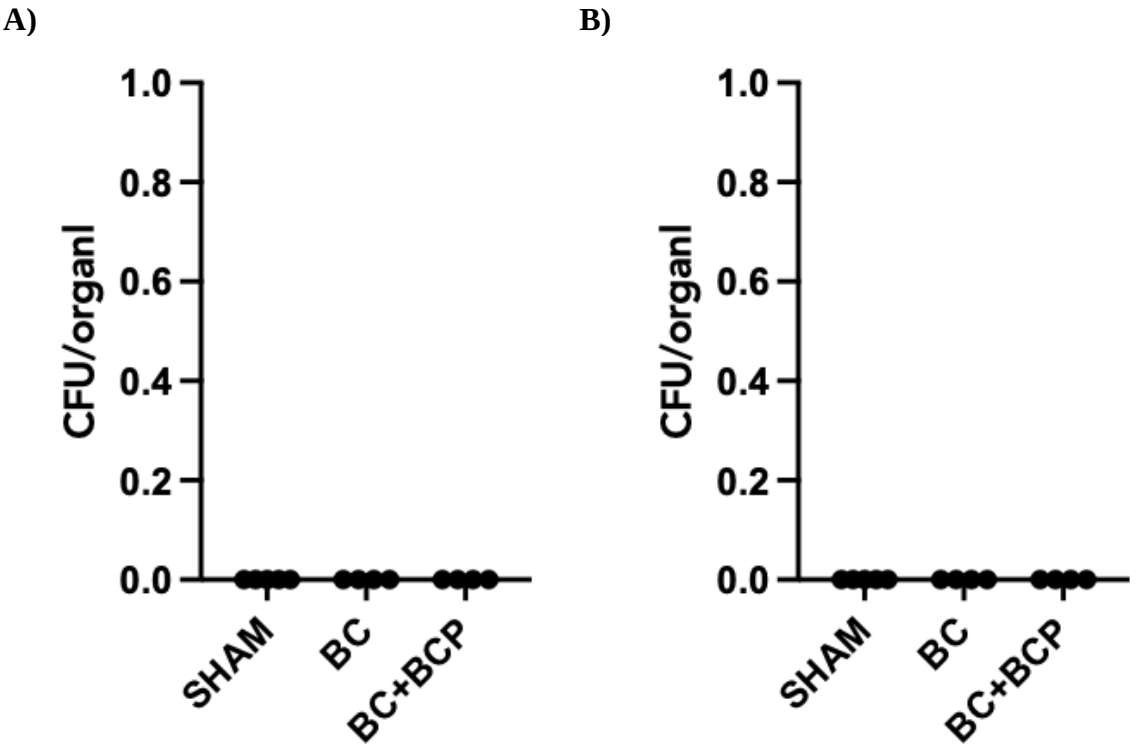

Figure 9. Bacterial burden within the left (A) and right (B) kidneys of BALB/c mice 24 hours after instillation of UPEC or PBS (SHAM). The following groups are included: sham (sham; n=5), untreated BC (BC; n=4) and BCP treated BC (BCP; n=4). Bacterial burdens are expressed as CFU/organ. Individual data points are shown.

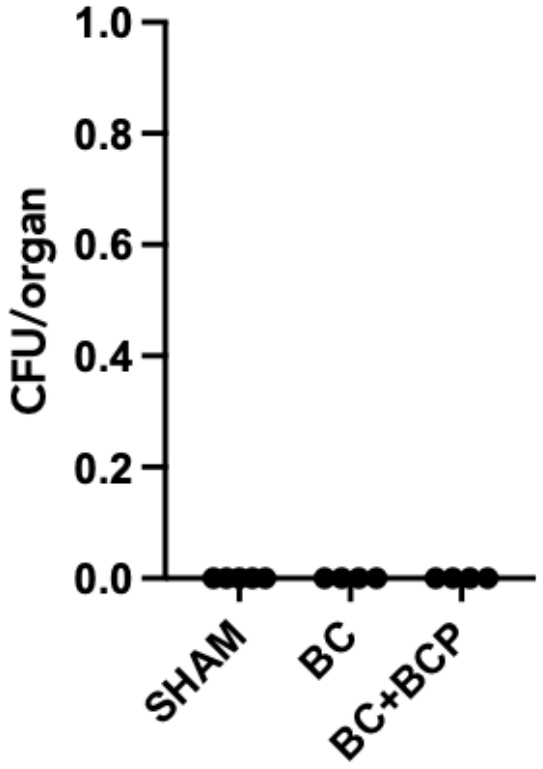

Figure 10. Bacterial burden within the spleen of BALB/c mice 24 hours after instillation of UPEC or PBS (SHAM). The following groups are included: sham (sham; n=5), untreated BC (BC; n=4) and BCP treated BC (BCP; n=4). Bacterial burdens are expressed as CFU/organ. Individual data points are shown.

3.2. Main Studies

3.2.1. Bacterial Burdens

3.2.1.1. Urine

Urine was collected from animals twenty-four hours after intravesical administration of UPEC. No bacteria were found in the urine of sham animals. Intravesical administration of UPEC significantly ($p<0.05$) increased bacterial burden in the urine of BC animals when compared to sham control. Treatment with BCP (100 mg/kg) was able to significantly ($p<0.05$) reduce bacterial growth compared to the untreated BC group. Similarly, treatment with Fosfomycin (10 mg/kg) alone and in combination with BCP (100 mg/kg) significantly ($p<0.05$) decreased bacterial growth compared to untreated BC animals (Figure 11).

3.2.1.2. Bladder

Bladder samples were collected from animals twenty-four hours after intravesical administration of UPEC. No bacteria were found in the bladder samples of sham animals. Intravesical administration of UPEC significantly ($p<0.05$) increased bacterial burden within the bladder of BC animals when compared to the sham control group. Treatment with BCP (100 mg/kg) was able to significantly ($p<0.05$) reduce bacterial growth compared to the untreated BC group. Similarly, treatment with Fosfomycin (10 mg/kg) alone and in combination with BCP (100 mg/kg) significantly ($p<0.05$) decreased bacterial growth in the bladder compared to untreated BC animals (Figure 12).

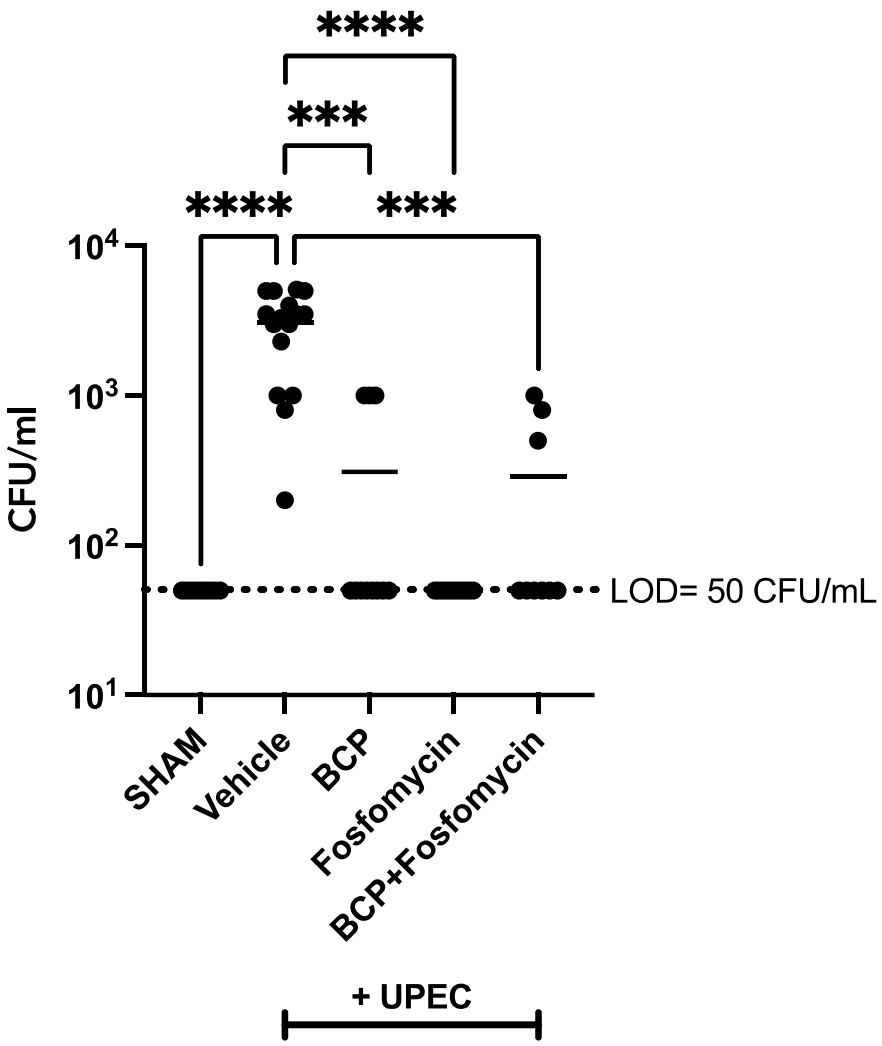

Figure 11. The effects of BCP and/or Fosfomycin treatment on bacterial growth in the urine of BALB/c mice 24 hours after instillation of UPEC or PBS (SHAM). The following groups are included: sham animals (sham; n=9), untreated BC (Vehicle; n=16), BCP treated BC (BCP, 100 mg/kg, n=12), Fosfomycin treated BC (Fosfomycin, 10 mg/kg, n=10) and combination BCP + Fosfomycin treated BC (BCP + Fosfomycin, n=10). Bacterial burdens are expressed as CFU/ml, LOD (Limit of Detection). Individual data points and group means are shown. * $p < 0.05$.

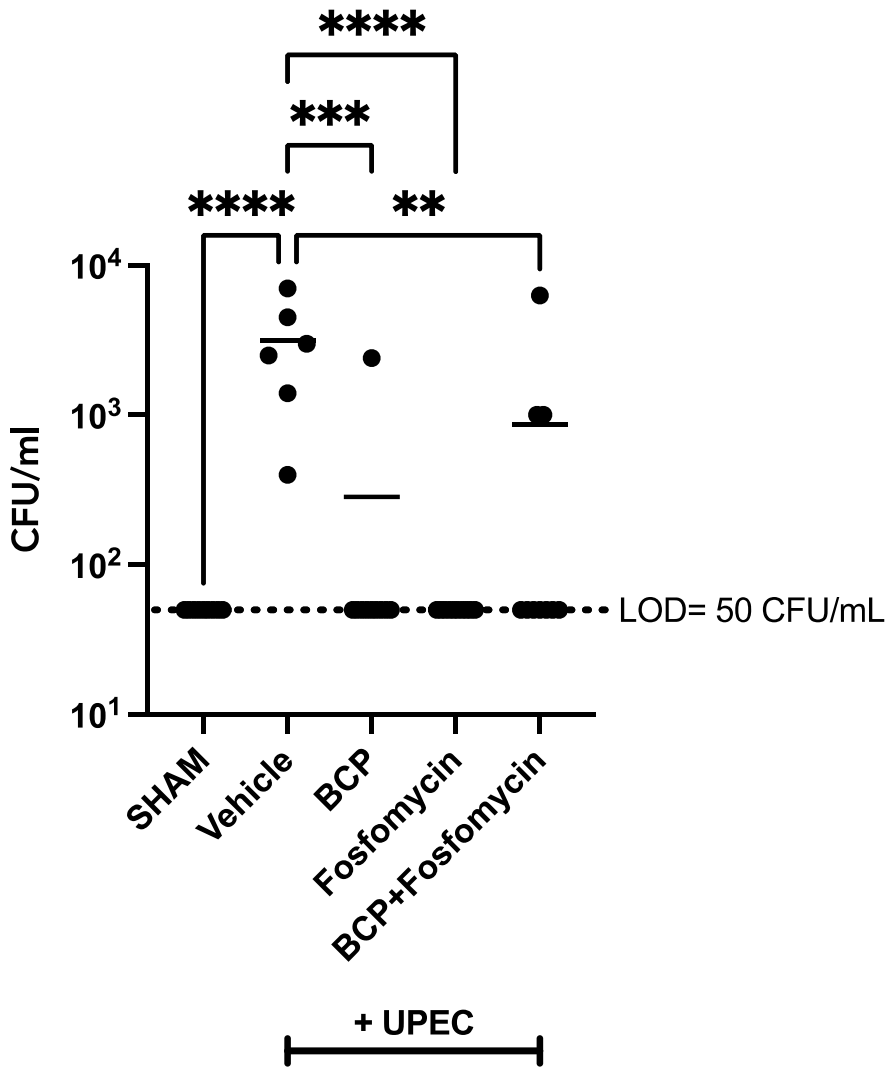

Figure 12. The effects of BCP and/or Fosfomycin treatment on bacterial growth in the bladder of BALB/c mice 24 hours after instillation of UPEC or PBS (SHAM). The following groups are included: sham animals (sham; n=9), untreated BC (Vehicle; n=6), BCP treated BC (BCP, 100 mg/kg, n=10), Fosfomycin treated BC (Fosfomycin, 10 mg/kg, n=10) and combination BCP + Fosfomycin treated BC (BCP + Fosfomycin, n=10). Bacterial burdens are expressed as CFU/ml, LOD (Limit of Detection). Individual data points and group means are shown. * $p < 0.05$.

3.2.2 IVM

3.2.2.1 Leukocyte Adhesion

Leukocyte adhesion was measured using intravital microscopy of the submucosal venules in the bladder twenty-four hours after intravesical administration of UPEC. The sham group showed low levels of leukocyte adhesion. BC significantly ($p<0.05$) increased the number of adherent leukocytes compared to the sham group. BCP (100 mg/kg) treatment significantly ($p<0.05$) decreased leukocyte adhesion when compared to animals in the BC group. The same effect was observed in animals who received Fosfomycin (10 mg/kg) treatment, which significantly ($p<0.05$) decreased leukocyte adhesion relative to BC animals. Combination treatment with BCP (100 mg/kg) and Fosfomycin (10 mg/kg) did not significantly ($p > 0.05$ reduce leukocyte adhesion when compared to animals in the BC group (Figure 13).

3.2.2.2 Leukocyte Rolling

Leukocyte slow rolling was measured using IVM of the submucosal venules in the bladder twenty-four hours after intravesical administration of UPEC. The sham group showed low levels of leukocyte rolling. BC significantly ($p<0.05$) increased the number of rolling leukocytes compared to the sham group. Leukocyte rolling was not significantly reduced ($p>0.05$) when treated with 100 mg/kg BCP, 10 mg/kg Fosfomycin or a combination of 100 mg/kg BCP + 10 mg/kg Fosfomycin (Figure 14).

3.2.2.3. Capillary Perfusion

Functional capillary density of the bladder microcirculation, a measure of microvascular perfusion, was significantly ($p<0.05$) reduced with intravesical administration of UPEC. Subsequent treatment with 100 mg/kg BCP restored FCD levels back to those of sham animals and was significantly ($p<0.05$) higher than that observed in the BC group (Figure 15). The same

effect was observed in animals who received Fosfomycin (10 mg/kg) treatment, which significantly ($p<0.05$) increased FCD levels relative to BC animals. Combination treatment with BCP (100 mg/kg) and Fosfomycin (10 mg/kg) significantly ($p<0.05$) increased FCD levels when compared to animals in the BC group (Figure 15).

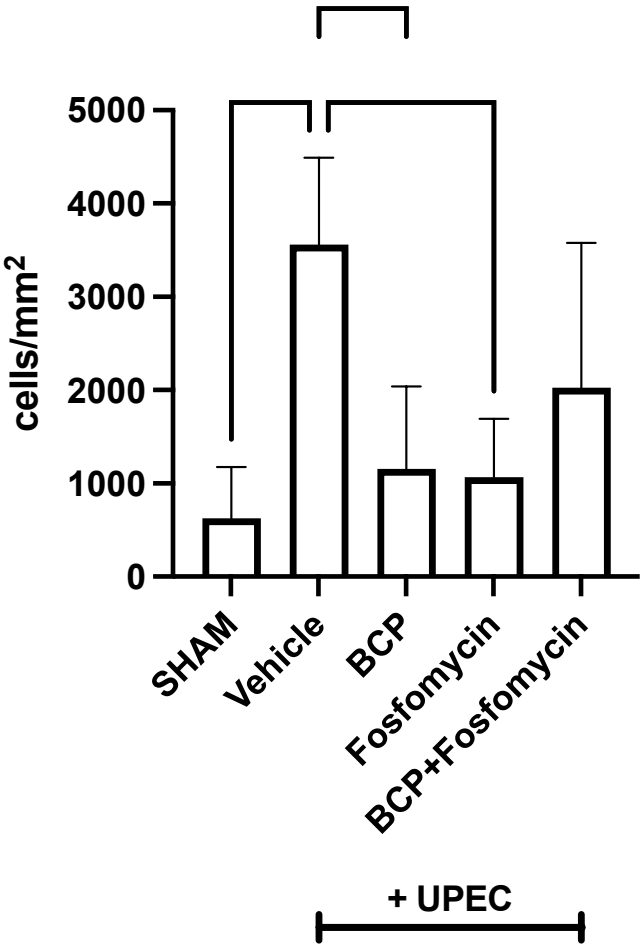

Figure 13. Leukocyte adhesion in the submucosal bladder venules of female BALB/c mice (cells/mm^2). The following groups are included: sham animals (SHAM; n=7), untreated BC (Vehicle; n=6), BCP treated BC (BCP, 100 mg/kg, n=5), Fosfomycin treated BC (10 mg/kg, n=5) and combination BCP + Fosfomycin treated BC (BCP + Fosfomycin, n=5). Leukocyte adhesion was evaluated 24 hours following intravesical administration of UPEC or PBS (SHAM). Data presented as mean± SD. * $p < 0.05$.

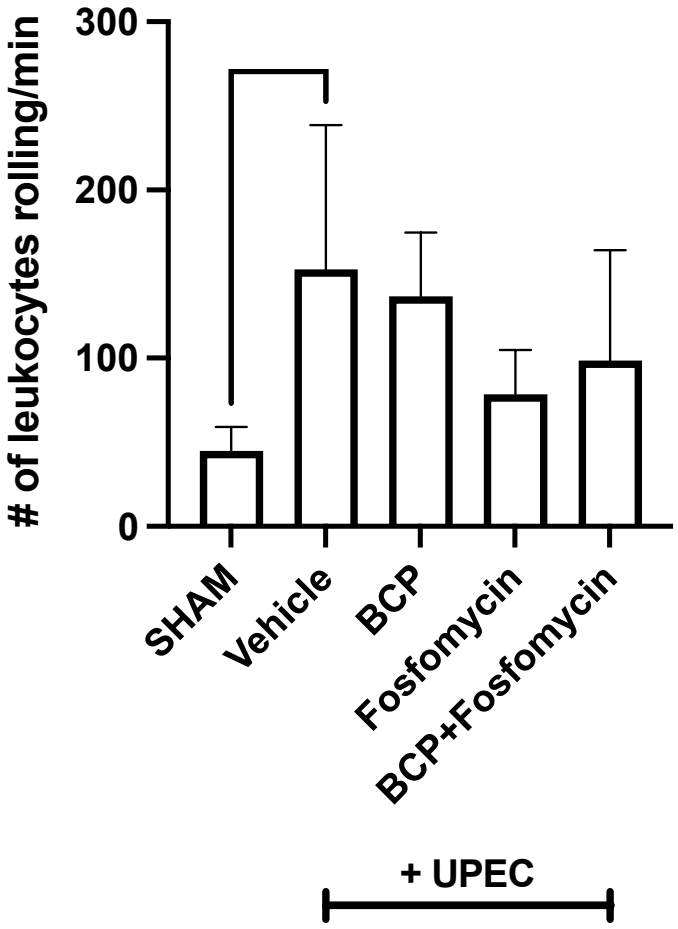

Figure 14. Leukocyte rolling in the submucosal bladder venules of female BALB/c mice (number of leukocytes rolling/min). The following groups are included: sham animals (SHAM; n=7), untreated BC (Vehicle; n=6), BCP treated BC (BCP, 100 mg/kg, n=5), Fosfomycin treated BC (10 mg/kg, n=5) and combination BCP + Fosfomycin treated BC (BCP + Fosfomycin, n=5). Leukocyte rolling was evaluated 24 hours following intravesical administration of UPEC or PBS (SHAM). Data presented as mean± SD. * $p < 0.05$.

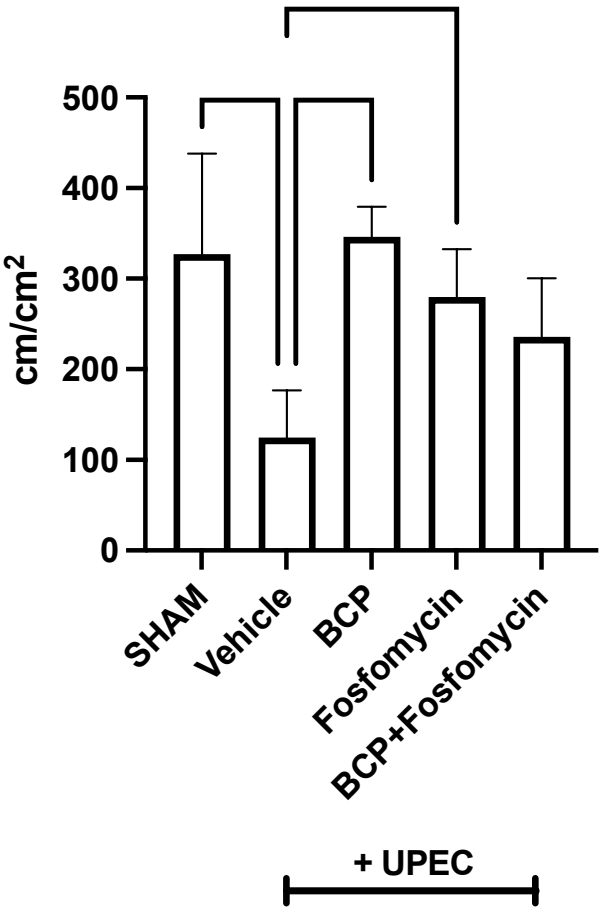

Figure 15. Capillary perfusion of the bladder microcirculation in of female BALB/c mice (cm/cm^2) The following groups are included: sham animals (SHAM; n=7), untreated BC (Vehicle; n=6), BCP treated BC (BCP, 100mg/kg, n=5), Fosfomycin treated BC (Fosfomycin, 10mg/kg, n=5) and combination BCP + Fosfomycin treated BC (BCP + Fosfomycin, n=5). FCD was evaluated 24 hours following intravesical administration of UPEC or PBS (SHAM). Data presented as mean± SD. * $p < 0.05$.

3.2.3. Pain and Behaviour

3.2.3.1. von Frey Aesthesiometry

Von Frey Aesthesiometry was performed to analyze changes in pain threshold by measuring the amount of force, in grams, tolerated when applied to the animal's pelvic region before withdrawal. Measurement was performed in all animals prior to intravesical UPEC instillation (T_0) to set an individual baseline measurement and again 24 hours after UPEC instillation. UPEC instillation resulted in a significant ($p<0.05$) decrease in withdrawal threshold when compared to sham animals. Treatment with 100 mg/kg BCP significantly ($p<0.05$) restored levels of withdrawal threshold back to those of sham animals. Furthermore, combination therapy with 100 mg/kg BCP and 10 mg/kg Fosfomycin was able to significantly improve withdrawal threshold when compared to untreated BC animals (Figure 16).

3.2.3.2. Behaviour

Changes in non-evoked behavioral responses were assessed as an alternative way to study pain in mice with BC. The scores for three behavioural parameters were summed to generate a cumulative behavioural score. Behavioural parameters were assessed in all animals prior to intravesical UPEC instillation (T_0) to set an individual baseline measurement and again 24 hours after UPEC instillation. Sham animals showed a minimal, non-significant increase in the total cumulative score. UPEC instillation significantly ($p<0.05$) increased cumulative scores compared to sham animals (Figure 16). Treatment with 100 mg/kg BCP significantly ($p<0.05$) improved this parameter, restoring behaviour to baseline. The same effect was observed in animals who received combination treatment of Fosfomycin (10 mg/kg) and BCP (100 mg/kg) which significantly ($p<0.05$) improved cumulative behavioural scores compared to BC animals (Figure 17).

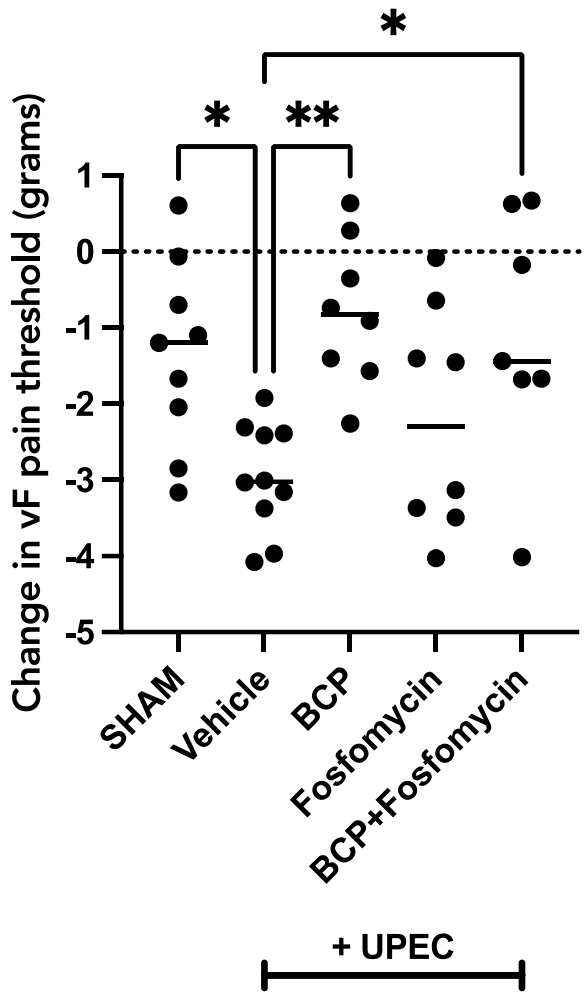

Figure 16. Change in withdrawal threshold (g) in female BALB/c mice. The following groups are included: sham animals (SHAM; n=9), untreated BC (Vehicle; n=10), BCP treated BC (BCP, 100 mg/kg, n=8), Fosfomycin treated BC (Fosfomycin, 10 mg/kg, n=8) and combination BCP + Fosfomycin treated BC (BCP + Fosfomycin, n=7). Withdrawal threshold was evaluated before induction (T_0) and 24 hours after intravesical administration of UPEC or PBS (SHAM, T_{24}). Individual data points and group means are shown. * $p < 0.05$.

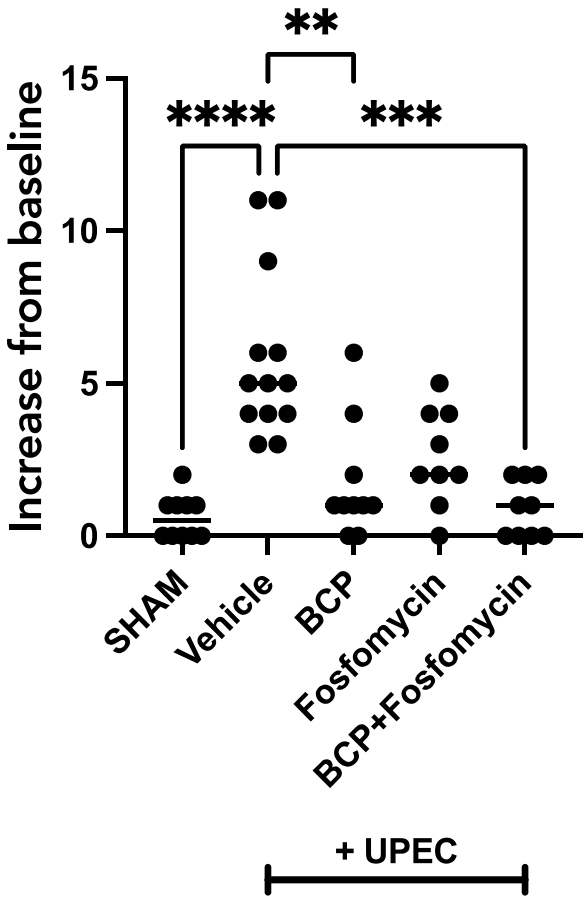

Figure 17. The increase in cumulative behavioural scores of female BALB/c mice. The following groups are included: sham animals (SHAM; n=10), untreated BC (Vehicle; n=13), BCP treated BC (BCP, 100mg/kg, n=10), Fosfomycin treated BC (Fosfomycin, 10mg/kg, n=9) and combination BCP + Fosfomycin treated BC (BCP + Fosfomycin, n=9). Behavioural parameters were evaluated before induction (T_0) and 24 hours after intravesical administration of UPEC or PBS (SHAM, T_{24}). Individual data points and group means are shown. * $p < 0.05$.

3.2.4. Histology

Intravesical administration of UPEC did not produce any significant morphological changes on bladder tissue (Figure 18) based on our inflammatory scoring system (Figure 19).

3.2.5. Cytokines

A custom designed mouse cytokine 10-plex kit was used to analyze the following cytokines, chemokines, and adhesion molecules: ICAM-1, IL-1, IL-10, IL-6, CXCL1, CXCL2, P-selectin, IFN-γ, LIX and TNF-α. Most cytokines were present in very low or undetectable levels (data not shown).

Intravesical administration of UPEC had no significant effect on the levels of the adhesion molecules, ICAM-1 and P-selectin (Figure 20).

Intravesical administration of UPEC had no significant effect on LIX levels. However, a two-tailed T-test between the sham and BC group was significant ($p<0.05$). No significant change in LIX levels was seen in any treatment groups. However, concentrations seen with BCP treatments, alone and combination, appear to be trending downwards, although not significant from the BC group ($p>0.05$) (Figure 21).

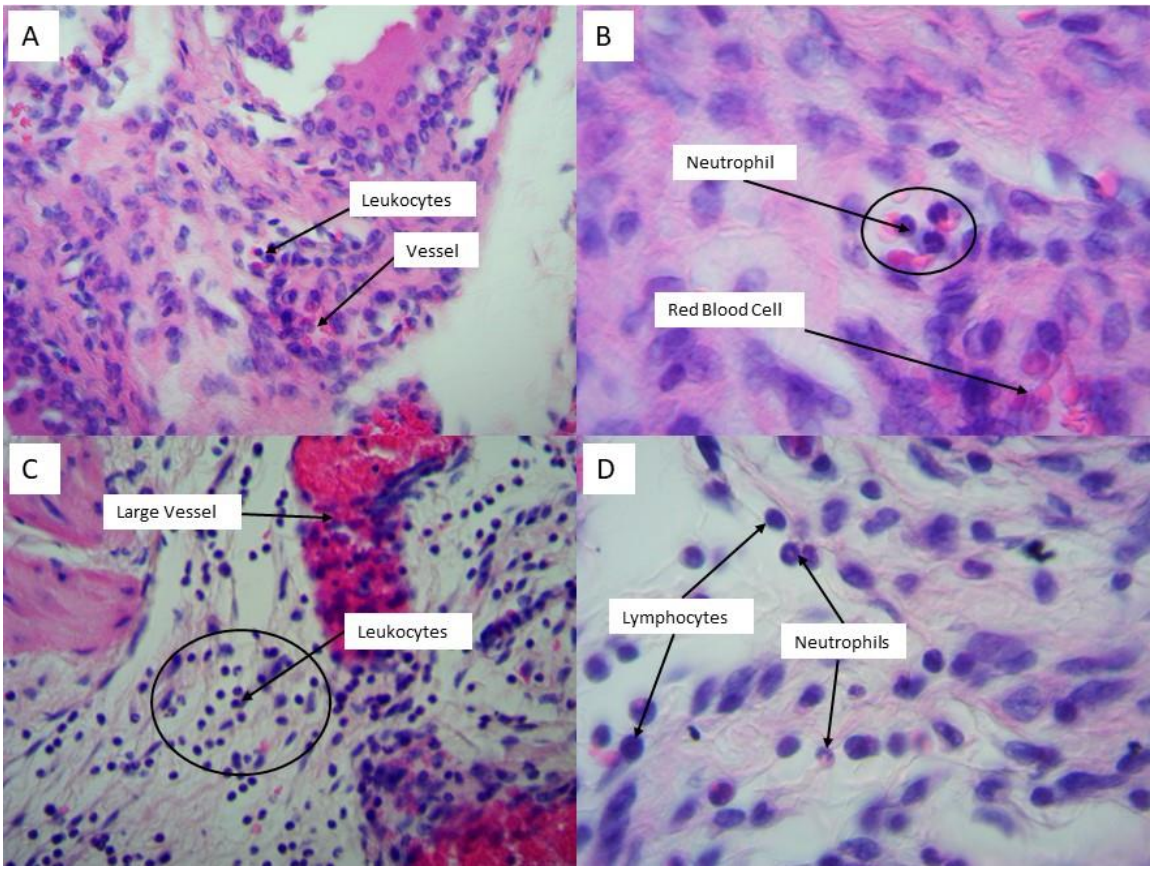

Figure 18. Representative histology images showing features of inflammation. Panel A/B shows a representative score of 0 taken from a SHAM animal. Panel A shows blood vessel confined immune cells (400x). Panel B shows the presence of neutrophils confined to a blood vessel (score = 0) under 1000x. Panels C/D is a bladder sample from a UPEC infected mouse. Panel C shows focal collections of immune cells further away from the blood vessels. Panel D shows focal collections of lymphocytes and neutrophils (score = 0.75).

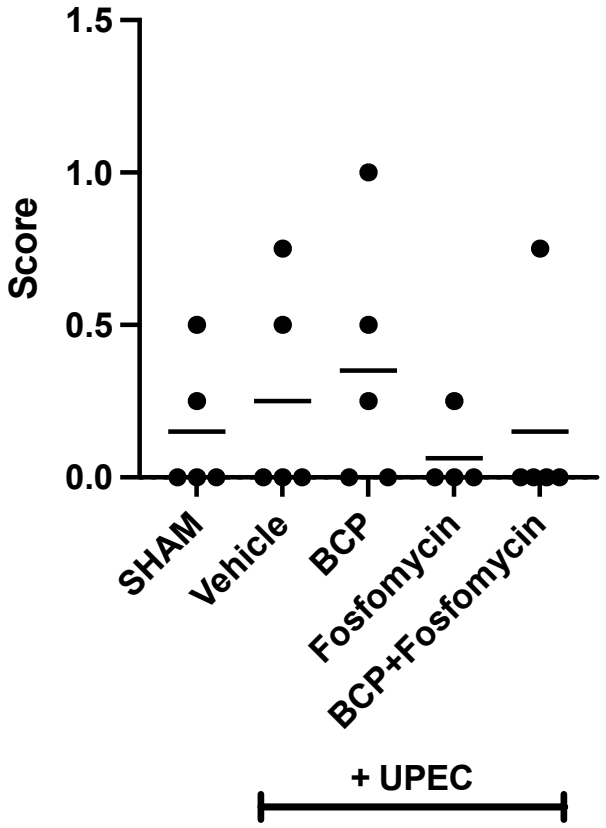

Figure 19. Bladder histopathology scores of female BALB/c mice hours after intravesical administration of UPEC or PBS (SHAM, T_{24}). Representative scores from the following groups: sham animals (SHAM; n=5), untreated BC (Vehicle; n=5), BCP treated BC (BCP, 100 mg/kg, n=4), Fosfomycin treated BC (Fosfomycin, 10 mg/kg, n=4) and combination BCP + Fosfomycin treated BC (BCP + Fosfomycin, n=5). Individual data points and group means are shown.

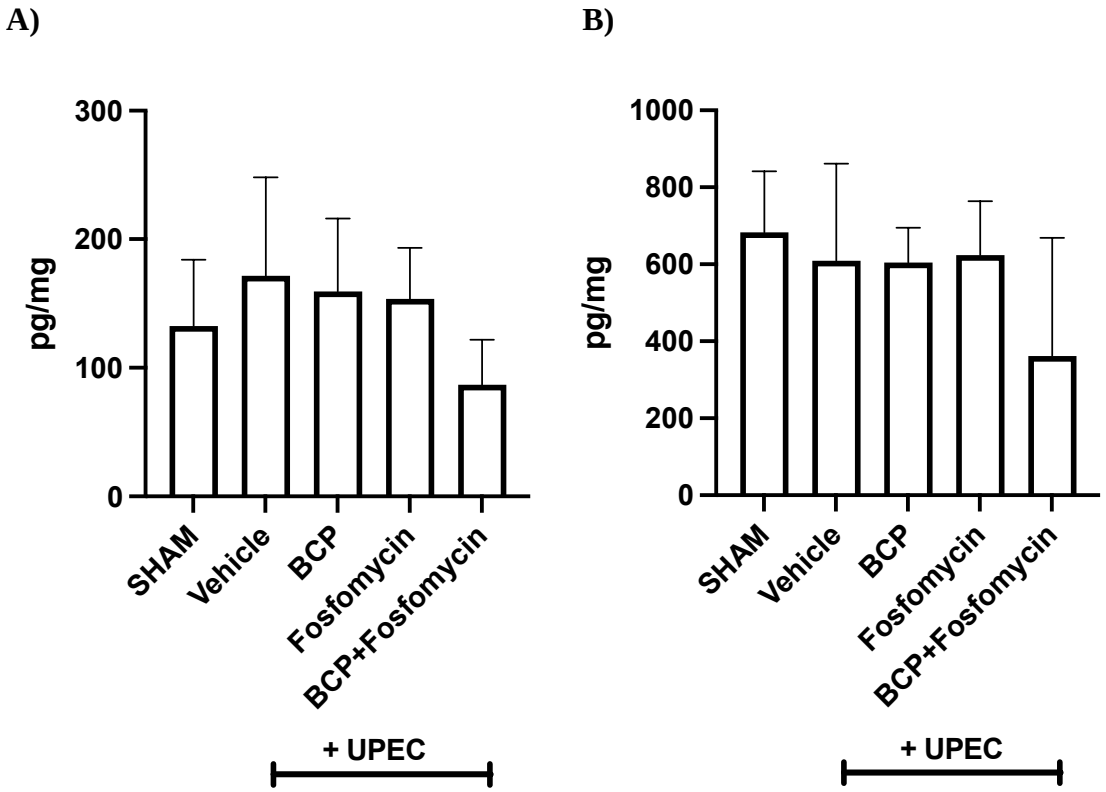

Figure 20. Concentrations of P-selectin (A), and ICAM-1 (B) in bladder tissue of female BALB/c mice 24 hours after intravesical administration of UPEC or PBS (SHAM). The following groups are included: sham animals (SHAM; n=4), untreated BC (Vehicle; n=6), BCP treated BC (BCP, 100 mg/kg, n=6), Fosfomycin treated BC (Fosfomycin, 10 mg/kg, n=6) and combination BCP + Fosfomycin treated BC (BCP + Fosfomycin, n=6). Two technical replicates were performed for each sample. Data presented as means ± SD.

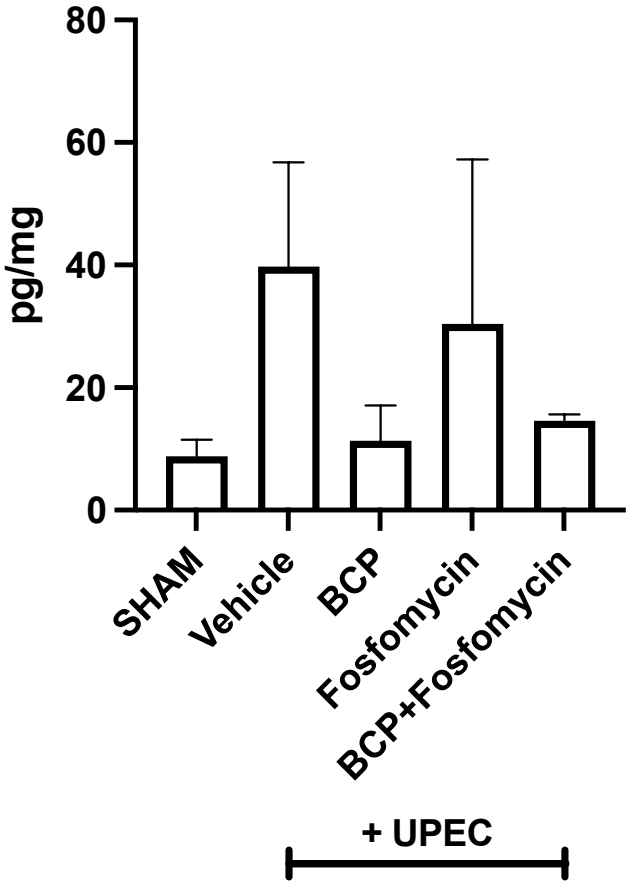

Figure 21. Concentrations of LIX in bladder tissue of female BALB/c mice 24 hours after intravesical administration of UPEC or PBS (SHAM). The following groups are included: sham animals (SHAM; n=3), untreated BC (Vehicle; n=3), BCP treated BC (BCP, 100 mg/kg, n=4), Fosfomycin treated BC (Fosfomycin, 10 mg/kg, n=4) and combination BCP + Fosfomycin treated BC (BCP + Fosfomycin, n=3). Two technical replicates were performed for each sample. Data presented as means ± SD.

3.3. Antagonist Studies

3.3.1 IVM

3.3.1.1. Leukocyte Adhesion

Leukocyte adhesion was measured using IVM of the submucosal venules in the bladder twenty-four hours after intravesical administration of UPEC. The sham group showed low levels of leukocyte adhesion. BC significantly ($p<0.05$) increased the number of adherent leukocytes compared to the sham group. BCP administration (100 mg/kg) significantly ($p<0.05$) decreased leukocyte adhesion when compared to animals in the BC group. Administration of the CB2R antagonist, AM630 (2.5 mg/kg), 30 minutes prior to BCP (100 mg/kg) reversed the effects of BCP, significantly ($p<0.05$) increasing leukocyte adhesion (Figure 22).

3.3.1.2 Leukocyte Rolling

Leukocyte slow rolling was measured using IVM of the submucosal venules in the bladder twenty-four hours after intravesical administration of UPEC. The sham group showed low levels of leukocyte rolling. BC significantly ($p<0.05$) increased the number of rolling leukocytes compared to the sham group. Leukocyte rolling was not significantly reduced ($p>0.05$) when treated with 100 mg/kg BCP. Additionally, AM630 (2.5 mg/kg) administration 30 minutes prior to BCP (100 mg/kg) treatment did not significantly ($p>0.05$) reduce leukocyte rolling (Figure 23).

3.3.1.3 Capillary Perfusion

Functional capillary density of the bladder microcirculation, a measure of microvascular perfusion, was significantly ($p<0.05$) reduced with intravesical administration of UPEC compared to sham animals. Subsequent treatment with 100 mg/kg BCP restored FCD levels back to those of sham animals and was significantly ($p<0.05$) higher than that observed in the BC

group. AM630 (2.5 mg/kg) administration, a CB2R antagonist, 30 minutes prior to BCP (100 mg/kg) treatment produced a non-significant reduction of FCD ($p>0.05$) compared to BC animals (Figure 24).

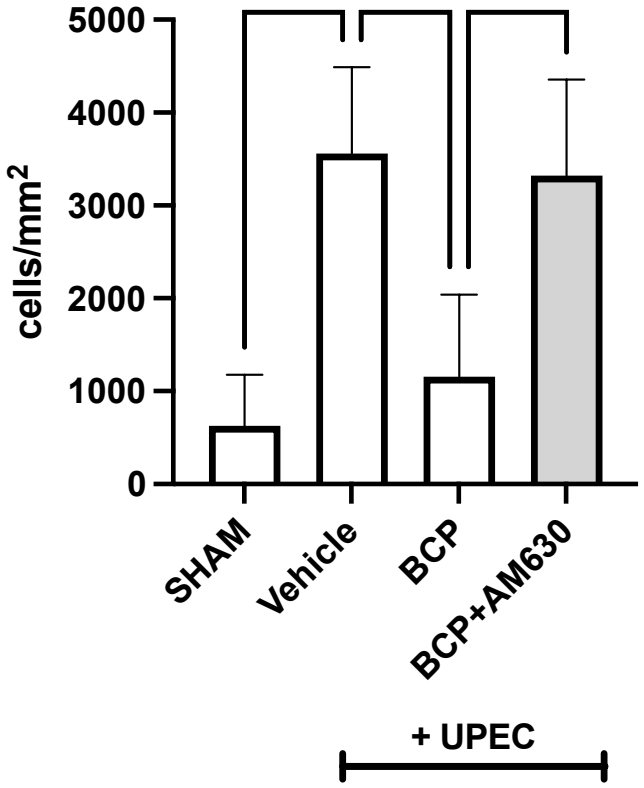

Figure 22. Leukocyte adhesion in the submucosal bladder venules of female BALB/c mice (cells/mm^2). The following groups are included: sham animals (SHAM; n=7), untreated BC (Vehicle; n=6), BCP treated BC (BCP, 100 mg/kg, n=5), AM630 treatment (AM630, 2.5 mg/kg, BCP, 100 mg/kg, n=6). Leukocyte adhesion was evaluated 24 hours following intravesical administration of UPEC or PBS (SHAM). Data presented as mean± SD. * $p < 0.05$.

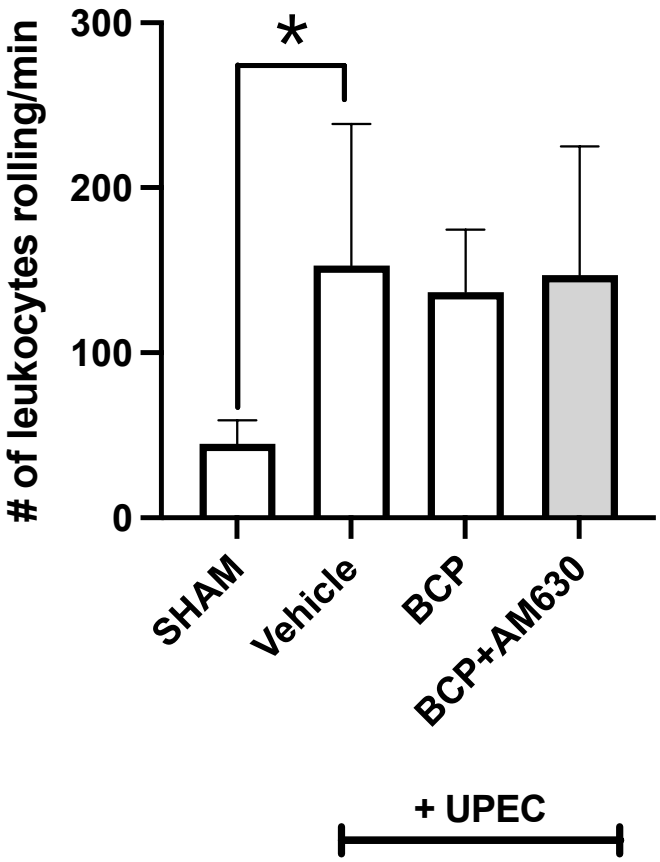

Figure 23. Leukocyte rolling in the submucosal bladder venules of female BALB/c mice (cells/mm^2). The following groups are included: sham animals (SHAM; n=7), untreated BC (Vehicle; n=6), BCP treated BC (BCP, 100 mg/kg, n=5), AM630 treatment (AM630, 2.5 mg/kg, BCP, 100 mg/kg, n=6). Leukocyte rolling was evaluated 24 hours following intravesical administration of UPEC or PBS (SHAM). Data presented as mean± SD. * $p < 0.05$.

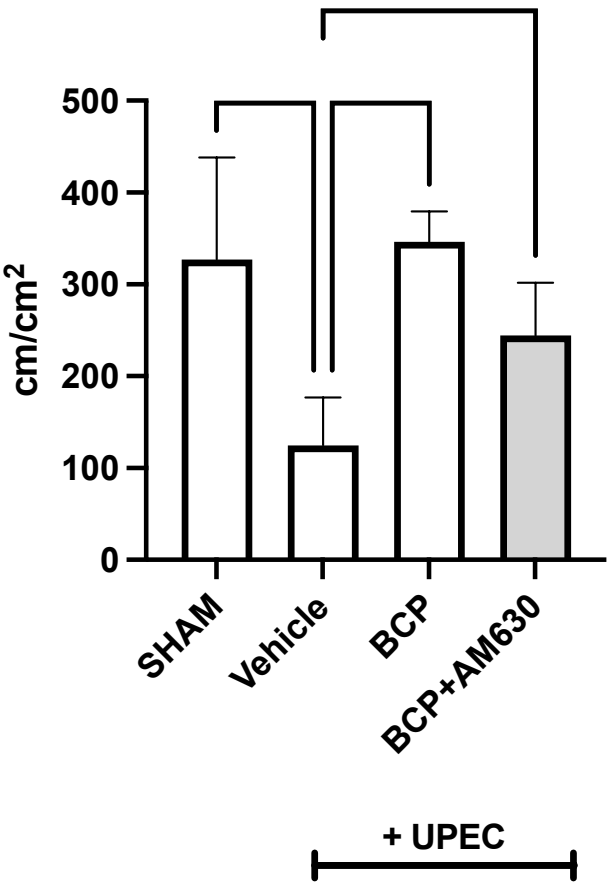

Figure 24. Capillary perfusion of the bladder microcirculation in of female BALB/c mice (cm/cm^2). The following groups are included: sham animals (SHAM; n=7), untreated BC (Vehicle; n=6), BCP treated BC (BCP, 100 mg/kg, n=5), AM630 treatment (AM630, 2.5 mg/kg, BCP, 100mg/kg, n=6). FCD was evaluated 24 hours following intravesical administration of UPEC or PBS (SHAM). Data presented as mean± SD. * $p < 0.05$.

3.3.2. Pain and Behaviour

3.3.2.1 von Frey Aesthesiometry

Von Frey Aesthesiometry was performed to analyze changes in pain threshold by measuring the amount of force, in grams, tolerated when applied to the animal's pelvic region before withdrawal. Measurements were performed in all animals prior to intravesical UPEC instillation (T_0) to set an individual baseline measurement and again 24 hours after UPEC instillation. UPEC instillation resulted in a significant ($p<0.05$) decrease in withdrawal threshold when compared to sham animals. Treatment with 100 mg/kg BCP significantly ($p<0.05$) restored levels of withdrawal threshold back to those of sham animals. Furthermore, AM630 (2.5 mg/kg) administration 30 minutes prior to BCP (100 mg/kg) treatment was able to significantly improve withdrawal threshold when compared to untreated BC animals (Figure 25). Blocking the CB2R with AM630 (2.5 mg/kg) did not significantly ($p>0.05$) change the withdrawal threshold when compared to animals treated with BCP alone.

3.3.2.1. Behaviour

Changes in non-evoked behavioral responses were assessed as an alternative way to study pain in mice with BC. The scores for three behavioural parameters were summed to generate a cumulative behavioural score. Behavioural parameters were assessed in all animals prior to intravesical UPEC instillation (T_0) to set an individual baseline measurement and again 24 hours after UPEC instillation Sham animals showed a minimal, non-significant increase in the total cumulative score. UPEC instillation significantly ($p<0.05$) increased cumulative scores compared to sham animals (Figure 26). Treatment with 100 mg/kg BCP significantly ($p<0.05$) improved this parameter, restoring behaviour to baseline. The same effect was observed in animals who received AM630 (2.5 mg/kg) administration 30 minutes prior to BCP (100 mg/kg) treatment, which

significantly ($p<0.05$) improved cumulative behavioural scores compared to BC animals. Blocking the CB2R with AM630 (2.5 mg/kg) did not significantly ($p>0.05$) change the increase in behavioural scores when compared to animals treated with BCP alone (Figure 26).

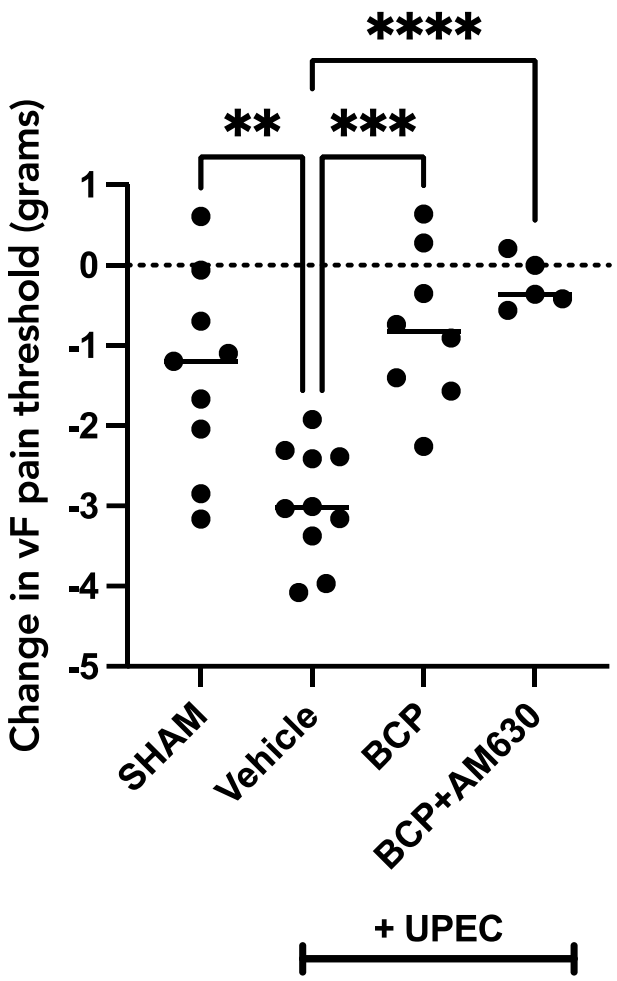

Figure 25. Change in withdrawal threshold (g) in female BALB/c mice. The following groups are included: sham animals (SHAM; n=9), untreated BC (Vehicle; n=10), BCP treated BC (BCP, 100 mg/kg, n=8), AM630 treatment (AM630, 2.5 mg/kg, BCP, 100 mg/kg, n=5). Withdrawal threshold was evaluated before induction (T_0) and 24 hours after intravesical administration of UPEC or PBS (SHAM, T_{24}). Individual data points and group means are shown. * $p < 0.05$.

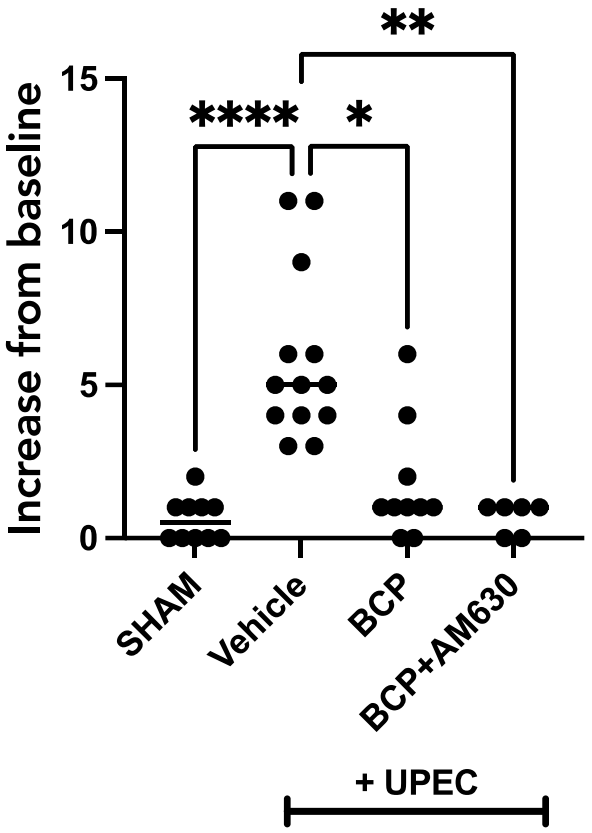

Figure 26. The increase in cumulative behavioural scores of female BALB/c mice. The following groups are included: sham animals (SHAM; n=9), untreated BC (Vehicle; n=10), BCP treated BC (BCP, 100 mg/kg, n=8), AM630 treatment (AM630, 2.5 mg/kg, BCP, 100 mg/kg, n=6). Behavioural parameters were evaluated before induction (T_0) and 24 hours after intravesical administration of UPEC or PBS (SHAM, T_{24}). Individual data points and group means are shown. * $p < 0.05$.

3.3.3 Bacterial Burden

3.3.3.1. Urine

Urine was collected from animals twenty-four hours after intravesical administration of UPEC. No bacteria were found in the urine of sham animals. Intravesical administration of UPEC significantly ($p<0.05$) increased bacterial burden in the urine of BC animals when compared to sham control. Treatment with BCP (100 mg/kg) was able to significantly reduce bacterial growth compared to the untreated BC group. Similarly, bacterial burden was significantly ($p<0.05$) reduced in animals who received AM630 (2.5 mg/kg) administration 30 minutes prior to BCP (100 mg/kg) treatment compared to BC animals (Figure 27).

3.3.3.2. Bladder

Bladder samples were collected from animals twenty-four hours after intravesical administration of UPEC. No bacteria were found in the bladders of sham animals. Intravesical administration of UPEC significantly ($p<0.05$) increased bacterial burden in the urine of BC animals when compared to sham control. Treatment with BCP (100 mg/kg) was able to significantly reduce bacterial growth compared to the untreated BC group. Similarly, bacterial burden was significantly ($p<0.05$) reduced in animals who received AM630 (2.5 mg/kg) administration 30 minutes prior to BCP (100 mg/kg) treatment compared to BC animals (Figure 28).

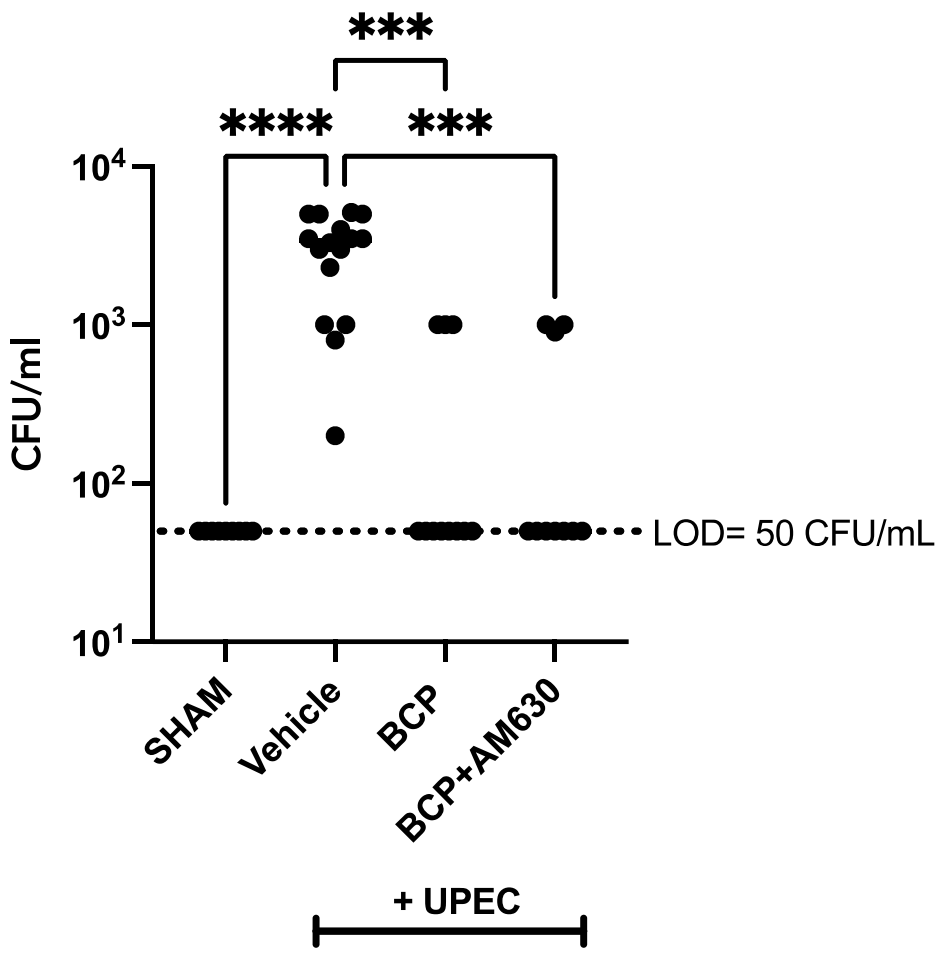

Figure 27. The effects of BCP treatment on bacterial growth in the urine of BALB/c mice 24 hours after instillation of UPEC or PBS (SHAM). The following groups are included: sham animals (sham; n=9), untreated BC (Vehicle; n=16), BCP treated BC (BCP, 100 mg/kg, n=12), AM630 treatment (AM630, 2.5 mg/kg, BCP, 100 mg/kg, n=10). Bacterial burdens are expressed as CFU/ml, LOD (Limit of Detection). Individual data points and group means are shown. * $p <$ 0.05.

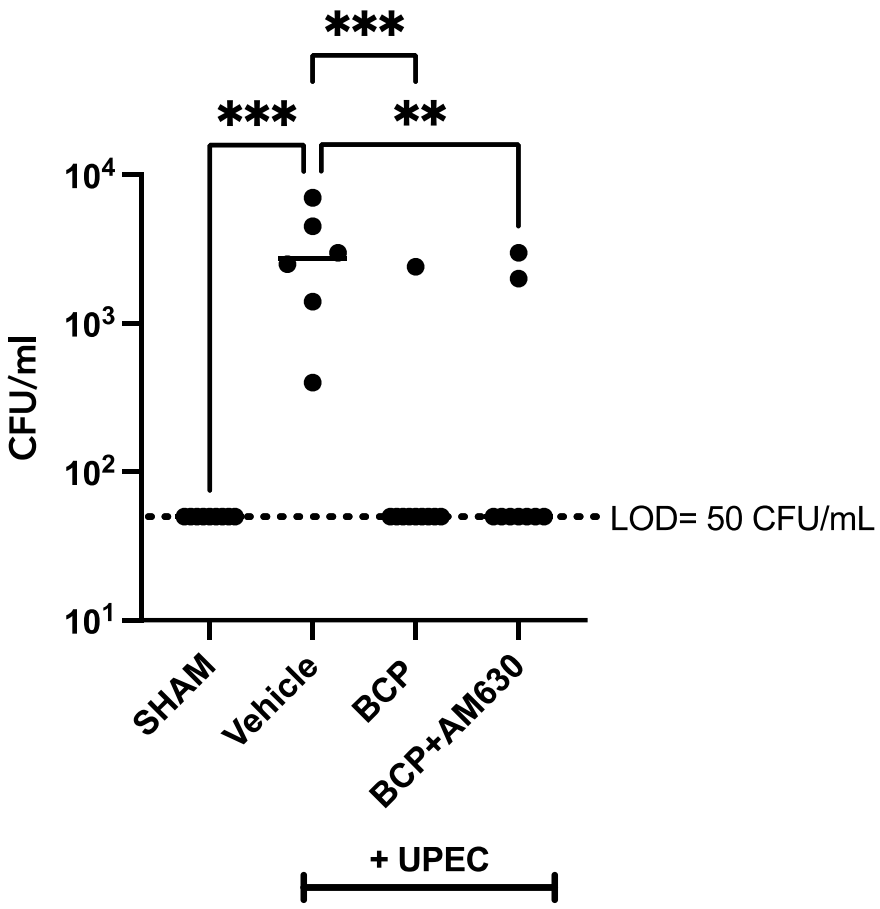

Figure 28. The effects of BCP treatment on bacterial growth in the bladder of BALB/c mice 24 hours after instillation of UPEC or PBS (SHAM). The following groups are included: sham animals (sham; n=9), untreated BC (Vehicle; n=6), BCP treated BC (BCP, 100 mg/kg, n=9), AM630 treatment (AM630, 2.5 mg/kg, BCP, 100 mg/kg, n=9). Bacterial burdens are expressed as CFU/ml, LOD (Limit of Detection). Individual data points and group means are shown. * $p <$ 0.05.

3.4. Bone Marrow Derived Macrophages

3.4.1. Intramacrophage Bacterial Killing

The effects of BCP on bacteria killing was monitored in mature bone marrow derived macrophages, with intracellular UPEC recovered from the macrophages at 1h and 2h post infection. To ensure only intracellular bacteria was evaluated, all extracellular bacteria were killed with gentamicin at 100μg/ml. Untreated UPEC controls had the highest recovered bacterial viability. BCP at all doses significantly enhanced ($p<0.05$) intracellular killing of UPEC in BMDMs at both 1h (Figure 29) and 2h (Figure 30) post infection, as measured by colony-forming units on tryptic soy agar. No significant ($p>0.05$) dose-dependent enhancement of intracellular killing was seen.

3.4.2. Nitric Oxide Assay

A nitric oxide assay was used to examine whether BCP effects NO release into the cell culture medium from monolayers of BMDMs colonized by UPEC. No significant difference ($p>0.05$) was found in NO release 1h post-infection between any groups (Figure 31).

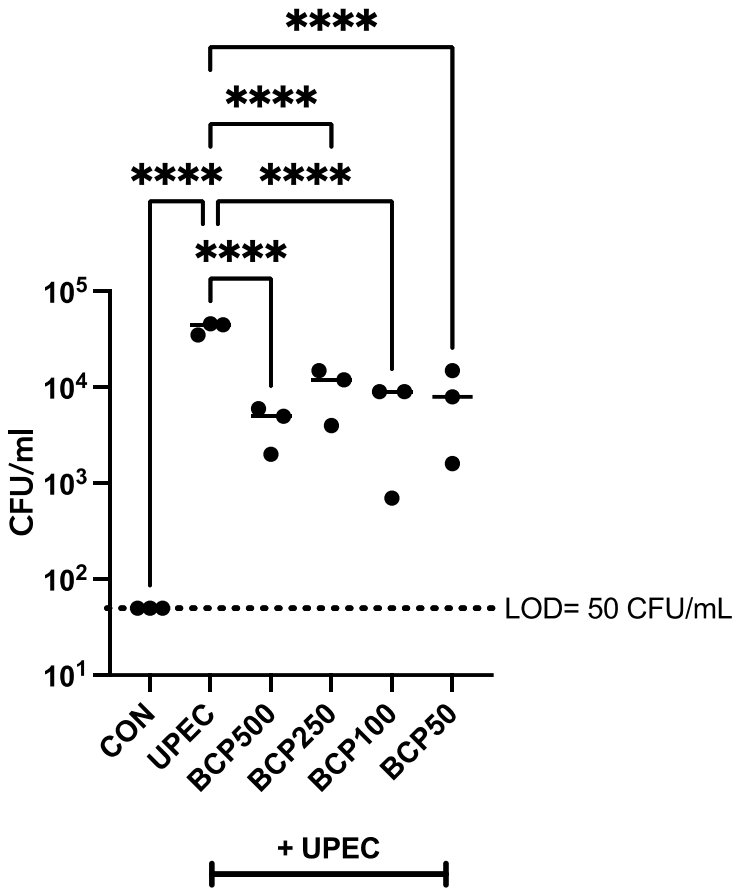

Figure 29. Effects of BCP at different doses on recovered intracellular UPEC bacteria from bone marrow derived macrophages, 1 hour post infection. Individual data points represent the number of viable bacterial colonies (CFU) recovered following gentamicin protection. The following groups are included: BMDM control, (CON, n=3), UPEC polysorbate 80 vehicle control (UPEC; n=3), UPEC+ BCP 500 μg/ml (BCP500; n=3), UPEC+ BCP 250μg/ml (BCP250; n=3), UPEC+ BCP 100μg/ml (BCP100; n=3), UPEC+ BCP 50μg/ml (BCP50; n=3), Bacterial counts are expressed as CFU/ml. Individual data points and group means are shown. * $p < 0.05$.

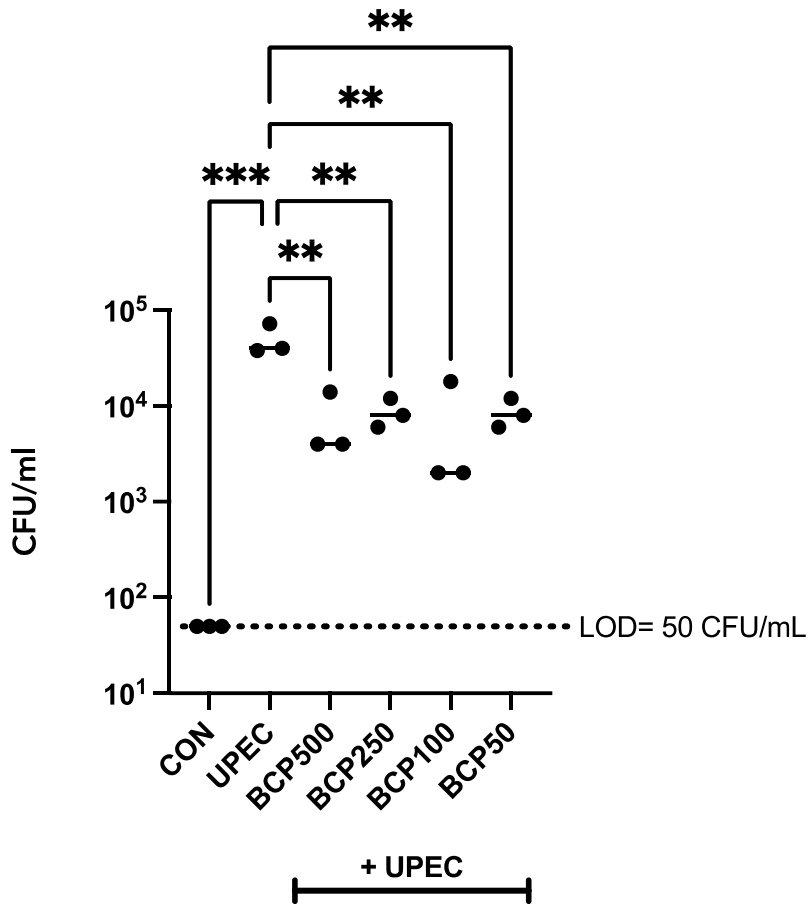

Figure 30. Effects of BCP at different doses on recovered intracellular UPEC bacteria from bone marrow derived macrophages, 2 hours post infection. Individual data points represent the number of viable bacterial colonies (CFU) recovered following gentamicin protection. The following groups are included: BMDM control, (CON, n=3), UPEC polysorbate 80 vehicle control (UPEC; n=3), UPEC+ BCP 500 μg/ml (BCP500; n=3), UPEC+ BCP 250 μg/ml (BCP250; n=3), UPEC+ BCP 100 μg/ml (BCP100; n=3), UPEC+ BCP 50 μg/m (BCP50l; n=3), Bacterial counts are expressed as CFU/ml. Individual data points and group means are shown. * $p < 0.05$.

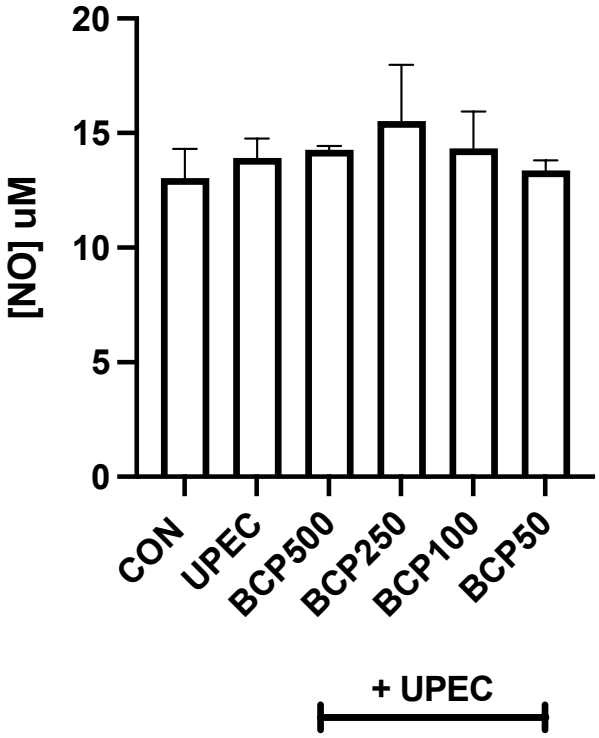

Figure 31. Extracellular nitric oxide (NO) production from bone marrow derived macrophages colonized with UPEC and treated with different doses of BCP (T_1). The following groups are included: BMDM control (CON, n=2), UPEC polysorbate 80 vehicle control (UPEC; n=2), UPEC+ BCP 500 μg/ml (BCP500; n=2), UPEC+ BCP 250 μg/ml (BCP250; n=2), UPEC+ BCP 100 μg/ml (BCP100; n=2), BCP50 (UPEC+ BCP 50 μg/ml; n=2). Data are expressed as means $\pm$ S.D. from two independent experiments. Samples were run in duplicates.

3.5. Human Bladder Epithelial Cells

3.5.1. Bacterial Burdens

The effects of BCP on bacterial adhesion and invasion into human bladder epithelial cells was monitored in BECs, with intracellular UPEC recovered 1h post infection. To ensure only intracellular bacteria was evaluated, all extracellular bacteria were killed with gentamicin (100 μg/ml). Untreated UPEC controls had the highest bacterial counts. BCP at all doses significantly enhanced ($p<0.05$) decreased bacterial invasion into BECs 1h post infection (Figure 32), as measured by colony-forming units on tryptic soy agar. A significant difference ($p<0.05$) was seen between BCP at 1000 μg/ml compared to BCP at 10 μg/ml.

3.5.2. Nitric Oxide Assay

A nitric oxide assay was used to examine whether BCP effects NO release into the cell culture medium from monolayers of BECs colonized by UPEC. No significant difference ($p>0.05$) was found in NO release 1h post-infection between any groups due to the high standard deviation in most of the groups (Figure 33). However, a t-test between the BCP500 and BCP250 group showed a significant difference ($p=0.003$).

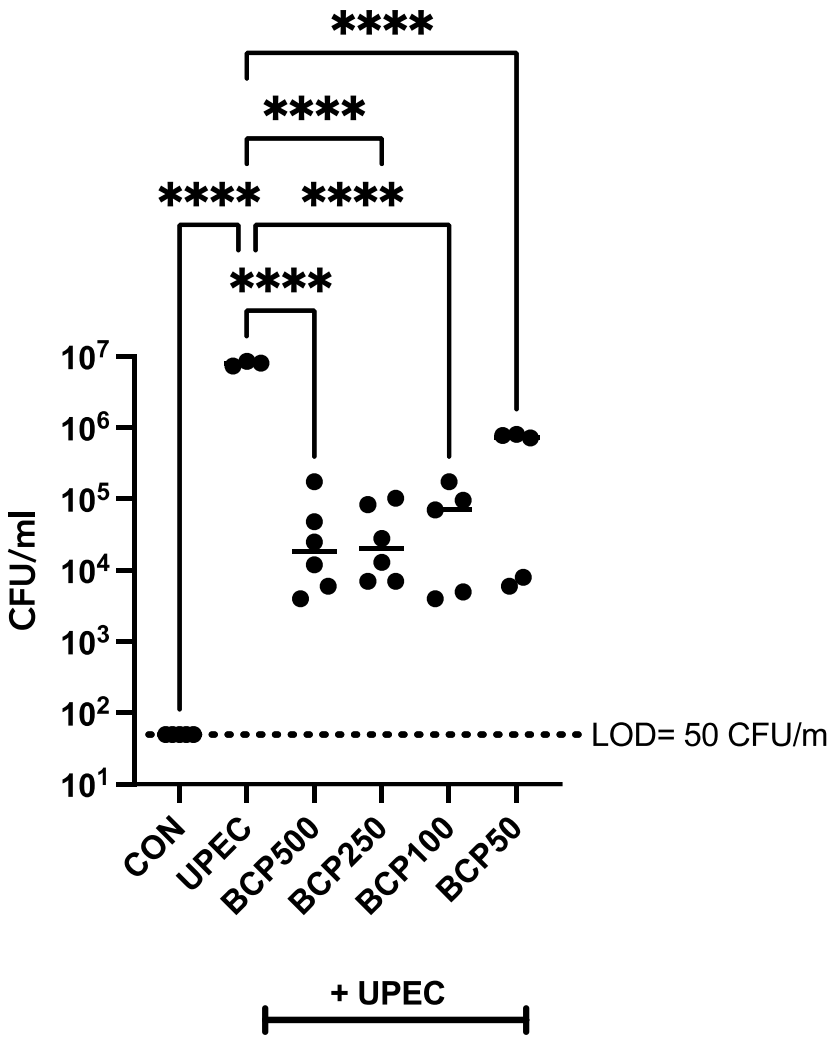

Figure 32. Effects of BCP at different doses on recovered intracellular UPEC bacteria from human bladder epithelial cells, 1 hours post infection. The following groups are included: BEC control, (CON, n=3), UPEC polysorbate 80 vehicle control (UPEC; n=3), UPEC+ BCP 500 μg/ml (BCP500; n=6), UPEC+ BCP 250 μg/ml (BCP250; n=6), UPEC+ BCP 100 μg/ml (BCP100; n=5), and UPEC+ BCP 50 μg/ml (BCP50; n=5). Bacterial counts are expressed as number of viable bacterial colonies (CFU) recovered following gentamicin protection. Group means are shown. * $p < 0.05$.

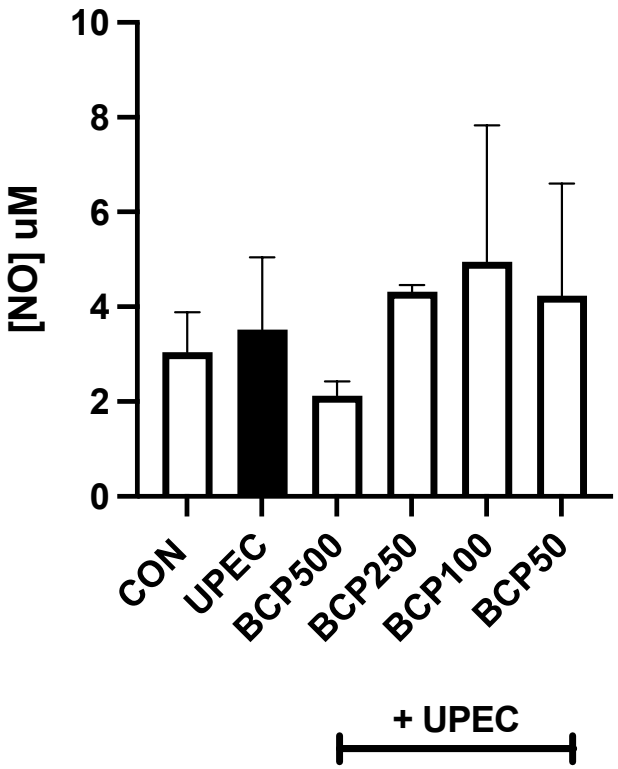

Figure 33. Extracellular nitric oxide (NO) production from bladder epithelial cells colonized with UPEC and treated with different doses of BCP (T_1). The following groups are included: BEC control, (CON, n=3), UPEC polysorbate 80 vehicle control (UPEC; n=3), UPEC+ BCP 500 μg/ml (BCP500; n=3), UPEC+ BCP 250 μg/ml (BCP250; n=3), UPEC+ BCP 100 μg/ml (BCP100; n=3) and UPEC+ BCP 50 μg/ml 0 (BCP50; n=3). Data are expressed as means $\pm$ S.D. from three independent experiments. Samples were run in duplicates.

Chapter 4: Discussion

The goal of this study was to evaluate the anti-inflammatory, anti-bacterial and analgesic activity of the CB2R agonist BCP in *in vitro* and *in vivo* models of acute UPEC-induced bacterial cystitis. Urinary tract infections are one of the most common bacterial infections encountered by clinicians (Tandogdu & Wagenlehner, 2016). While uncomplicated UTIs are typically manageable with a course of antibiotics, they are not effective against rising multi-drug resistant uropathogens, are ineffective at reducing recurrences and provide no immediate analgesia. BCP is a selective CB2R agonist shown to have anti-inflammatory (Zhang et al., 2021), anti-bacterial (Yoo & Jwa, 2018) and local anesthetic (Ghelardini, Galeotti, Di Cesare Mannelli, Mazzanti, & Bartolini, 2001) properties. The beneficial effects shown by BCP along with its ability to modulate the endocannabinoid system through CB2R activation, make it a promising target for the pharmacological treatment of BC.

To our knowledge, the present study is the first to show anti-inflammatory, anti-bacterial and analgesic effects of BCP in experimental BC in mice.

4.1. The Anti-Bacterial Effects of Beta-Caryophyllene *in vivo*

Bacterial cystitis is a form of urinary tract infection, confined to the lower urinary tract (i.e., bladder and urethra). Our pilot studies aimed to ensure that our model accurately simulates BC and did not lead to the development of an upper urinary tract infection nor a systemic infection. Results from these studies found that intravesical UPEC administration significantly increased bacterial burdens in both the urine and bladder tissue. No bacteria were found in either the left or right kidney demonstrating that intravesical UPEC administration did not lead to the development of pyelonephritis at the 24-hour timepoint. Similarly, no bacteria were found in the spleen tissue indicating that our model does not lead to a systemic infection after 24 hours. Once

confirming bacterial burdens within the urine and bladder unaccompanied by infection within the kidney and spleen tissues, our pilot studies aimed to examine the effects of BCP treatment (100 mg/kg) at T_0. No bacteria were found in kidney and spleen tissues following UPEC instillation. Accordingly, BCP had no effect on bacterial growth in these organs. In both urine and bladder samples, BCP was shown to significantly reduce bacterial growth 24 hours after UPEC instillation. Our pilot studies administered BCP treatment immediately after UPEC instillation. Therefore, in order to improve upon the clinical relevancy of our model, we delayed treatment until 6 hours following UPEC instillation (T_6) for our main and antagonist studies.

Results from our pilot bacterial studies were confirmed in our main studies which also saw a significant increase in bacterial burdens within the urine and bladders of female mice 24 hours after UPEC instillation. Treatment with BCP (100 mg/kg) was able to significantly decrease bacterial burdens in the urine and bladders of female mice. Previously, BCPs anti-bacterial activity on *E. coli* has been demonstrated *in vitro*. Studies by Neta et al. (2017) found that BCP induced bacterial killing in murine hepatoma cells infected with *E. coli* (Neta et al., 2017). Similarly, in studies by Dahham et al. (2015) BCP exhibited antimicrobial activity against six bacterial strains, with MIC values ranging from 3 to 14 μM, including *E. coli* with an MIC value of 9 ± 2.2 μM. (Dahham et al., 2015). In addition to *E. coli*, BCPs anti-bacterial activity has been studied in other bacteria such as Streptococcus *mutans.* Studies by Pieri et al. (2016) found that BCP at concentrations between 1.56 and 6.25 mg/ml inhibited bacterial adherence of *Streptococcus* isolates *in vitro* and BCP at 50 mg/ml decreased bacteria dental plaque formation by over 40% in dogs (Pieri et al., 2016).

Our main bacterial studies included fosfomycin as a positive control. Fosfomycin is a first-line treatment option for uncomplicated urinary tract infections, that is 75-90% effective in

clearing UTIs (Gardiner, Stewardson, Abbott, & Peleg, 2019). As expected, fosfomycin treatment (10 mg/kg) significantly reduced bacterial burdens in both the urine and bladder samples of female mice. Additionally, fosfomycin in combination with BCP significantly reduced bacterial burdens in both the urine and bladder. No significant differences were found between treatment groups, suggesting that BCP has similar anti-bacterial efficacy to fosfomycin in UPEC-induced bacterial cystitis.

4.2. The Anti-Inflammatory Effects of Beta-Caryophyllene

Uropathogenic *Escherichia coli*, the most common cause of UTIs, induce an inflammatory response, including leukocyte recruitment to the bladder. IVM was used as a method to assess the inflammatory response in UPEC-induced BC. Here, we showed that intravesical administration of UPEC produces an inflammatory response characterized by increased recruitment of leukocytes to the site of infection, as seen by a significant increase in leukocyte adhesion and rolling compared to sham animals. Similar findings were shown by Haraoka et al. (1999) who showed that intravesical administration of UPEC in female mice resulted in a marked increase in neutrophil recruitment compared to sham animals, as assessed by urine neutrophil numbers (Haraoka et al., 1999). To the best of our knowledge, no studies to date have used IVM as a method of studying the effects of intravesical administration of UPEC on the microcirculation of the urinary bladder. However, studies have been done using LPS from *Escherichia coli* administered intravesical. Studies by Kowalewska et al. (2011) found that LPS administration resulted in a significant increase in leukocyte adhesion and rolling in the bladder microcirculation (Kowalewska, Burrows, & Fox-Robichaud, 2011). It is known that leukocyte extravasation first begins with P-selectin mediated rolling along the endothelial surface, followed by firm attachment involving Ig adhesion molecules such as ICAM-1 (Collins et al., 2000).

Therefore, we performed a Luminex assay to quantify the levels of P-selectin and ICAM-1 in the urinary bladder. In this study, UPEC instillation did not cause a significant upregulation of P-selectin or ICAM-1 compared to sham animals. Similarly, Kowalewska et al. (2011) showed that the bladder endothelium expressed P-selectin and ICAM-1 after intravesical saline instillation, and that the expression of both adhesion molecules did not significantly increase following *E. coli* LPS administration (Kowalewska et al., 2011). These results suggest that there may be a basal level of inflammation maintained in the murine bladder under normal conditions. Overall, cytokine and adhesion molecule levels were low in all tissue samples, indicating low-grade local inflammation associated with BC induction at the 24-hour time point. These results are in line with our histopathology data which found no significant histological changes in the bladder tissue of UPEC-infected mice compared to sham animals. Few studies have examined the histological changes associated with UPEC-induced BC. Studies by Rugo et al. (1992) used a model close in methodology to ours but instead looked at histological changes in the kidneys. Similarly, to our results, their authors found only moderate focal infiltrates of neutrophils into the kidneys, 12 hours after *E. coli* bladder inoculation (Rugo et al., 1992). Our histopathology data differs from studies by Luna-Pineda et al. (2019) who found polymorphonuclear infiltration in the submucosa accompanied by edema and cellular exfoliation in the bladders of UPEC infected mice (Luna-Pineda et al., 2019). However, these conflicting results may be due to model variances. Their authors used a more robust infectious model consisting of double the inoculation volume and a longer 48-hour timepoint, allowing for greater development of infection. Therefore, our data, as assessed by bladder tissue adhesion molecule measurements and histopathology, suggests that intravesical UPEC administration at the 24-hour timepoint

produces low grade local tissue inflammation, with early inflammatory markers evaluated by IVM of the bladder microcirculation.

IVM allows for the bladder microcirculation to be assessed *in vivo* making it a valuable tool for studying the potential effects ECS modulation. In this study BCP was used as an anti-inflammatory treatment for UPEC-induced BC. Our studies found that IP delivery of BCP at 100 mg/kg causes a significant decrease in the number of adherent leukocytes compared to vehicle control (olive oil). These results are in line with previous work in our lab investigating the role of CB2R activation in the urinary bladder of LPS induced interstitial cystitis. Studies by Berger et al. (2019) found that intravesical instillation of BCP or the CB2R agonist, HU308, significantly reduced the number of adhering leukocytes in the submucosal bladder venules (Berger et al., 2019). Intravital microscopy represents a novel method of studying the role CB2R activation in the bladder microcirculation. However, CB2R activation has been studied via IVM in other organs. Szczesniak et al. (2017) found that the CB2R agonist, HU308, significantly decreased leukocyte adhesion in the iridial microcirculation in a murine model of proliferative vitreoretinopathy (Szczesniak et al., 2017). Similarly, Sardinha et al. (2014) studied CB2R-mediated immune modulation in sepsis, finding that HU308 treatment significantly reduced the number of adherent leukocytes in the submucosal venules of endotoxemic mice (Sardinha et al., 2014). In order to further investigate the role of CB2R activation in immune modulation, we blocked CB2R activation with AM630, a CB2R antagonist/inverse agonist. AM630 reversed the BCP induced reduction in leukocyte adhesion, maintaining the number of adherent leukocytes induced by intravesical UPEC administration. Our results correspond with the previously mentioned study investigating vitreoretinopathy, who found AM630 co-administration with HU308 blocked the therapeutic effects of HU308, increasing the number of adherent leukocytes

back to the levels seen in untreated, LPS animals (Szczesniak et al., 2017). Similarly, in a murine model of experimental sepsis, AM630 was shown to reverse the protective effects of FAAH inhibitor URB597 on the LPS-induced increase in leukocyte adhesion in intestinal venules (Kianian, Al-Banna, Kelly, & Lehmann, 2013). Together, these results suggest that CB2R activation has anti-inflammatory properties, reducing the number of adherent leukocytes in a wide variety of tissues and inflammatory models.

Leukocyte slow rolling was assessed as an additional method to evaluate the leukocyte trafficking in the microcirculation of UPEC-induced BC. Our results showed no significant reduction in leukocyte rolling with BCP treatment. To our knowledge, CB2R-mediated effects on leukocyte rolling have not yet been shown using IVM of the urinary bladder. However, studies measuring leukocyte rolling in a model of acute joint inflammation found that inhibiting endocannabinoid degradation via high doses of the FAAH inhibitor, URB597, had no inhibitory effect on leukocyte rolling when compared to vehicle (Krustev, Reid, & McDougall, 2014). Similarly, IVM on the intestinal microvasculature of LPS-challenged mice showed that HU308 treatment was unable to return the number of rolling leukocytes to the levels seen in control animal. Additionally, AM630 in combination with HU308 showed no significant change in the number of rolling leukocytes when compared to HU308 treated animals (Sardinha et al., 2014). These results are in line with our antagonist studies that showed no significant difference in the number of rolling leukocytes when CB2R were blocked with AM630 prior to BCP treatment. Together these results suggest that leukocyte slow rolling is an inflammatory response initiated independently of CB2R signaling. Additional studies must be done in order to further detail the role of CB2R signaling on leukocyte slow rolling. Alternatively, our studies did not administer BCP treatment until 6 hours following BC induction, so it is possible that the innate immune

response initiating leukocyte slow rolling had already begun prior to the 6-hour timepoint and therefore BCP did not produce any anti-inflammatory action on slow rolling.

Lastly, IVM was used as a method of evaluating capillary perfusion by quantifying the functional capillary density in the bladder microcirculation. Our results confirm findings seen for leukocyte rolling and adhesion. UPEC administration resulted in a significant decrease in FCD after 24 hours that was significantly improved with BCP treatment. These results are in line with studies on interstitial cystitis, finding that both, BCP and HU308, restored FCD of the bladder microcirculation to levels seen in healthy control animals, following an LPS-induced reduction in capillary perfusion (Berger et al., 2019). Similarly, HU308 was able to restore FCD in the mucosal villi of mice in an LPS-induced model of endotoxemia (Sardinha et al., 2014). In order to further verify our findings that CB2R activation through BCP reduces UPEC-induced microcirculatory damage, we blocked CB2R activation with AM630. While trends show a decrease in FCD levels following AM630 pre-treatment, this effect was not statistically significant. A similar effect was seen in the above-mentioned study finding no significant difference in FCD following BCP treatment with or without AM630 (Sardinha et al., 2014). While our results, along with those seen in previous studies, suggest a potential role for CB2R agonists in diminishing microcirculatory damage, microcirculatory perfusion is a complex process regulated through the interplay of many different pathways. Microcirculatory perfusion becomes compromised with immune dysregulation, e.g. due to decreased deformability of red blood cells with increased viscosity, intravascular activation of coagulation, increased percentage of activated neutrophils obstructing the microvasculature and increased capillary compression due to capillary leakage-induced edema (Spronk, Zandstra, & Ince, 2004). Therefore,

modulating the CB2R pathway may play a role in restoring irregular microcirculation but is not the only pathway involved.

As an additional method of investigating the therapeutic benefits of BCP as a treatment for BC, we compared its efficacy to that of antibiotic treatment using fosfomycin. Results from our adhesion molecule measurements, histopathology and IVM data found no significant difference between BCP and fosfomycin in terms of anti-inflammatory action, indicating that BCP has similar anti-inflammatory efficacy as the current standard clinical treatment for UTIs.

4.3. The Analgesic Effects of Beta-Caryophyllene

BCP demonstrated anti-inflammatory effects comparable to that of antibiotics in our murine model of bacterial cystitis. Despite a decrease in inflammation with antibiotic treatment, painful symptoms often persist in patients for 24-48 hours following initiation of treatment. Therefore, adjunctive therapy with phenazopyridine, which has a local analgesic effect on the urinary tract, is recommended to provide symptom relief (Bono, Reygaert, & Doerr, 2021). In order to further investigate the use of BCP as a treatment for bacterial cystitis we then examined its analgesic effects using studies of evoked and non-evoked pain tolerance. The von Frey aesthesiometry is a commonly used method to evaluate mechanical hyperalgesia in bladder pain by measuring the maximum force of mechanical stimuli applied to the pelvic area before the animal withdrawals. This method is more commonly used in interstitial cystitis and bladder pain syndrome which is associated with referred pain to the pelvic region (Lai et al., 2016). However, bladder hyperalgesia and suprapubic pain are common symptoms of UTIs (Foxman, 2014) making von Frey aesthesiometry a valuable method of studying clinical UTI symptoms in an animal model.

UPEC instillation into the bladders of mice caused a significant reduction in the withdrawal threshold to stimulation of the lower abdomen. No significant difference was found in withdrawal threshold between groups *prior* to intravesical instillation of saline or *E. coli* (baseline) and instillation of saline (control) had no effect on pain threshold. Our results in experimental BC are in line with studies by Rudick et al. (2011) and Montalbetti et al. (2022) who both showed that *E. coli* instillation into the bladders of female mice induced pelvic allodynia as assessed by von Frey aesthesiometry (Montalbetti et al., 2022; Rudick et al., 2011). IP injection of BCP at 100mg/kg alone or in combination with fosfomycin reversed the *E. coli* induced reduction in withdrawal threshold, suggesting that BCP reduces pain levels. fosfomycin treatment alone had no significant impact on withdrawal threshold when compared to untreated BC animals. To our knowledge this is the first study to assess the analgesic effects of CB2R activation in bacterial cystitis. However, CB2R activation by BCP at 100 mg/kg has shown to improve von Frey aesthesiometry withdrawal threshold in an animal model of interstitial cystitis (Berger et al., 2019). Furthermore, the analgesic effects of BCP have been investigated in other animal models of pain. *In vivo* studies on mice after partial sciatic nerve ligation found that BCP treatment at 10 mg/kg over the course of three days significantly increased mechanical withdrawal thresholds as measured by von Frey aesthesiometry (Klauke et al., 2014). Additionally, studies by Ghelardini et al. (2001) demonstrated the analgesic properties of BCP both *in vitro* and *in vivo*. Authors found that BCP dose-dependently reduces the electrically evoked contractions of the rat phrenic hemidiaphragm *in vitro*, eliciting a similar effect to the local anaesthetic procaine. Furthermore, *in vivo* studies using conjunctival reflex test in rabbits found that BCP permitted a dose-dependent increase in the number of stimuli needed to provoke the reflex (Ghelardini et al., 2001).

As an alternative method of assessing non-evoked pain in UPEC-induced BC, we employed a behavioural scoring system of inflammatory visceral pain based off Boucher et al. 2000 (Boucher et al., 2000). Our behavioural scoring system used three clinical signs and behaviors that are commonly used in research to indicate pain in mice including hunched posture, orbital tightness and decreased motor activity (Carstens & Moberg, 2000). Our results showed that UPEC instillation into the bladders of female mice significantly decreased cumulative behavioural scores. This decrease in behavioural scores was reversed with BCP treatment at 100 mg/kg, alone or in combination with fosfomycin, suggesting a reduction in overall pain levels. Fosfomycin treatment alone showed no significant improvement on cumulative behavioural scores in UPEC-induced BC. Our results are similar to previous studies using a murine model of interstitial cystitis that found BCP at 100 mg/kg produced significant improvements in posture, orbital tightness and motor activity (Berger et al., 2019). To date, this is the only known study using behavioural scoring as a method of measuring CB2R activation on visceral pain in bacterial cystitis. However, studies by Mittal et al. (2016) found similar results quantifying cold hyperalgesia in a murine model of sickle cell disease. Authors found that sickle mice demonstrated increased back curvature and orbital tightness in response to cold. Treatment of sickle mice with the cannabinoid agonist CP55,940 resulted in a decrease in back curvature and orbital tightness when placed on the cold plate (A. Mittal, Gupta, Lamarre, Jahagirdar, & Gupta, 2016).

Results from our von Frey aesthesiometry and behavioural assessment demonstrated that UPEC instillation into the bladders of mice resulted in heightened nociceptive pain despite only producing low-grade tissue inflammation. Studies show that acute UTI pain is mediated by LPS and is independent of inflammation (Rudick et al., 2011). A mouse model of UTI compared pain

associated with the UPEC strain NU14 and the asymptomatic strain 83972. Both strains colonized the bladder indicating that pelvic pain was not correlated with colonization at 24 hours. The authors then assessed myeloperoxidase (MPO), a marker of inflammation. MPO levels in the urine did not significantly differ between 83972 and NU14 infected mice and pelvic pain was not correlated with MPO levels 24 hours post infection. These results support the idea that UPEC induced pelvic pain is not correlated with bladder inflammation. Based on these results, authors hypothesized that UPEC induced pelvic pain is associated with LPS. In order to test this hypothesis, LPS was purified from 83972 or NU14 and instilled directly into the bladder of mice. NU14 purified LPS resulted in a significantly greater pain response when compared to 83972 purified LPS. It is well described that LPS acts through the TLR4 receptor. In order to further support the idea that pelvic pain in UTIs is associated with LPS, authors used TLR4-deficient mice and found that they exhibited significantly reduced pelvic pain compared to wild-type mice following NU14 LPS instillation indicating that NU14 LPS acts through TLR4 to initiate pelvic pain (Rudick et al., 2011). Although the specific mechanisms behind how TLR4 contributes to pain are not fully elucidated it is thought that LPS triggers UTI pain peripherally via its activation of microglia which leads to NF$-\kappa$B dependent COX-2 upregulation that has been shown to contribute to central sensitization in a murine model of neuropathy (Tanga, Nutile-McMenemy, & DeLeo, 2005). A TLR4 dependent pathway of initiating pelvic pain is of particular interest in our model which found higher pain levels in fosfomycin treated animals compared to BCP treated animals. Studies by Zoppi et al. (2014) demonstrated that the CB2R agonist, JWH-133, prevented a stress-induced NF-κB and COX-2 increase in wild-type but not $CB2^{-/-}$ mice, indicating a CB2R-mediated anti-inflammatory response (Zoppi et al., 2014).

Together, these results suggest that CB2R agonists but not antibiotics may mitigate UTI pain via the downregulation of COX-2.

Additionally, BCP is the only CB2R agonist to demonstrate local anesthetic properties. Studies by Ghelardini et al. (2001) showed local anaesthetic activity of BCP in rabbits using the conjunctival reflex test. Which they proposed was strictly dependent on BCPs chemical structure (Ghelardini et al., 2001). Our studies administered BCP via IP injections which likely produced a numbing effect in the urinary bladder of mice. Therefore, the analgesic effects of BCP but not fosfomycin, shown in our evoked and non-evoked pain tolerance could be explained by BCPs local anesthetic activity.

In order to further investigate the CB2R mediated analgesic effects of BCP we administered the CB2R antagonist/inverse agonist, AM630 (2.5 mg/kg), 30 minutes prior to BCP treatment. Our results showed no effect of pre-treatment with the AM630 on BCP-induced anti-nociception in both evoked and non-evoked pain assessment. These results are in line with studies by Krustev et al. (2014) who found that increasing tissue anandamide levels using the selective FAAH inhibitor, URB597, produced anti-nociceptive pain in a murine model of acute joint inflammation, as assessed by von Frey aesthesiometry and hindlimb weight bearing. However, similar to our results, pre-treatment with the CB2R antagonist, AM630 (0.2 mg/kg), had no effect on URB597-induced anti-nociception in both hindlimb weight bearing and von Frey hair secondary allodynia studies (Krustev et al., 2014). Together, these results raise questions on the involvement of CB2R activation involvement in pain desensitization. Both studies used low doses of AM630 (e.g., 2.5 mg/kg and 0.2 mg/kg) so it is possible that full CB2R blockage was not achieved at these doses. Therefore, the effects of higher AM630 dosing on CB2R agonist-induced analgesia must be studied further.

Alternatively, research has shown that cannabinoids can act synergistically with opioid receptors to produce analgesic effects (Ibrahim et al., 2005). *In vivo* studies investigating BCP's ability to prevent a capsaicin-induced nociceptive response found that BCP induced antinociception in a dose-dependent manner. However, these results were blocked when pretreated with either the opioid receptor naloxone hydrochloride or selective μ-opioid receptor antagonist β-FNA but not by the δ-opioid receptor antagonist NTI and the κ-opioid receptor antagonist nor-BNI (Katsuyama et al., 2013). These results further the hypothesis that BCP may have analgesic properties related to the release of endogenous β-endorphins activating opioid receptors in peripheral never terminals of sensory neurons. Future research must be done to further our understanding on the potential synergism between BCPs and opioid receptors.

4.4. Beta-Caryophyllene Treatment in UPEC-Infected Bone Marrow Derived Macrophages

In addition to the anti-bacterial effects of BCP seen in our murine model of UPEC-induced bacterial cystitis, we also aimed to study the effects of BCP in bone marrow derived macrophages. Macrophages play a crucial role in pathological processes, protecting against invading pathogens by promoting phagocytosis and clearance. Our studies examined the bactericidal activity of BMDMs by quantifying the CFU/ml of recovered intracellular *E. coli* from UPEC infected BMDM lysates. Our results found that BMDMs treated with BCP were able to more effectively clear bacteria at both 1 hour and 2 hours post-infection compared to untreated controls. There was no difference in the response over the full dose range. Similar results were seen by Yang et al. 2014 who found that the CB2R agonist, JWH133, reversed the impaired phagocytosis of peritoneal macrophages collected from cirrhotic rats (Yang et al., 2014). Similarly, studies by Shiratsuchi et al. (2008) demonstrated that the endocannabinoid, 2-AG, augmented phagocytosis of zymosan by mouse macrophages. This increase was abolished in the

presence of the CB2R antagonist, SR144528, but not the CB1 antagonist, AM251, indicating that the increase in phagocytosis by 2-AG is CB2R-mediated (Shiratsuchi, Watanabe, Yoshida, & Nakanishi, 2008). To our knowledge, this is the first study to examine the effects of CB2R agonist treatment on UPEC clearance in BMDMs. Together with the literature, these results suggest that BCP enhances bacterial clearance by macrophages in a CB2R-mediated manner. However, our results are limited by the lack of a CB2R antagonist group. Future research should be done, in order to support the idea that BCP treatment enhances bacterial clearance in macrophages through CB2R activation.

Lastly, we aimed to examine the effects of BCP treatment on NO production of BMDMs colonized with UPEC. NO is part of the innate immune response and has been shown to be produced enzymatically by nitric oxide synthase (NOS). Three major isoforms of NOS are known: two constitutive forms, the neuronal isoform (nNOS) and the endothelial isoform (eNOS) in addition to one inducible isoform (iNOS). iNOS can be induced in a wide variety of cells of the immune system including macrophages, neutrophils and epithelial cells (Svensson, Poljakovic, Demirel, Sahlberg, & Persson, 2018). During bacterial infections, increased levels of both NO and iNOS have been found in patients suffering from UTIs (Lundberg et al., 1997, 1996). Our results found low levels of NO production in UPEC-infected BMDMs 1-hour post-infection. No significant effect was seen with BCP treatment. The literature describes a lag phase of several hours between cell activation and NO synthesis (Geller & Billiar, 1998). Our model collected supernatant one-hour post-infection. Therefore, it is possible that NO synthesis had not yet been affected by UPEC colonization at the one-hour timepoint. Similar results were seen by Mittal et al. (2010) who found low levels of NO in UPEC infected peritoneal macrophages two hours post infection. However, their results showed a significant increase in NO levels by the six

hours timepoint (R. Mittal, Gonzalez-Gomez, Goth, & Prasadarao, 2010). Longer timepoints should be investigated in order to further study the effects of BCP treatment on NO production in UPEC-infected BMDMs.

4.5. Beta-Caryophyllene Treatment in UPEC-Infected Bladder Epithelial Cells

The ability of UPEC to adhere and invade host bladder epithelial cells in considered the most critical factor in uropathogenicity (Martinez, Mulvey, Schilling, Pinkner, & Hultgren, 2000). CB2R have been shown on the urothelium and detrusor muscle in the human bladder (Bakali et al., 2013). Our studies examined the effects of BCP at different doses on UPEC invasion into BECs. Our results found that BCP at all doses significantly reduced UPEC invasion into BECs compared to control. Although the exact mechanisms behind UPEC invasion into BECs remain incomplete, there are some CB2R-mediated mechanisms that could potentially explain a CB2R agonist induced decrease in UPEC invasion into BECs. Studies by Ellermann et al. (2020) found that the endocannabinoid, 2-AG, protected mice from enteric bacterial infection by inhibiting virulence factors essential for infection. It was shown that 2-AG directly modulates the virulence of pathogenic *Enterobacteriaceae* by inhibiting the activation of the pro-virulence receptor QseC. (Ellermann et al., 2020). Interestingly, studies by Kostakioti et al. (2009) demonstrated that QseC deletion significantly attenuated intracellular bacterial communities (IBC) and UPEC virulence. Authors also found that QseC deletion severely decreased type 1 pili (Kostakioti, Hadjifrangiskou, Pinkneer, & Scott, 2009). Type 1 pilus adhesin, FimH, mediates not only bacterial adherence but is necessary for UPEC invasion of human bladder epithelial cells (Martinez et al., 2000). If BCP is able to antagonize the bacterial receptor QseC similarly to 2-AG it could provide rationale for a BCP-induced decrease in UPEC invasion into BECs.

These results are of particular importance in terms of UTI recurrence. Once internalized into epithelial cells, UPEC can enter a dormant state protected from natural bacterial flushing through the urine. Research has shown that intracellular UPEC can survive for extended amounts of time in the absence of clinical symptoms, later egressing to promote recurrent UTIs (Kim, Shea, Kim, & Daaka, 2018). BCPs ability to decrease UPEC invasion into epithelial cells may decrease the recurrence of UTIs, unlike antibiotic treatment. Additionally, BCP treatment has been described to enhance cell proliferation in the epidermis and dermis (Koyama et al., 2019). To date, no research has been done studying the effects of BCP treatment on urothelial proliferation. However, research has shown that improving urothelial cell proliferation may restore urothelial health and prevent UTI recurrences. (Jiang et al., 2021).

Preventing UTI recurrences is of particular importance as lower urinary tract symptoms (LUTS) are often seen in women who were successfully treated by antibiotics against the microorganism (Rodrigues, Hering, & Campagnari, 2014). LUTS are thought to persist following bladder ischemia, seen in our IVM data, which promotes detrusor overactivity due to structural damage to the urothelium and disruption of the mucosa (Azadzoi, Tarcan, Kozlowski, Krane, & Siroky, 1999). Women with a history of recurrent UTIs ($\geq$ 3 per year) are more likely to develop bladder hypersensitivity, characterized by chronic bladder pain long after the bacterial load has cleared. Antibiotic treatment is unable to prevent recurrent UTIs and the associated chronic bladder pain therefore longitudinal studies should be done on the potential ability of BCP to decrease recurrences.

Similarly, to our *in vitro* studies using BMDMs we aimed to examine the effects of BCP treatment on NO production in bladder epithelial cells colonized with UPEC. Again, our results found low levels of NO in all groups. Low levels were expected in control BECs as basal NO

production has been demonstrated in urothelial cells (Mastrangelo, Baertschi, Roatti, Amherdt, & Iselin, 2003). No significant effect was seen with BCP treatment. Similarly, Poljakovic et al. 2005 demonstrated that three different strains of UPEC did not stimulate NO production (NO concentration < 5μM) in culture medium of A498 human kidney epithelial cells one-hour post-infection. Low levels of NO were seen in infected and control A498 cells. Their studies found that UPEC in the presence of IFN-γ produced a slight increase in NO production, of which was weak compared to the response evoked by cytokines (Poljakovic, Svensson, & Persson, 2005). Additionally, studies by Poljakovic et al. 2002) demonstrated *in vitro* that the delay in iNOS expression by uroepithelial cells is at least in part due to the finding that iNOS expression in uroepithelial cells is not triggered directly by UPEC but by cytokines released by the activated urothelium and by infiltrating inflammatory cells (Poljakovic, Karpman, Svanborg, & Persson, 2002). Together with the literature, these results suggest that UPEC are weak inducers of human uroepithelial iNOS and that NO production is not part of the first line of defence against UPEC.

Lastly, these results are in line with our BMDM results, highlighting the possibility that NO synthesis is not yet affected by UPEC colonization at the one-hour timepoint. Poljakovic et al. 2001 demonstrated that uroepithelial cells expressed iNOS in the later phase of *in vivo* UPEC infections, peaking between 6 and 12 hours (Poljakovic et al., 2001). Therefore, longer time points should be explored in order to determine the role of UPEC in the induction of human uroepithelial iNOS.

4.6. Experimental Model of BC

4.6.1. Limitations and Future Considerations

The UPEC-induced model of bacterial cystitis has been used extensively to research the development and treatment of UTIs. This model is advantageous as it requires only temporary

anesthesia and UPEC can be delivered directly into the bladder by means of catheterization in 2-3 minutes. Additionally, the mouse is a desirable model system for mammalian UTIs as the bladder structure and cellular composition mimic those of the human bladder (Hannan & Hunstad, 2016). However, some limitations can be identified in our model.

Our model of UPEC-induced bacterial cystitis found lower levels of bacterial counts in homogenized bladder tissue than what is commonly described in the literature. Studies by Chockalingam et al. (2019) used similar methods to our work, infecting Balb/c mice via intravesical inoculation of 1 x 10^8 CFU/ml of CFT073 UPEC. Their work found median bacteria counts of 10^6 CFU/ml at 24 hours post-infection whereas our results found levels of UPEC between 10^3 and 10^4 CFU/ml in bladder tissue. Interestingly, they did find counts as low as 10^2 (Chockalingam et al., 2019). These results highlight the variability seen in the model of UPEC-induced bacterial cystitis. One issue we saw was that despite manually voiding the bladder prior to UPEC infection, some animals void their bladder while recovering from anesthesia, thereby flushing the inoculated UPEC from their bladder almost immediately following BC induction. In order to minimize potential effects of anesthesia, mice were taken off isoflurane immediately following UPEC instillation. However, once conscious we are unable to ethically prevent bladder voiding. Therefore, varying degrees of infection may be related to the length of time UPEC inoculation remained in the bladder prior to voiding. Additionally, Chockalingam et al. (2019) saw median bacterial counts of 10^5 CFU/ml in kidney tissues 24 hours post-infection whereas our model found no bacteria within the kidney tissues (Chockalingam et al., 2019). A satisfactory murine model of ascending UTI must avoid inoculation induced vesicoureteral reflux. Therefore, during BC induction we instilled the inoculation volume slowly over 10 seconds in order to prevent reflux into the kidneys as described in the literature (Johnson &

Brown, 1996). Most studies using the UPEC-induced model of bacterial cystitis do not discuss slow infusion rate in their methods. Furthermore, our model used rifampicin resistant (RR) strain of CFT073 UPEC. This mutation could potentially decrease bacterial activity, resulting in lower infection levels. Studies by Huseby et al. (2020) demonstrated that there are at least 120 different mutations tolerated in the rifampicin-resistance-determining region, including frameshift mutations with largely unknown consequences for phenotype (Huseby, Brandis, Alzrigat, & Hughes, 2020). Lastly, our model used female Balb/c mice infected with CFT073 (UPEC). In the case of both the mice and *E. coli* used, these strains are less commonly seen in research on UPEC-induced BC. Many studies who have previously examined UPEC-induced BC have used C57BL/6 mice who are known to have different innate immune responses compared to Balb/c mice (Bleul et al., 2021). Therefore, strain differences may hinder the generalization of our results.

Another limitation of our study is that only female mice were used. The prevalence of UTIs is significantly higher for women than men due to the proximity between the urethral opening to the vaginal cavity and rectum, which harbor large bacterial communities (Foxman, 2010). However, bacteria live around the urethral opening in both men and women and can colonize the urethra of both sexes. Although, transurethral catheterization to instill UPEC is an effective model for UTIs in mice, it is challenging to reproduce in males due to differences in the gross anatomy. In female mice the urethra is easy to visualize and catharize. Whereas the male urethra is longer and mor tortuous, making transurethral catherization much more difficult. Due to the inability to easily catharize male mice, the majority of research on UTIs has been done on female mice and as a result the effects of sex differences in UTIs remain understudied. Recently, Lamanna et al. (2020) has designed a novel catheter that allows for the control and flexibility to

navigate through the tortuous male urethra (Lamanna, Hsieh, & Forster, 2020) . This technique should be employed in future studies to facilitate the use of male mice in UTI research and expand upon sex differences in UTI treatments.

Additionally, there is potential that our model induces low levels of pain through catheterization and i.p. injections. Although both catheterization and treatment should be relatively pain free, we cannot confirm that no pain was inflicted during these procedures. However, all animals were catheterized and received the same amount of i.p. injections. Therefore, if pain was inflicted, it would be present across all treatment groups.

Lastly, future experiments should also test a second or multiple doses of BCP *in vivo* to improve efficacy. Our *in vivo* model is limited by the use of only one treatment dose and timepoint. To date, there is no known pharmacokinetic or pharmacodynamic data for BCP. Although our drug dose was chosen based on previous literature, without this knowledge we are unable to know the optimal timing and dosage of BCP treatment. Although little to no dose-response was seen in our *in vitro* UPEC infections, it is possible that the same might not be true in an animal model where different tissues with multiple cell types are interacting. Dose-dependent differences should be assessed in *in vivo* in order to determine if there is an optimal dose of BCP that effectively provides anti-inflammatory, anti-bacterial and analgesic effects.

4.7. Conclusion

This study aimed to investigate the anti-bacterial, anti-inflammatory, and analgesic properties of BCP, a phyto-derived CB2R agonist, in a murine model of BC. Our results demonstrated that BCP (100 mg/kg) treatment produced strong anti-bacterial effects, reducing bacterial counts in the urine and bladder samples of BC animals. Next, BCP treatment (100mg/kg) showed anti-inflammatory action *in vivo*, producing a significant decrease in

leukocyte adhesion and reversing the UPEC-induced reduction in capillary perfusion in the bladder microcirculation of BC animals. Antagonizing the CB2R with AM630 reversed BCPs reduction in leukocyte adhesion, alluding to potential anti-inflammatory actions mediated through the CB2R. Results from bladder tissue adhesion molecule measurements and histopathology, suggests that intravesical UPEC administration at the 24-hour timepoint produces low grade local tissue inflammation. Using fosfomycin as a positive control, BCP was shown to have similar anti-inflammatory and anti-bacterial efficacy as the standard clinical therapy for BC. BCP was also able to restore the UPEC-induced pelvic sensitivity to both evoked and non-evoked pain, performing better than antibiotics. These analgesic effects were not blocked by AM630 pre-treatment, demonstrating that other physiological pathways may be involved in pain associated with BC. Lastly, *in vitro* studies revealed BCPs (50μg/ml-1000μg/ml) ability to enhance bacterial clearance by bone marrow derived macrophages and reduce UPEC invasion into human BECs. In summary, this study shows that BCP has potential as a novel adjunct treatment for the management of BC based on its ability to reduce levels of bacterial burden, pain and inflammatory markers in experimental BC.

References

Abraham, S. N., & Miao, Y. (2015). The nature of immune responses to urinary tract infections. *Nature Reviews Immunology*, *15*(10), 655–663. https://doi.org/10.1038/nri3887

Aguiniga, L. M., Yaggie, R. E., Schaeffer, A. J., & Klumpp, D. J. (2016). Lipopolysaccharide domains modulate urovirulence. *Infection and Immunity*, *84*(11), 3131–3140. https://doi.org/10.1128/IAI.00315-16

Al-Taee, H., Azimullah, S., Meeran, M. F. N., Alaraj Almheiri, M. K., Al Jasmi, R. A., Tariq, S., … Ojha, S. (2019). β-caryophyllene, a dietary phytocannabinoid attenuates oxidative stress, inflammation, apoptosis and prevents structural alterations of the myocardium against doxorubicin-induced acute cardiotoxicity in rats: An in vitro and in vivo study. *European Journal of Pharmacology*, *858*(September 2018), 1–10. https://doi.org/10.1016/j.ejphar.2019.172467

Asadi Karam, M. R., Oloomi, M., Mahdavi, M., Habibi, M., & Bouzari, S. (2013). Vaccination with recombinant FimH fused with flagellin enhances cellular and humoral immunity against urinary tract infection in mice. *Vaccine*, *31*(8), 1210–1216. https://doi.org/10.1016/j.vaccine.2012.12.059

Azadzoi, K. M., Tarcan, T., Kozlowski, R., Krane, R. J., & Siroky, M. B. (1999). Overactivity and structural changes in the chronically ischemic bladder. *Journal of Urology*, *162*(5), 1768–1778. https://doi.org/10.1016/S0022-5347(05)68236-5

Bakali, E., Elliott, R. A., Taylor, A. H., Willets, J., Konje, J. C., & Tincello, D. G. (2013). Distribution and function of the endocannabinoid system in the rat and human bladder. *International Urogynecology Journal and Pelvic Floor Dysfunction*, *24*(5), 855–863. https://doi.org/10.1007/s00192-012-1954-1

Beerepoot, M. A. J. (2012). Lactobacilli vs Antibiotics to Prevent Urinary Tract Infections. *Archives of Internal Medicine*, *172*(9), 704–712. https://doi.org/10.1001/archinternmed.2012.777

Berger, G., Arora, N., Burkovskiy, I., Xia, Y., Chinnadurai, A., Westhofen, R., … Lehmann, C. (2019). Experimental cannabinoid 2 receptor activation by phyto-derived and synthetic cannabinoid ligands in LPS-Induced interstitial cystitis in mice. *Molecules*, *24*(23), 1–4. https://doi.org/10.3390/molecules24234239

Bishop, B. L., Duncan, M. J., Song, J., Li, G., Zaas, D., & Abraham, S. N. (2007). Cyclic AMP-regulated exocytosis of Escherichia coli from infected bladder epithelial cells. *Nature Medicine*, *13*(5), 625–630. https://doi.org/10.1038/nm1572

Bleul, T., Zhuang, X., Hildebrand, A., Lange, C., Böhringer, D., Schlunck, G., … Lapp, T. (2021). Different Innate Immune Responses in BALB/c and C57BL/6 Strains following Corneal Transplantation. *Journal of Innate Immunity*, *13*(1), 49–59. https://doi.org/10.1159/000509716

Bono, M. J., Reygaert, W. C., & Doerr, C. (2021). *Urinary Tract Infection (Nursing)*. *StatPearls*.

Booth, J. K., & Bohlmann, J. (2019). Terpenes in Cannabis sativa – From plant genome to humans. *Plant Science*, *284*, 67–72. https://doi.org/10.1016/j.plantsci.2019.03.022

Boucher, M., Meen, M., Codron, J. P., Coudore, F., Kemeny, J. L., & Eschalier, A. (2000). Cyclophosphamide-induced in freely-moving conscious rats: Behavioral approach to a new model of visceral pain. *Journal of Urology*, *164*, 203–208. https://doi.org/10.1016/S0022-5347(05)67495-2

Bourne, R., & Bourne, R. (2010). ImageJ. *Fundamentals of Digital Imaging in Medicine*, *9*(7), 185–188. https://doi.org/10.1007/978-1-84882-087-6_9

Cabral, G. A., Rogers, T. J., & Lichtman, A. H. (2015). Turning Over a New Leaf: Cannabinoid and Endocannabinoid Modulation of Immune Function. *Journal of Neuroimmune Pharmacology*, *10*(2), 193–203. https://doi.org/10.1007/s11481-015-9615-z

Calignano, A., Rana, G. La, Giuffrida, A., & Piomelli, D. (1998). Control of pain initiation by endogenous cannabinoids. *Nature*, *394*(6690), 277–281. https://doi.org/10.1038/28393

Carstens, E., & Moberg, G. P. (2000). Recognizing pain and distress in laboratory animals. *ILAR Journal*, *41*(2), 62–71. https://doi.org/10.1093/ilar.41.2.62

Chockalingam, A., Stewart, S., Xu, L., Gandhi, A., Matta, M. K., Patel, V., … Rouse, R. (2019). Evaluation of immunocompetent urinary tract infected Balb/C mouse model for the study of antibiotic resistance development using Escherichia Coli CFT073 infection. *Antibiotics*, *8*(4), 1–18. https://doi.org/10.3390/antibiotics8040170

Chromek, M., Slamová, Z., Bergman, P., Kovács, L., Podracká, L., Ehrén, I., … Brauner, A. (2006). The antimicrobial peptide cathelicidin protects the urinary tract against invasive bacterial infection. *Nature Medicine*, *12*(6), 636–641. https://doi.org/10.1038/nm1407

Chu, C. M., & Lowder, J. L. (2018). Diagnosis and treatment of urinary tract infections across age groups. *American Journal of Obstetrics and Gynecology*, *219*(1), 40–51. https://doi.org/10.1016/j.ajog.2017.12.231

Collins, R. G., Velji, R., Guevara, N. V., Hicks, M. J., Chan, L., & Beaudet, A. L. (2000). P-selectin or intercellular adhesion molecule (ICAM)-1 deficiency substantially protects against atherosclerosis in apolipoprotein E-deficient mice. *Journal of Experimental Medicine*, *191*(1), 189–194. https://doi.org/10.1084/jem.191.1.189

Comelli, F., Giagnoni, G., Bettoni, I., Colleoni, M., & Costa, B. (2007). The inhibition of monoacylglycerol lipase by URB602 showed an anti-inflammatory and anti-nociceptive effect in a murine model of acute inflammation. *British Journal of Pharmacology*, *152*(5), 787–794. https://doi.org/10.1038/sj.bjp.0707425

Costola-de-Souza, C., Ribeiro, A., Ferraz-de-Paula, V., Calefi, A. S., Aloia, T. P. A., Gimenes-Júnior, J. A., … Palermo-Neto, J. (2013). Monoacylglycerol Lipase (MAGL) Inhibition Attenuates Acute Lung Injury in Mice. *PLoS ONE*, *8*(10), 1–16. https://doi.org/10.1371/journal.pone.0077706

Critchley, I. A., Nicole Cotroneo, Pucci, M. J., & Rodrigo Mendes. (2019). The burden of antimicrobial resistance among urinary tract isolates of Escherichia coli in the United States in 2017. *PLoS ONE*, *14*(12), 1–11. https://doi.org/10.1371/journal.pone.0220265

Dahham, S. S., Tabana, Y. M., Iqbal, M. A., Ahamed, M. B. K., Ezzat, M. O., Majid, A. S. A., & Majid, A. M. S. A. (2015). The anticancer, antioxidant and antimicrobial properties of the sesquiterpene β-caryophyllene from the essential oil of Aquilaria crassna. *Molecules*, *20*(7), 11808–11829. https://doi.org/10.3390/molecules200711808

Dubbs, S. B., & Sommerkamp, S. K. (2019). Evaluation and Management of Urinary Tract Infection in the Emergency Department. *Emergency Medicine Clinics of North America*, *37*(4), 707–723. https://doi.org/10.1016/j.emc.2019.07.007

Ellermann, M., Pacheco, A. R., Jimenez, A. G., Russell, R. M., Cuesta, S., Kumar, A., … Sperandio, V. (2020). Endocannabinoids Inhibit the Induction of Virulence in Enteric Pathogens. *Cell*, *183*(3), 650-665.e15. https://doi.org/10.1016/j.cell.2020.09.022

Fihn, S. D. (2003). Acute uncomplicated urinary tract infection in women. *New England Journal of Medicine*, *349*(3), 259–266. https://doi.org/10.1056/NEJMcp030027

Fontes, L. B. A., Dias, D. dos S., Aarestrup, B. J. V., Aarestrup, F. M., Da Silva Filho, A. A., & Corrêa, J. O. do A. (2017). β-Caryophyllene ameliorates the development of experimental autoimmune encephalomyelitis in C57BL/6 mice. *Biomedicine and Pharmacotherapy*, *91*, 257–264. https://doi.org/10.1016/j.biopha.2017.04.092

Foxman, B. (2010). The epidemiology of urinary tract infection. *Nature Reviews Urology*, *7*(12), 653–660. https://doi.org/10.1038/nrurol.2010.190

Foxman, B. (2014). Urinary tract infection syndromes. Occurrence, recurrence, bacteriology, risk factors, and disease burden. *Infectious Disease Clinics of North America*, *28*(1), 1–13. https://doi.org/10.1016/j.idc.2013.09.003

Francomano, F., Caruso, A., Barbarossa, A., Fazio, A., La Torre, C., Ceramella, J., … Sinicropi, M. S. (2019). β-Caryophyllene: A Sesquiterpene with Countless Biological Properties. *Applied Sciences*, *9*(24), 1–19. https://doi.org/10.3390/app9245420

Galiègue, S., Mary, S., Marchand, J., Dussossoy, D., Carrière, D., Carayon, P., … Casellas, P. (1995). Expression of Central and Peripheral Cannabinoid Receptors in Human Immune Tissues and Leukocyte Subpopulations. *European Journal of Biochemistry*, *232*(1), 54–61. https://doi.org/10.1111/j.1432-1033.1995.tb20780.x

Gardiner, B. J., Stewardson, A. J., Abbott, I. J., & Peleg, A. Y. (2019). Nitrofurantoin and fosfomycin for resistant urinary tract infections: old drugs for emerging problems. *Australian Prescriber*, *42*(1), 14. https://doi.org/10.18773/austprescr.2019.002

Geller, D. A., & Billiar, T. R. (1998). Molecular biology of nitric oxide synthases. *Cancer and Metastasis Reviews*, *17*(1), 7–23. https://doi.org/10.1023/A:1005940202801

Gertsch, J., Leonti, M., Raduner, S., Racz, I., Chen, J.-Z., Xie, X.-Q., … Zimmer, A. (2008). Beta-caryophyllene is a dietary cannabinoid. *Proceedings of the National Academy of Sciences*, *105*(26), 9099–9104. https://doi.org/10.1073/pnas.0803601105

Ghelardini, C., Galeotti, N., Di Cesare Mannelli, L., Mazzanti, G., & Bartolini, A. (2001). Local anaesthetic activity of β-caryophyllene. *Farmaco*, *56*(5–7), 387–389. https://doi.org/10.1016/S0014-827X(01)01092-8

Grimes, C. L., & Lukacz, E. S. (2011). Urinary tract infections. *Female Pelvic Medicine and Reconstructive Surgery*, *17*(6), 272–278. https://doi.org/10.1097/SPV.0b013e318237b99d

Gupta, K., Stapleton, A. E., Hooton, T. M., Roberts, P. L., Fennell, C. L., & Stamm, W. E. (1998). Inverse Association of H2O2-Producing Lactobacilli and Vaginal Escherichia coli Colonization in Women with Recurrent Urinary Tract Infections. *Journal of Infectious Diseases*, *178*(2), 446–450. https://doi.org/10.1086/515635

Hagan, E. C., Lloyd, A. L., Rasko, D. A., Faerber, G. J., & Mobley, H. L. T. (2010). Escherichia coli global gene expression in urine from women with urinary tract infection. *PLoS Pathogens*, *6*(11), 1–18. https://doi.org/10.1371/journal.ppat.1001187

Hannan, T. J., & Hunstad, D. A. (2016). A murine model for Escherichia coli urinary tract infection, *1333*, 1–15. https://doi.org/10.1007/978-1-4939-2854-5

Hannan, T. J., Totsika, M., Mansfield, K. J., Moore, K. H., Schembri, M. A., & Hultgren, S. J. (2012). Host-pathogen checkpoints and population bottlenecks in persistent and intracellular uropathogenic Escherichia coli bladder infection. *FEMS Microbiology Reviews*, *36*(3), 616–648. https://doi.org/10.1111/j.1574-6976.2012.00339.x

Hanuš, L., Breuer, A., Tchilibon, S., Shiloah, S., Goldenberg, D., Horowitz, M., … Fride, E. (1999). HU-308: A specific agonist for CB2, a peripheral cannabinoid receptor. *Proceedings of the National Academy of Sciences of the United States of America*, *96*(25), 14228–14233. https://doi.org/10.1073/pnas.96.25.14228

Haraoka, M., Hang, L., Frendéus, B., Godaly, G., Burdick, M., Strieter, R., & Svanborg, C. (1999). Neutrophil Recruitment and Resistance to Urinary Tract Infection. *The Journal of Infectious Diseases*, *180*(4), 1220–1229. https://doi.org/10.1086/315006

Hayes, B. W., & Abraham, S. N. (2016). Innate Immune Reesponse to Bladder Infection. *Physiology & Behavior*, *4*(6), 1–11. https://doi.org/10.1128/microbiolspec.UTI-0024-2016

Hermanson, D. J., Gamble-George, J. C., Marnett, L. J., & Patel, S. (2014). Substrate-selective COX-2 inhibition as a novel strategy for therapeutic endocannabinoid augmentation. *Trends in Pharmacological Sciences*, *35*(7), 358–367. https://doi.org/10.1016/j.tips.2014.04.006

Hooton, T. M., Scholes, D., Stapleton, A. E., Roberts, P. L., Winter, C., Gupta, K., … Stamm, W. E. (2000). A prospective study of asymptomatic bacteriuria in sexually active young women. *New England Journal of Medicine*, *343*(14), 992–997. https://doi.org/10.1056/NEJM200010053431402

Hopkins, W. J., Gendron-Fitzpatrick, A., Balish, E., & Uehling, D. T. (1998). Time course and host responses to Escherichia coli urinary tract infection in genetically distinct mouse strains. *Infection and Immunity*, *66*(6), 2798–2802. https://doi.org/10.1128/iai.66.6.2798-2802.1998

Howlett, A. C., & Abood, Mary, E. (2017). CB1 & CB2 Receptor Pharmacology. *Adv Pharmacol*, *80*, 169–206. https://doi.org/10.1016/bs.apha.2017.03.007.CB

Huseby, D. L., Brandis, G., Alzrigat, L. P., & Hughes, D. (2020). Antibiotic resistance by high-level intrinsic suppression of a frameshift mutation in an essential gene. *Proceedings of the National Academy of Sciences of the United States of America*, *117*(6), 3185–3191. https://doi.org/10.1073/pnas.1919390117

Ibrahim, M. M., Porreca, F., Lai, J., Albrecht, P. J., Rice, F. L., Khodorova, A., … Malan, T. P. (2005). CB2 cannabinoid receptor activation produces antinociception by stimulating peripheral release of endogenous opioids. *Proceedings of the National Academy of Sciences of the United States of America*, *102*(8), 3093–3098. https://doi.org/10.1073/pnas.0409888102

Ibrahim, M. M., Rude, M. L., Stagg, N. J., Mata, H. P., Lai, J., Vanderah, T. W., … Malan, T. P. (2006). CB2 cannabinoid receptor mediation of antinociception. *Pain*, *122*(1–2), 36–42. https://doi.org/10.1016/j.pain.2005.12.018

Ibsen, M. S., Connor, M., & Glass, M. (2017). Cannabinoid CB 1 and CB 2 Receptor Signaling and Bias . *Cannabis and Cannabinoid Research*, *2*(1), 48–60. https://doi.org/10.1089/can.2016.0037

Jaillon, S., Moalli, F., Ragnarsdottir, B., Bonavita, E., Puthia, M., Riva, F., … Mantovani, A. (2014). The humoral pattern recognition molecule PTX3 is a key component of innate immunity against urinary tract infection. *Immunity*, *40*(4), 621–632. https://doi.org/10.1016/j.immuni.2014.02.015

Jancel, T., & Dudas, V. (2002). Medicine Cabinet: Management of uncomplicated urinary tract infections. *The Western Journal of Medicine*, *176*, 51–55. Retrieved from http://www.ncbi.nlm.nih.gov/pubmed/18751171%0Ahttp://www.pubmedcentral.nih.gov/articlerender.fcgi?artid=PMC1305769

Javed, H., Azimullah, S., Haque, M. E., & Ojha, S. K. (2016). Cannabinoid type 2 (CB2) receptors activation protects against oxidative stress and neuroinflammation associated dopaminergic neurodegeneration in rotenone model of parkinson's disease. *Frontiers in Neuroscience*, *10*(AUG), 1–15. https://doi.org/10.3389/fnins.2016.00321

Jepson, R., Williams, G., & Craig, J. (2012). Cranberries for preventing urinary tract infections. *Cochrane Database Syst Rev*, (10), 1–70. https://doi.org/10.1002/14651858.CD001321.pub5.www.cochranelibrary.com

Jiang, Y. H., Jhang, J. F., Hsu, Y. H., Ho, H. C., Lin, T. Y., Birder, L. A., & Kuo, H. C. (2021). Urothelial health after platelet-rich plasma injection in intractable recurrent urinary tract infection: Improved cell proliferation, cytoskeleton, and barrier function protein expression. *LUTS: Lower Urinary Tract Symptoms*, *13*(2), 271–278. https://doi.org/10.1111/luts.12364

Johansson, J., Gudmundsson, G. H., Rottenberg, M. E., Berndt, K. D., & Agerberth, B. (1998). Conformation-dependent antibacterial activity of the naturally occurring human peptide LL-37. *Journal of Biological Chemistry*, *273*(6), 3718–3724. https://doi.org/10.1074/jbc.273.6.3718

Johnson, J. R., & Brown, J. J. (1996). Defining inoculation conditions for the mouse model of ascending urinary tract infection that avoid immediate vesicoureteral reflux yet produce renal and bladder infection. *Journal of Infectious Diseases*, *173*(3), 746–749. https://doi.org/10.1093/infdis/173.3.746

Jung, D. H., Park, M. H., Kim, C. J., Lee, J. Y., Keum, C. Y., Kim, I. S., … Lee, Y. C. (2020). Effect of β-caryophyllene from cloves extract on helicobacter pylori eradication in mouse model. *Nutrients*, *12*(4), 1–13. https://doi.org/10.3390/nu12041000

Katsuyama, S., Mizoguchi, H., Kuwahata, H., Komatsu, T., Nagaoka, K., Nakamura, H., … Sakurada, S. (2013). Involvement of peripheral cannabinoid and opioid receptors in b-caryophyllene-induced antinociception. *European Journal of Pain (United Kingdom)*, *17*(5), 664–675. https://doi.org/10.1002/j.1532-2149.2012.00242.x

Kerr, D. M., Burke, N. N., Ford, G. K., Connor, T. J., Harhen, B., Egan, L. J., … Roche, M. (2012). Pharmacological inhibition of endocannabinoid degradation modulates the expression of inflammatory mediators in the hypothalamus following an immunological stressor. *Neuroscience*, *204*, 53–63. https://doi.org/10.1016/j.neuroscience.2011.09.032

Kianian, M., Al-Banna, N. A., Kelly, M. E. M., & Lehmann, C. (2013). Inhibition of endocannabinoid degradation in experimental endotoxemia reduces leukocyte adhesion and improves capillary perfusion in the gut. *Journal of Basic and Clinical Physiology and Pharmacology*, *24*(1), 27–33. https://doi.org/10.1515/jbcpp-2012-0065

Kim, W. J., Shea, A. E., Kim, J. H., & Daaka, Y. (2018). Uropathogenic Escherichia coli invades bladder epithelial cells by activating kinase networks in host cells. *Journal of Biological Chemistry*, *293*(42), 16518–16527. https://doi.org/10.1074/jbc.RA118.003499

Kinane, D. F., Blackwell, C. C., Brettle, R. P., Weir, D. M., Winstanley, F. P., & Elton, R. A. (1982). ABO Blood Group, Secretor State, And Susceptibility To Recurrent Urinary Tract Infection In Women. *British Medical Journal (Clinical Research Edition)*, *285*(6334), 7–9. Retrieved from https://www.jstor.org/stable/29507048

Kishimoto, S., Gokoh, M., Oka, S., Muramatsu, M., Kajiwara, T., Waku, K., & Sugiura, T. (2003). 2-Arachidonoylglycerol Induces the Migration of HL-60 Cells Differentiated into Macrophage-like Cells and Human Peripheral Blood Monocytes through the Cannabinoid CB2 Receptor-dependent Mechanism. *Journal of Biological Chemistry*, *278*(27), 24469–24475. https://doi.org/10.1074/jbc.M301359200

Kishimoto, S., Muramatsu, M., Gokoh, M., Oka, S., Waku, K., & Sugiura, T. (2005). Endogenous cannabinoid receptor ligand induces the migration of human natural killer cells. *Journal of Biochemistry*, *137*(2), 217–223. https://doi.org/10.1093/jb/mvi021

Klauke, A. L., Racz, I., Pradier, B., Markert, A., Zimmer, A. M., Gertsch, J., & Zimmer, A. (2014). The cannabinoid CB2 receptor-selective phytocannabinoid beta-caryophyllene exerts analgesic effects in mouse models of inflammatory and neuropathic pain. *European Neuropsychopharmacology*, *24*(4), 608–620. https://doi.org/10.1016/j.euroneuro.2013.10.008

Kostakioti, M., Hadjifrangiskou, M., Pinkner, J., & Scott, H. (2009). QseC-mediated dephosphorylation of QseB is required for expression of genes associated with virulence in uropathogenic Escherichia coli. *Mol Microbiol*, *73*(6), 1020–1031. https://doi.org/10.1111/j.1365-2958.2009.06826.x.QseC-mediated

Kowalewska, P. M., Burrows, L. L., & Fox-Robichaud, A. E. (2011). Intravital Microscopy of the Murine Urinary Bladder Microcirculation. *Microcirculation*, *18*(8), 613–622. https://doi.org/10.1111/j.1549-8719.2011.00123.x

Koyama, S., Purk, A., Kaur, M., Soini, H. A., Novotny, M. V., Davis, K., … Mescher, A. (2019). *Beta-caryophyllene enhances wound healing through multiple routes*. *PLoS ONE* (Vol. 14). https://doi.org/10.1371/journal.pone.0216104

Krustev, E., Reid, A., & McDougall, J. J. (2014). Tapping into the endocannabinoid system to ameliorate acute inflammatory flares and associated pain in mouse knee joints. *Arthritis Research and Therapy*, *16*(1), 1–12. https://doi.org/10.1186/s13075-014-0437-9

Kurihara, R., Tohyama, Y., Matsusaka, S., Naruse, H., Kinoshita, E., Tsujioka, T., … Yamamura, H. (2006). Effects of peripheral cannabinoid receptor ligands on motility and polarization in neutrophil-like HL60 cells and human neutrophils. *Journal of Biological Chemistry*, *281*(18), 12908–12918. https://doi.org/10.1074/jbc.M510871200

Lai, H. H., IV, R. W. G., Luo, Y., O'Donnell, M., Rudick, C. N., Pontari, M., … Klumpp, D. J. (2016). Animal Models of Urologic Chronic Pelvic Pain Network. *Urology*, *85*(6), 1454–1465. https://doi.org/10.1016/j.urology.2015.03.007.ANIMAL

Lamanna, O. K., Hsieh, M. H., & Forster, C. S. (2020). Novel catheter design enables transurethral catheterization of male mice. *American Journal of Physiology-Renal Physiology*, *319*(1), F29–F32. https://doi.org/10.1152/ajprenal.00121.2020

Lewis, A. L., & Gilbert, N. M. (2020). Roles of the vagina and the vaginal microbiota in urinary tract infection: evidence from clinical correlations and experimental models. *GMS Infectious Diseases*, *8*(2195–8831), 1–11. https://doi.org/10.3205/id000046

Lillington, J., Geibel, S., & Waksman, G. (2014). Biogenesis and adhesion of type 1 and P pili. *Biochimica et Biophysica Acta - General Subjects*, *1840*(9), 2783–2793. https://doi.org/10.1016/j.bbagen.2014.04.021

Lourbopoulos, A., Grigoriadis, N., Lagoudaki, R., Touloumi, O., Polyzoidou, E., Mavromatis, I., … Simeonidou, C. (2011). Administration of 2-arachidonoylglycerol ameliorates both acute and chronic experimental autoimmune encephalomyelitis. *Brain Research*, *1390*, 126–141. https://doi.org/10.1016/j.brainres.2011.03.020

Luna-Pineda, V. M., Moreno-Fierros, L., Cázares-Domínguez, V., Ilhuicatzi-Alvarado, D., Ochoa, S. A., Cruz-Córdova, A., … Xicohtencatl-Cortes, J. (2019). Curli of Uropathogenic Escherichia coli Enhance Urinary Tract Colonization as a Fitness Factor. *Frontiers in Microbiology*, *10*(2063), 1–10. https://doi.org/10.3389/fmicb.2019.02063

Lundberg, J. O. N., Carlsson, S., Engstrand, L., Morcos, E., Wiklund, N. P., & Weitzberg, E. (1997). Urinary nitrite: More than a marker of infection. *Urology*, *50*(2), 189–191. https://doi.org/10.1016/S0090-4295(97)00257-4

Lundberg, J. O. N., Ehrén, I., Jansson, O., Adolfsson, J., Lundberg, J. M., Weitzberg, E., … Wiklund, N. P. (1996). Elevated nitric oxide in the urinary bladder in infectious and noninfectious cystitis. *Urology*, *48*(5), 700–702. https://doi.org/10.1016/S0090-4295(96)00423-2

Maki, K. C., Kaspar, K. L., Khoo, C., Derrig, L. H., Schild, A. L., & Gupta, K. (2016). Consumption of a cranberry juice beverage lowered the number of clinical urinary tract infection episodes in women with a recent history of urinary tract infection. *American Journal of Clinical Nutrition*, *103*(6), 1434–1442. https://doi.org/10.3945/ajcn.116.130542

Martinez, J. J., Mulvey, M. A., Schilling, J. D., Pinkner, J. S., & Hultgren, S. J. (2000). Type 1 pilus-mediated bacterial invasion of bladder epithelial cells. *EMBO Journal*, *19*(12), 2803–2812. https://doi.org/10.1093/emboj/19.12.2803

Mastrangelo, D., Baertschi, A. J., Roatti, A., Amherdt, M., & Iselin, C. E. (2003). Nitric oxide production within rat urothelial cells. *Journal of Urology*, *170*(4 I), 1409–1414. https://doi.org/10.1097/01.ju.0000083492.80217.20

McLellan, L. K., & Hunstad, D. A. (2016). Urinary Tract Infection: Pathogenesis and Outlook. *Trends in Molecular Medicine*, *22*(11), 946–957. https://doi.org/10.1016/j.molmed.2016.09.003

Mittal, A., Gupta, M., Lamarre, Y., Jahagirdar, B., & Gupta, K. (2016). Quantification of pain in sickle mice using facial expressions and body measurements. *Blood Cells, Molecules, and Diseases*, *57*, 58–66. https://doi.org/10.1016/j.bcmd.2015.12.006

Mittal, R., Gonzalez-Gomez, I., Goth, K. A., & Prasadarao, N. V. (2010). Inhibition of inducible nitric oxide controls pathogen load and brain damage by enhancing phagocytosis of Escherichia coli K1 in neonatal meningitis. *American Journal of Pathology*, *176*(3), 1292–1305. https://doi.org/10.2353/ajpath.2010.090851

Molina-Holgado, F., Molina-Holgado, E., & Guaza, C. (1998). The endogenous cannabinoid anandamide potentiates interleukin-6 production by astrocytes infected with Theiler's murine encephalomyelitis virus by a receptor-mediated pathway. *FEBS Letters*, *433*, 139–142.

Molina-Holgado, F., Molina-Holgado, E., Guaza, C., & Rothwell, N. J. (2002). Role of CB1 and CB2 receptors in the inhibitory effects of cannabinoids on lipopolysaccharide-induced nitric oxide release in astrocyte cultures. *Journal of Neuroscience Research*, *67*(6), 829–836. https://doi.org/10.1002/jnr.10165

Montalbetti, N., Dalghi, M., Bastacky, S., Clayton, D., Ruiz, W., Apodaca, G., & Carattino, M. (2022). Bladder infection with uropathogenic Escherichia coli increases the excitability of afferent neurons. *Am J Physiol Renal Physiol*, *322*(1), F1–F13.

Moo, C. L., Yang, S. K., Osman, M. A., Yuswan, M. H., Loh, J. Y., Lim, W. M., … Lai, K. S. (2020). Antibacterial activity and mode of action of β-caryophyllene on Bacillus cereus. *Polish Journal of Microbiology*, *69*(1), 49–54. https://doi.org/10.33073/pjm-2020-007

Muller, W. A. (2013). Getting Leukocytes to the Site of Inflammation. *Veterinary Pathology*, *50*(1), 7–22. https://doi.org/10.1177/0300985812469883

Neta, M. C. S., Vittorazzi, C., Guimarães, A. C., Martins, J. D. L., Fronza, M., Endringer, D. C., & Scherer, R. (2017). Effects of β-caryophyllene and Murraya paniculata essential oil in the murine hepatoma cells and in the bacteria and fungi 24-h time-kill curve studies. *Pharmaceutical Biology*, *55*(1), 190–197. https://doi.org/10.1080/13880209.2016.1254251

Nicolle, L. E., Bradley, S., Colgan, R., Rice, J. C., Schaeffer, A., & Hooton, T. M. (2005). Infectious Diseases Society of America Guidelines for the Diagnosis and Treatment of Asymptomatic Bacteriuria in Adults. *Clinical Infectious Diseases*, *40*(5), 643–654. https://doi.org/10.1086/427507

Nielsen, K. L., Dynesen, P., Larsen, P., Jakobsen, L., Andersen, P. S., & Frimodt-Møller, N. (2014). Role of urinary cathelicidin LL-37 and human β-defensin 1 in uncomplicated escherichia coli urinary tract infections. *Infection and Immunity*, *82*(4), 1572–1578. https://doi.org/10.1128/IAI.01393-13

Ojha, S., Javed, H., Azimullah, S., & Haque, M. E. (2016). β-Caryophyllene, a phytocannabinoid attenuates oxidative stress, neuroinflammation, glial activation, and salvages dopaminergic neurons in a rat model of Parkinson disease. *Molecular and Cellular Biochemistry*, *418*(1–2), 59–70. https://doi.org/10.1007/s11010-016-2733-y

Ortega-Gutiérrez, S., Molina-Holgado, E., & Guaza, C. (2005). Effect of anandamide uptake inhibition in the production of nitric oxide and in the release of cytokines in astrocyte cultures. *Glia*, *52*(2), 163–168. https://doi.org/10.1002/glia.20229

Pacher, P., Bátkai, S., & Kunos, G. (2006). The endocannabinoid system as an emerging target of pharmacotherapy. *Pharmacological Reviews*, *58*(3), 389–462. https://doi.org/10.1124/pr.58.3.2

Paragas, N., Kulkarni, R., Werth, M., Schmidt-Ott, K. M., Forster, C., Deng, R., … Barasch, J. (2014). α-Intercalated cells defend the urinary system from bacterial infection. *Journal of Clinical Investigation*, *124*(7), 2963–2976. https://doi.org/10.1172/JCI71630

Pertwee, R. G., Howlett, A. C., Abood, M. E., Alexander, S. P. H., Di Marzo, V., Elphick, M. R., … Ross, R. A. (2010). International Union of Basic and Clinical Pharmacology. LXXIX. Cannabinoid receptors and their ligands: Beyond CB1 and CB2. *Pharmacological Reviews*, *62*(4), 588–631. https://doi.org/10.1124/pr.110.003004

Pieri, F. A., Souza, M. C. de C., Vermelho, L. L. R., Vermelho, M. L. R., Perciano, P. G., Vargas, F. S., … Moreira, M. A. S. (2016). Use of β-caryophyllene to combat bacterial dental plaque formation in dogs. *BMC Veterinary Research*, *12*(1), 1–8. https://doi.org/10.1186/s12917-016-0842-1

Poljakovic, M., Karpman, D., Svanborg, C., & Persson, K. (2002). Human renal epithelial cells express iNOS in response to cytokines but not bacteria. *Kidney International*, *61*(2), 444–455. https://doi.org/10.1046/j.1523-1755.2002.00138.x

Poljakovic, M., Svensson, L., & Persson, K. (2005). The influence of uropathogenic escherichia coli and proinflammatory cytokines on the inducible nitric oxide synthase response in human kidney epithelial cells. *Journal of Urology*, *173*(3), 1000–1003. https://doi.org/10.1097/01.ju.0000150711.69933.95

Poljakovic, M., Svensson, M. L., Svanborg, C., Johansson, K., Larsson, B., & Persson, K. (2001). Escherichia coli-induced inducible nitric oxide synthase and cyclooxygenase expression in the mouse bladder and kidney. *Kidney International*, *59*(3), 893–904. https://doi.org/10.1046/j.1523-1755.2001.059003893.x

Quartilho, A., Mata, H. P., Ibrahim, M. M., Vanderah, T. W., Porreca, F., Makriyannis, A., & Malan, T. P. (2003). Inhibition of inflammatory hyperalgesia by activation of peripheral CB 2 cannabinoid receptors. *Anesthesiology*, *99*(4), 955–960. https://doi.org/10.1097/00000542-200310000-00031

Rhodes, A., Evans, L. E., Alhazzani, W., Levy, M. M., Antonelli, M., Ferrer, R., … Dellinger, R. P. (2017). Surviving Sepsis Campaign: International Guidelines for Management of Sepsis and Septic Shock: 2016. *Critical Care Medicine*, *45*(3), 486–552. https://doi.org/10.1097/CCM.0000000000002255

Rodrigues, P., Hering, F., & Campagnari, J. C. (2014). Involuntary detrusor contraction is a frequent finding in patients with recurrent urinary tract infections. *Urologia Internationalis*, *93*(1), 67–73. https://doi.org/10.1159/000356063

Rudick, C. N., Billips, B. K., Pavlov, V. I., Yaggie, R. E., Anthony, J., & Klumpp, D. J. (2011). Host-Pathogen Interactions Mediating Pain of Urinary Tract Infection. *J Infect Dis*, *201*(8), 1240–1249. https://doi.org/10.1086/651275.Host-Pathogen

Rugo, H. S., O'Hanley, P., Bishop, A. G., Pearce, M. K., Abrams, J. S., Howard, M., & O'Garra, A. (1992). Local cytokine production in a murine model of Escherichia coli pyelonephritis. *Journal of Clinical Investigation*, *89*(3), 1032–1039. https://doi.org/10.1172/JCI115644

Sardinha, J., Kelly, M. E. M., Zhou, J., & Lehmann, C. (2014). Experimental cannabinoid 2 receptor-mediated immune modulation in sepsis. *Mediators of Inflammation*, *2014*, 1–7. https://doi.org/10.1155/2014/978678

Scandiffio, R., Geddo, F., Cottone, E., Querio, G., Antoniotti, S., Gallo, M. P., … Bovolin, P. (2020). Protective Effects of (E)-β-Caryophyllene (BCP) in Chronic Inflammation. *Nutrients*, *12*(3273), 1–24. https://doi.org/10.1016/j.adaj.2018.07.009

Schiwon, M., Weisheit, C., Franken, L., Gutweiler, S., Dixit, A., Meyer-Schwesinger, C., … Engel, D. R. (2014). Crosstalk between sentinel and helper macrophages permits neutrophil migration into infected uroepithelium. *Cell*, *156*(3), 456–468. https://doi.org/10.1016/j.cell.2014.01.006

Scholes, D., Hooton, T. M., Roberts, P. L., Stapleton, A. E., Gupta, K., & Stamm, W. E. (2000). Risk Factors for Recurrent Urinary Tract Infection in Young Women. *The Journal of Infectious Diseases*, *182*(4), 1177–1182. https://doi.org/10.1086/315827

Shang, Y., & Tang, Y. (2017). The central cannabinoid receptor type-2 (CB2) and chronic pain. *International Journal of Neuroscience*, *127*(9), 812–823. https://doi.org/10.1080/00207454.2016.1257992

Shiratsuchi, A., Watanabe, I., Yoshida, H., & Nakanishi, Y. (2008). Involvement of cannabinoid receptor CB2 in dectin-1-mediated macrophage phagocytosis. *Immunology and Cell Biology*, *86*(2), 179–184. https://doi.org/10.1038/sj.icb.7100121

Singh, I., Gautam, L. K., & Kaur, I. R. (2016). Effect of oral cranberry extract (standardized proanthocyanidin-A) in patients with recurrent UTI by pathogenic E. coli: a randomized placebo-controlled clinical research study. *International Urology and Nephrology*, *48*(9), 1379–1386. https://doi.org/10.1007/s11255-016-1342-8

Sommano, S. R., Chittasupho, C., Ruksiriwanich, W., & Jantrawut, P. (2020). The Cannabis Terpenes. *Molecules (Basel, Switzerland)*, *25*(24), 1–16. https://doi.org/10.3390/molecules25245792

Song, J., Duncan, M. J., Li, G., Chan, C., Grady, R., Stapleton, A., & Abraham, S. N. (2007). A novel TLR4-mediated signaling pathway leading to IL-6 responses in human bladder epithelial cells. *PLoS Pathogens*, *3*(4), 541–552. https://doi.org/10.1371/journal.ppat.0030060

Spronk, P. E., Zandstra, D. F., & Ince, C. (2004). Bench-to-bedside review: Sepsis is a disease of the microcirculation. *Critical Care*, *8*(6), 462–468. https://doi.org/10.1186/cc2894

Stapleton, A. E., Au-Yeung, M., Hooton, T. M., Fredricks, D. N., Roberts, P. L., Czaja, C. A., … Stamm, W. E. (2011). Randomized, placebo-controlled phase 2 trial of a lactobacillus crispatus probiotic given intravaginally for prevention of recurrent urinary tract infection. *Clinical Infectious Diseases*, *52*(10), 1212–1217. https://doi.org/10.1093/cid/cir183

Svensson, L., Poljakovic, M., Demirel, I., Sahlberg, C., & Persson, K. (2018). Host-Derived Nitric Oxide and Its Antibacterial Effects in the Urinary Tract. In *Advances in Microbial Physiology* (1st ed., Vol. 73, pp. 1–62). Elsevier Ltd. https://doi.org/10.1016/bs.ampbs.2018.05.001

Szczesniak, A. M., Porter, R. F., Toguri, J. T., Borowska-Fielding, J., Gebremeskel, S., Siwakoti, A., … Kelly, M. E. M. (2017). Cannabinoid 2 receptor is a novel anti-inflammatory target in experimental proliferative vitreoretinopathy. *Neuropharmacology*, *113*, 627–638. https://doi.org/10.1016/j.neuropharm.2016.08.030

Takahashi, S., Hamasuna, R., Yasuda, M., Arakawa, S., Tanaka, K., Ishikawa, K., … Matsumoto, T. (2013). A randomized clinical trial to evaluate the preventive effect of cranberry juice (UR65) for patients with recurrent urinary tract infection. *Journal of Infection and Chemotherapy*, *19*(1), 112–117. https://doi.org/10.1007/s10156-012-0467-7

Tandogdu, Z., & Wagenlehner, F. M. E. (2016). Global epidemiology of urinary tract infections. *Current Opinion in Infectious Diseases*, *29*(1), 73–79. https://doi.org/10.1097/QCO.0000000000000228

Tanga, F. Y., Nutile-McMenemy, N., & DeLeo, J. A. (2005). The CNS role of Toll-like receptor 4 in innate neuroimmunity and painful neuropathy. *Proceedings of the National Academy of Sciences of the United States of America*, *102*(16), 5856–5861. https://doi.org/10.1073/pnas.0501634102

Terlizzi, M. E., Gribaudo, G., & Maffei, M. E. (2017). UroPathogenic Escherichia coli (UPEC) infections: Virulence factors, bladder responses, antibiotic, and non-antibiotic antimicrobial strategies. *Frontiers in Microbiology*, *8*(1566), 1–23. https://doi.org/10.3389/fmicb.2017.01566

Thumbikat, P., Waltenbaugh, C., Schaeffer, A. J., & Klumpp, D. J. (2006). Antigen-Specific Responses Accelerate Bacterial Clearance in the Bladder. *The Journal of Immunology*, *176*(5), 3080–3086. https://doi.org/10.4049/jimmunol.176.5.3080

Uehling, D. T., Hopkins, W. J., Elkahwaji, J. E., Schmidt, D. M., & Leverson, G. E. (2003). Phase 2 clinical trial of a vaginal mucosal vaccine for urinary tract infections. *Journal of Urology*, *170*(3), 867–869. https://doi.org/10.1097/01.ju.0000075094.54767.6e

Wawrysiuk, S., Naber, K., Rechberger, T., & Miotla, P. (2019). Prevention and treatment of uncomplicated lower urinary tract infections in the era of increasing antimicrobial resistance—non-antibiotic approaches: a systemic review. *Archives of Gynecology and Obstetrics*, *300*(4), 821–828. https://doi.org/10.1007/s00404-019-05256-z

Woo, H. J., Yang, J. Y., Lee, M. H., Kim, H. W., Kwon, H. J., Park, M., … Kim, J. B. (2020). Inhibitory effects of β-caryophyllene on helicobacter pylori infection in vitro and in vivo. *International Journal of Molecular Sciences*, *21*(3), 1–14. https://doi.org/10.3390/ijms21031008

Yang, Y. Y., Hsieh, S. L., Lee, P. C., Yeh, Y. C., Lee, K. C., Hsieh, Y. C., … Lin, H. C. (2014). Long-term cannabinoid type 2 receptor agonist therapy decreases bacterial translocation in rats with cirrhosis and ascites. *Journal of Hepatology*, *61*(5), 1004–1013. https://doi.org/10.1016/j.jhep.2014.05.049

Yoo, H. J., & Jwa, S. K. (2018). Inhibitory effects of β-caryophyllene on Streptococcus mutans biofilm. *Archives of Oral Biology*, *88*(January), 42–46. https://doi.org/10.1016/j.archoralbio.2018.01.009

Zhang, Y., Zhang, H., Li, Y., Wang, M., & Qian, F. (2021). β-Caryophyllene attenuates lipopolysaccharide-induced acute lung injury via inhibition of the MAPK signalling pathway. *Journal of Pharmacy and Pharmacology*, *73*(10), 1319–1329. https://doi.org/10.1093/jpp/rgab074

Zimmer, A., Zimmer, A. M., Hohmann, A. G., Herkenham, M., & Bonner, T. I. (1999). Increased mortality, hypoactivity, and hypoalgesia in cannabinoid CB1 receptor knockout mice. *Proceedings of the National Academy of Sciences of the United States of America*, *96*(10), 5780–5785. https://doi.org/10.1073/pnas.96.10.5780

Zoppi, S., Madrigal, J. L., Caso, J. R., García-Gutiérrez, M. S., Manzanares, J., Leza, J. C., & García-Bueno, B. (2014). Regulatory role of the cannabinoid CB2 receptor in stress-induced neuroinflammation in mice. *British Journal of Pharmacology*, *171*(11), 2814–2826. https://doi.org/10.1111/bph.12607

Zou, S., & Kumar, U. (2018). Cannabinoid receptors and the endocannabinoid system: Signaling and function in the central nervous system. *International Journal of Molecular Sciences*, *19*(3), 1–23. https://doi.org/10.3390/ijms19030833